Unraveling molecular mechanisms underlying the progression of pathology in Parkinson s disease

Dijkstra, A.A.

2014

document version
Publisher's PDF, also known as Version of record

Chapter 3

Evidence for immune response, axonal dysfunction and reduced endocytosis in the substantia nigra in early stage Parkinson's disease

3

Anke A. Dijkstra
Angela Ingrassia
Renée X. de Menezes
Ronald E. van Kesteren
Annemieke J.M. Rozemuller
Peter Heutink
Wilma D.J. van de Berg

Submitted to Plos One

Abstract

Subjects with incidental Lewy body disease (iLBD) may represent the premotor stage of Parkinson's disease (PD). To elucidate molecular mechanisms underlying neuronal dysfunction and α-synuclein pathology in the premotor phase of PD, we investigated the transcriptome of the substantia nigra (SN) of well-characterized iLBD, PD donors and age-matched controls with Braak α-synuclein stage ranging from 0-6.

In Braak α-synuclein stages 1 and 2, we observed deregulation of pathways linked to axonal degeneration, immune response and endocytosis, including axonal guidance signaling, mTOR signaling, EIF2 signaling and clathrin-mediated endocytosis in the SN. In Braak stages 3 and 4, we observed deregulation of pathways involved in protein translation and cell survival, including mTOR and EIF2 signaling. In Braak stages 5 and 6, we observed deregulation of dopaminergic signaling, axonal guidance signaling and thrombin signaling. Throughout the progression of PD pathology, we observed a deregulation of mTOR, EIF2 and regulation of eIF4 and p70S6K signaling in the SN.

Our results indicate that molecular mechanisms related to axonal dysfunction, endocytosis and immune response are an early event in PD pathology, whereas mTOR and EIF2 signaling are impaired throughout disease progression. These pathways may hold the key to altering the disease progression in PD.

Introduction

Substantial dopaminergic cell loss in the substantia nigra (SN) is considered to be the pathoanatomical substrate of the motor symptoms in Parkinson's disease (PD) (1). The neuronal loss in the SN is accompanied by the presence of Lewy bodies (LBs) and Lewy neurites (LNs) which are abnormal protein aggregates, mainly consisting of misfolded α-synuclein (2). The α-synuclein pathology in PD is however not limited to the SN, but observed in many brain regions (3-6). It has been postulated that the α-synuclein pathology in the brain starts in the lower brainstem and then advances to the limbic and neocortical brain regions during progression of the disease (6-8). α-Synuclein pathology and nigrostriatal loss (9, 10) have been observed in aged individuals without evidence of parkinsonism or dementia during life and defined pathologically as incidental Lewy Body (iLBD) subjects, suggesting that these subjects may represent the premotor stage of PD (11-14). Studying post-mortem SN tissue of iLBD subjects may, therefore, provide insight into molecular mechanisms involved in α-synuclein aggregation and neuronal dysfunction in early stage PD and shed light on its pathogenesis.

The etiology of PD remains largely unknown, but the role of genetic factors in PD development has been firmly established during the past decade with the identification of 16 'PARK' loci (15). These loci have mainly been identified in patients with familial PD, but also patients with sporadic PD, using Genome Wide Association Studies (GWAS) (16, 17). The identified genes have provided useful insight in the molecular pathways that contribute to the pathogenesis of PD (18). In addition, advanced genomics and proteomics techniques have been applied to discover the molecular signature of sporadic PD. For example, transcriptome analysis of brain structures, such as striatum, SN and locus coeruleus (LC) of PD patients and controls revealed changes in the expression of genes involved in a variety of pathways and cellular processes, including ubiquitination and proteasomal degradation of proteins, oxidative stress, vesicle trafficking, cytoskeletal stability, axonal guidance, dopamine neurotransmission and metabolism, neurotrophic signaling, inflammation and programmed cell death (19-32). The involvement of the mitochondrial dysfunction and synaptic loss in the pathogenesis of PD has been successfully confirmed in animal and *in vitro* models in PD (for review: (33, 34)). However, it is still unknown if these processes contribute to the early stages of PD, in particular the premotor stage.

In the present study, we aimed to identify molecular pathways that play a key role in the progression of α-synuclein pathology by studying the transcriptome of the post-mortem SN of well-characterized PD patients, iLBD subjects and age-matched controls using microarray analysis. To elucidate the mechanisms underlying the α-synuclein aggregation and nigral neuronal death in early stage PD, we focused on transcriptome changes prior to appearance of α-synuclein aggregates in the SN, in Braak α-synuclein stage 1 and 2, and those affected during disease progression in PD.

Methods

Post-mortem human SN tissue

Snap-frozen post-mortem SN tissue was obtained from the Netherlands Brainbank (NBB) and the department of Pathology of VU University Medical Center (VUmc, Amsterdam, The Netherlands). All donors had given informed consent for using the brain tissue and the extensive neuropathological and clinical information for scientific research, in compliance with ethical and legal guidelines. Records including a summary of medical history were available of all patients and controls included in this study.

All subjects were neuropathologically evaluated by experts (AJMR, WK and WvB) and classified for

Braak Alzheimer (neurofibrillary tangles; NFTs score 0-VI (35); amyloid-β plaques stage 0-C (36) and Braak α-synuclein stages 0-6 (3). The distribution and density of NFTs were determined using Bodian staining and immunohistochemistry for hyperphosphorylated tau (Clone AT-8; dilution 1:300 pretreatment in Tris-buffered saline pH 9.0 in the microwave, Innogenetics, Belgium), and the α-synuclein pathology was determined routinely using immunohistochemistry for α-synuclein in several sections throughout the assessed structures by two investigators (WK,WvB) (KM51 antibody, Novocastra, Newcastle upon Tyne, UK; dilution 1:500; pretreatment: citrate buffer (pH 6.0) in the microwave and 80% formic acid). Senile plaques were immunohistochemically stained for amyloid-β (clone M0872, dilution 1:500; DAKO, Denmark pretreatment: citrate buffer (pH 6.0) in the microwave and 80% formic acid).

In total, 28 donors with Braak α-synuclein stages ranging from 0 to 6 were included in the present study; 8 iLBD subjects, 12 clinically diagnosed and pathologically confirmed PD donors and 8 age-matched non-demented controls. Age-matched non-demented controls had no history of neurological or psychiatric disorders. ILBD subjects had no history of neurological or psychiatric disorders and revealed α-synuclein pathology in the medulla oblongata (MO) and olfactory bulb (OB) (Braak α-synuclein stage 1) or MO, OB and LC (Braak α-synuclein stage 2) or MO, LC and SN (Braak α-synuclein stage 3). PD patients were clinically diagnosed with PD or PD with dementia (PDD) by neurologists and/or geriatricians and had no history of cancer or concomitant disease of the central nervous system. The distribution pattern of the PD patients was consistent with Braak α-synuclein stage 4-6. Only sporadic PD patients with an age of onset > 45 years of age were included. The demographic data, including mean age at death, gender, and Braak stages for PD and Alzheimer's disease pathology of the PD patients, iLBD subjects and controls are listed in table 1. A detailed overview of all the demographic, clinical and pathological data including the density of neuromelanin containing neurons of all subjects included in the present study is given in supplementary table 3.1.

Table 1. Clinical and pathological characteristics of donors included in the study.

	Braak α-synuclein stage 0 (n=8)	Braak α-synuclein stage 1-2 (n=5)	Braak α-synuclein stage 3-4 (n=7)	Braak α-synuclein stage 5-6 (n=8)	p-value
Male, n (%)	4 (50%)	2 (40%)	4 (57%)	4 (50%)	0.95[b]
Female, n (%)	4 (50%)	3 (60%)	3 (43%)	4 (50%)	
Age of onset (SD)	n/a	n/a	50 (n=1)	63.6 (11.2)	
PD duration (SD)	n/a	n/a	24 (n=1)	17.7 (6.7)	
Estimated H&Y, median (range)	n/a	n/a	4.0 (n=1)	5.0 (4.0-5.0)	
Demented, n (%)	n/a	n/a	100% (n=1)	4 (50%)	
Age at death, y (SD)	75.5 (7.6)	79.4 (7.1)	78.8(8.5)	78.5 (8.5)	0.81[a]
Tangle score, median (range)	1(0-2)	2(0-2)	1 (0-2)	1 (0-2)	0.76[b]
Amyloid-β score, median (range)	0 (0-B)	A (0-B)	0 (0-C)	A (0-C)	0.38[b]
Neuronal cell density, mean (SD)	6659 (960)	5022 (930)	4682(1440)	2575 (530)	<0.001[a]

Abbreviations: SD= standard deviation; H&Y= Hoehn & Yahr; n/a=not known. [a]ANOVA; [b]Kruskal-Wallis, n/a not answered.

Tissue processing for microarray analysis and morphometry

The SN was identified macroscopically in snap-frozen post-mortem tissue of the mesencephalon and subsequently dissected in a cryostat (-18°C). The SN was marked and serial 40-µm-thick sections were made to microscopically verify that all neuromelanin-containing neurons of the SN were located within the punch. Every 10th section collected throughout the SN of all donors was used to estimate the number of neuromelanin-containing neurons in the SN using the optical fractionator method (37), as described in previously (38). The mean neuromelanin-containing cell density is listed in table 1. The average neuromelanin-containing neuron density in the SN of the controls was 6659 (sd=960), Braak α-synuclein stage 1 and 2 was 5022 (sd=930); Braak α-synuclein stage 3 and4 4682 (sd=1440) and Braak α-synuclein stage 5-6: 2575 (sd=530). An ANOVA revealed that the cell density between groups is statistically different ($F(3)=19.57$, $p<0.001$). Punches were collected throughout the entire SN in 2mL RNAse free Eppendorf tubes). Total RNA was isolated with a Trizol® Reagent (Invitrogen, Carlsbad, CA, USA)/ chloroform protocol. RNA concentration and purity were determined using a NanoDrop ND-1000 spectrophotometer (Nanodrop Technologies, Wilmington, DE, USA) and RNA integrity was determined by the RNA integrity number (RIN) using an Agilent TM 2100 Bioanalyzer and a RNA 6000 Nano LabChip Kit (Agilent Technologies, Palo Alto, CA, USA). The RIN values varied from 5.8 to 8.1 (mean RIN = 7.1).

Sample labelling and microarray hybridization

Five micrograms of total RNA per subject were used to synthesize cDNA. cDNA synthesis and *in vitro* transcription reactions for biotin-labeled complement RNA (cRNA) were carried out using One-Cycle cDNA synthesis kit and the GeneChip ® IVT labeling kit (Affymetrix). The biotinylated cRNA was then cleaned up and fragmented and hybridization cocktails were prepared according to the manufacturer's protocol. All labeled targets underwent a quality control step with hybridization on Gene Chip® Test 3 arrays (Affymetrix, Inc., Santa Clara, California, USA) before the hybridization on Gene Chip expression arrays. All cRNA samples had a 3'/5'-ratio ≤ 3 for housekeeping gene glyceraldehydes-3-phosphate dehydroxygenase (GAPDH) and ≤10 for housekeeping gene actin. Subsequently, the samples were hybridized for 16 hrs on the GeneChip® Human Genome U 133 Plus 2.0 arrays and scanned using a GeneChip® Scanner 3000 (Affymetrix).

Microarray analysis and bioinformatics

The cell intensity files (CEL) generated from images of the scanned arrays were analyzed with Expression Console™ software (v.1.1) to create probe set summarization (CHP) files, evaluate the success of the individual hybridizations and identify possible outliers in the data set. The CEL files were then imported into Partek® Genomics SuiteTM (Partek Incorporated, St. Louis, MO, USA) using a RMA (Robust Multi-chip Average) method, that includes quantile normalization, log2 transformation and median polish of probe-level intensities. The data discussed in this manuscript have been deposited in NCBI's Gene Expression Omnibus (39) and are accessible through GEO Series accession number GSE49036 (http://www.ncbi.nlm.nih.gov/geo/query/acc.cgi?acc=GSE49036).

Microarray data of all subjects were first subjected to an unsupervised hierarchical cluster analysis (Euclidian distance, average linkage) to explore the overlap in gene expression patterns among groups without pre-grouping the samples based upon clinical or pathological characteristics. Unsupervised hierarchical clustering analysis did not support any relation between SN gene expression changes and age, gender, post-mortem delay (PMD) or scan date of the included

subjects. Moreover, no significant correlation between the 3'/5'-ratio of the two housekeeping genes GAPDH and actin and the pH of cerebrospinal fluid was observed (data not shown).
An analysis of covariance (ANCOVA) algorithm (with RIN as covariate to control for the variation caused by partial degradation of RNA) was used to compare probe set expression profiles between groups. To identify gene expression profiles differentially expressed during the progression of PD pathology, gene expression was compared between 1) controls, 2) Braak α-synuclein 1-2, 3) Braak α-synuclein 3-4, 4) Braak α-synuclein 5-6. Lists of probe sets were generated from the ANCOVAs using an BH-FDR=0.05 (40). The lists of probe sets with significantly altered expression levels based on the uncorrected p-values in the separate groups compared to controls were used to investigate pathway alterations in the premotor stage and progression of PD pathology.

Pathway analysis
Each ranked list of the ANCOVAs from the different groups (Braak α-synuclein 1-2, Braak α-synuclein 3-4 and Braak α-synuclein 5-6) compared to controls with uncorrected p-value <0.05 was imported into the software package Ingenuity Pathways Analysis version 8.8 (IPA; Ingenuity Systems, www.ingenuity.com) to assign pathway affiliation. Genes were assigned molecular pathways based on their GO annotation and Entrez Gene information (http://www.ncbi.nlm.nih.gov/gene). The p-value is determined by the probability that the association between the genes in the dataset and the canonical pathway is explained by chance alone. The significance value for pathway over-representation was calculated using a BH-FDR (40). A p-value <0.05 was considered significant.

Validation

Quantitative PCR
Using quantitative PCR (qPCR), the expression levels of selected genes were studied in SN homogenates of 5 controls, 1 Braak α-synuclein stage 1-2, 3 Braak α-synuclein stage 3-4 and 4 α-synuclein stage 5-6 of subjects which were included from the microarray study which are listed in supplementary table 3.1. Six genes, were chosen among the ones with significance (p-value ≤ 0.001) in the PD patients or the iLBD group compared to the control group: eukaryotic translation initiation factor 4A2 (EIF4A2), synaptophysin-like 1 (SYPL1), heat shock 70kDa protein 8 (HSPA8), lysosomal-associated membrane protein 2 (LAMP2), glutamate receptor, metabotropic 3 (GRM3) and fatty acid binding protein 7, brain (FABP7). The housekeeping genes ribosomal protein L27 (RPL27) and ribosomal protein S13 (RPS13) were selected from the list of housekeeping genes as these genes had the most stable expression profiles among all groups in the SN based on the microarray analyses. For reverse transcription of total RNA from SN homogenates, iScriptTM cDNA Synthesis Kit (BioRad Laboratories, Hercules, CA, USA) was used. TaqMan® assays spanning genomic intron-exon junctions were designed in the 3'-end of the gene sequences. Forward and reverse primer sequences were checked for possible secondary structures and dimer formation with the primer analysis tool available at OligoFaktory web portal (http://164.15.232.115/oligofaktory/index.jsp?tool=analysis) and at http://www.eurofinsgenomics.eu. All primers were purchased from Eurogentec S.A. (Liege, Belgium), and suitable probes were selected from the Human Universal Probe Library (Roche Applied Science, Mannheim, Germany). Sequences of the primers and melting temperature (Tm) of the reactions are listed in supplementary table 3.2. All PCR reactions were prepared with TaqMan Fast Universal PCR Master Mix (Applied Biosystems, 11 Norwalk, CT) and performed using a StepOne Plus Real-Time PCR instrument (Applied Biosystems). Standard curves were

generated for each assay run. The relative expression ratio of each target gene was calculated using the efficiency-corrected delta Cq method (41).
The results of the quantitative PCR and normalized microarray expression were statistically analyzed using a Pearson correlation coefficient. A p-value <0.05 was considered significant.

In situ hybridization
Using *in situ* hybridization, localization of the mRNA transcript was studied in unfixed frozen SN sections of PD, iLBD and control subjects. RNA probes for HSPA8, EIF4A2 and LAMP2 were generated using cDNA synthesized from total human brain RNA (iScriptTM cDNA Synthesis Kit, BioRad Laboratories, Hercules, CA, USA). A PCR amplification was performed with Phusion High-fidelity PCR kit (# F553L, Thermo Scientific) using primers containing T_3 (sense) or T_7 (antisense) promoters (sequences; supplementary table 3.3). Digoxigenin labeled RNA probes were generated by linear amplification using Maxiscript T_7/T_3 kit (#AM1322, Ambion) and DIG RNA labeling mix containing digoxigenin-UTP (#11277073910, Roche). Probes were checked for size on 1% agarose gel, and sequenced using an ABI3730 DNA analyzer (Applied Biosystems).
Unfixed frozen SN of PD was sectioned (40 µm) with a cryostat at -18°C, mounted on Superfrost Plus slides (Thermo Scientific) and stored at -80°C. Before the hybridization, slides were kept at room temperature for 30 minutes, fixed with 4% buffered PFA for 20 minutes, then washed with PBS and acetylated with 0.25% acetic anhydride in triethanolamine buffer for 10 minutes. After ethanol dehydration and chloroform treatment, sections were rehydrated and washed with PBS, followed by 2x saline sodium citrate buffer (SSC buffer). The probes were added to the hybridization mix (containing 50% formamide, 4x SSC, tRNA, 50x Denhards reagent and 10% dextran). The hybridization was performed overnight at 60°C. Post-hybridization washes were carried out with 1xSSC in a 60°C water bath and at room temperature, and with 2xSSC containing 0.3 units/ml Rnase A (Roche) in a 37°C water bath. Slides were then pre-incubated for 1 hour with a blocking solution containing 1% blocking powder (DIG nucleid acid detection kit, # 11 175 041 910, Roche) and subsequently incubated overnight at 4°C in humid chamber with anti-DIG AP Fab fragments (#11093274910, Roche) diluted 1:1500 in blocking solution. After buffer washings, the alkaline phosphatase colour reaction was started, incubating the slides with NBT/BCIP (diluted 1:50; #11681451001, Roche) at room temperature in humid chamber. The reaction was stopped in a stop buffer containing 1mM EDTA. Slides were then air dried and coverslipped with Merckoglas (Merck, New Jersey, USA).

Results

Clustering of gene expression profiles
In order to identify differences in genome wide gene expression patterns between PD, iLBD and controls, we performed microarray analysis of the SN. First, an unbiased hierarchical cluster analysis was applied to the microarray dataset to study the clustering of the gene expression data of the 3 pathological groups (figure 1). Within the cluster, there was full separation between PD and control samples, indicating substantial differences in gene expression profiles. The expression profiles of the iLBD subjects clustered either together with the control cases, or with the PD, but they didn't form their own cluster, indicating that their expression levels are intermediate between control and PD gene expression profiles. Unexpectedly, several samples clustered separately from the two main clusters. There were no technical reasons however, to exclude these donors from the analysis.

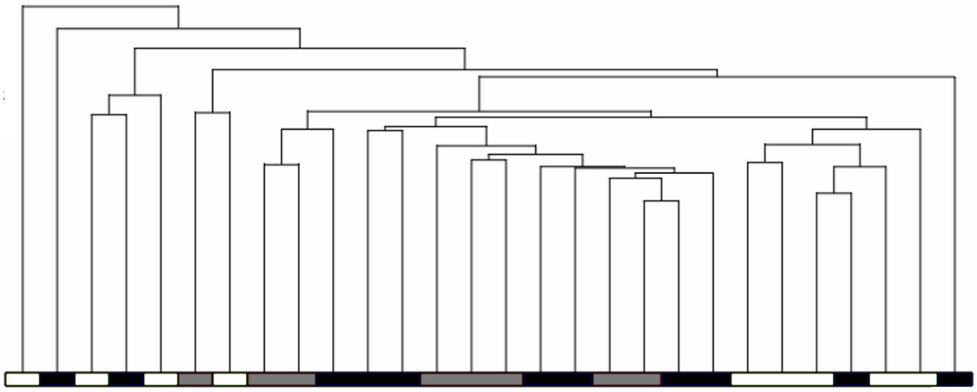

Figure 1. Unbiased hierarchical clustering of all gene expression profiles of iLBD, PD and control donors included. Grey is control, black is iLBD and white is PD donor. The two main clusters are formed by 1) controls and iLBD and 2) PD and iLBD, indicating that the expression of iLBD is heterogenous and intermediate between control and PD.

Molecular pathways involved in end-stage PD compared to control in the SN

In total, 2657 probe sets, of which 976 were up regulated, and 1681 down regulated (BH-FDR <0.05), were altered in PD patients with Braak α-synuclein 5-6 compared to controls. The altered probe sets which displayed a fold change of ±1.50 or more are shown in supplementary table 3.4. Ingenuity Pathway analysis of differentially expressed genes at Braak stage 5-6 (12199 probe sets, ANCOVA unadjusted p<0.05) revealed 47 deregulated pathways (BH-FDR<0.05), which included PI3K/AKT signaling (BH-FDR=0.00032), signaling by Rho family GTPases (BH-FDR=0.00032), and EIF2 signaling (BH-FDR=0.00032).

The following pathways were deregulated in SN tissue of PD patients with Braak α-synuclein stage 5-6 (BH-FDR<0.05) and have been previously described by others (19, 22, 24-26, 28, 32, 42): PI3K/AKT signaling (BH-FDR=0.00032), PTEN signaling (BH-FDR=0.00096), B cell receptor signaling (BH-FDR=0.0019), mTOR signaling (BH-FDR=0.0053), dopamine receptor signaling (BH-FDR=0.03), ephrin receptor signaling (BH-FDR=0.03), Huntington's disease signaling (BH-FDR=0.02), and axonal guidance signaling (BH-FDR=0.02). Other previously identified pathways, such as estrogen receptor signaling and IGF-1 signaling, were not altered in our PD group. In table 2, an overview of novel and previously identified deregulated pathways in end-stage PD is given. Novel pathways included signaling by rho family GTPases (BH-FDR=0.00032), RhoGDI signaling (BH-FDR=0.00072) and protein kinase A signaling (BH-FDR=0.0026).

Altered pathways in the SN in different stages of pathological progression

The ANCOVA of the four groups resulted in the identification of 137 probe sets (BH-FDR 0.05). Pathway analysis showed that 23 pathways were altered among all groups (8475 probe sets, unadjusted p<0.05). Pathways with alterations throughout disease progression in PD included EIF2 signaling (BH-FDR= 0.00000047), breast cancer regulation by stathim 1 (BH-FDR=0.000051), regulation of eIF4 and p70S6K Signaling (BH-FDR=0.00014), dopamine-DARPP32 feedback in cAMP signaling (BH-FDR=0.00018) and mTOR signaling (BH-FDR=0.00019). These pathways are involved in protein translation shut down, immune response and axonal degeneration.

In addition to confirming the involvement of several previously described pathways in end-stage PD, our dataset revealed other molecular alterations, which parallel the progression of PD pathology. Differentially expressed probe sets with unadjusted p<0.05 between Braak

Table 2. Molecular pathways associated with the up- or down-regulated genes in end-stage PD (Braak 5-6) versus controls in our study, compared to other transcriptome studies. * novel pathways in the SN in PD compared to control ** BH-FDR<0.05 displayed;***Fisher p-value<0.05 displayed. LSN= lateral substantia nigra, MSN= medial substantia nigra.

IPA pathway category	PD compared to control**	Elstner et al. 2011***	Bossers et al. 2009***	Simunovic et al. 2009 ***	Lesnick et al. 2007 ***	Moran et al. 2006-LSN ***	Moran et al. 2006-MSN***	Hauser et al. 2005 ***	Zhang et al 2005. ***
EIF2 signaling	0.00032	$1.10*10^{-3}$		$3.98*10^{-4}$					
PI3K/AKT sigaling	0.00032	0.03		$1.82*10^{-3}$	0.01				0.02
Signaling by Rho Family GTPases	0.00032*								
RhoGDI Signaling	0.00072*								
PTEN signaling	0.0010		0.03		0.01	0.03	0.02		
Regulation of stathmin/Breast Cancer Regulation by Stathmin1	0.0013	$8.91*10^{-5}$		$7.76*10^{-4}$					
B Cell Receptor signaling	0.0019						0.01		$1.31*10^{-3}$
Role of NFAT in Cardiac Hypertrophy	0.0026		0.02						
Protein Kinase A Signaling	0.0026*								
Rac signaling	0.0027	0.01		0.02					
Phospholipase C Signaling	0.0041*								
mTOR sigaling	0.0052	0.02		0.02					
Regulation of eIF4 and p70S6K signaing	0.0062	$1.78*10^{-2}$		$1.58*10^{-2}$					
Fcγ Receptor-mediated Phagocytosis in Macrophages and Monocytes	0.0062*								
RhoA Signaling	0.013*								
CXCR4 signaling	0.015	0.02	0.02	0.02					
Tight Junction Signaling	0.018*								
NGF Signaling	0.018*								
Gap Junction Signaling	0.018*								
Axonal Guidance Signaling	0.018	0.02		$8.51*10^{-4}$	0.05	0.01			
Huntington's Disease signalling	0.019	0.01	$1.77*10^{-3}$	$1.48*10^{-3}$		$4.79*10^{-3}$	$9.12*10^{-4}$	0.02	

Table 2 (continued)

IPA pathway category	PD compared to control**	Elstner et al. 2011***	Bossers et al. 2009***	Simunovic et al. 2009 ***	Lesnick et al. 2007 ***	Moran et al. 2006-LSN ***	Moran et al. 2006-MSN***	Hauser et al. 2005 ***	Zhang et al 2005. ***
Cellular Effects of Sildenafil (Viagra)	0.019*								
Gα12/13 Signaling	0.019		0.03						
p70S6K signaling	0.019	0.01		$9.12*10^{-5}$					
Virus entry via endocytic pathways	0.019	0.04		$2.51*10^{-4}$					
G Beta Gamma Signaling	0.027*								
Ephrin Receptor signaling	0.028	$2.51*10^{-3}$							0.03
Molecular Mechanisms of Cancer	0.028*								
CTLA4 Signaling in Cytotoxic T	0.028*								
Regulation of IL-2 Expression	0.028*								
GNRH Signaling	0.030		$3.24*10^{-3}$						
Role of NFAT in Regulation	0.030*								
SAPK/JNK Signaling	0.030*								
Telomerase Signaling	0.030*								
CDK5 Signaling	0.030*								
Ceramide Signaling	0.030*								
Chronic Myeloid Leukemia Signaling	0.030*								
PI3K Signaling in B Lymphocytes	0.030*								
Dopamine Receptor signaling	0.030				0.03	$3.02*10^{-3}$	0.01	0.01	$6.31*10^{-3}$
Germ cell-sertoli cell junction signaling	0.035	0.03		$2.19*10^{-3}$					
Reelin signaling in neurons	0.035	$3.63*10^{-3}$		0.01					
ILK signaling	0.036	0.01		0.02					
Thrombin signaling	0.045	0.03		$2.51*10^{-3}$					
α-Adrenergic Signaling	0.045		0.01						
ERK/MAPK Signaling	0.046*								
HGF Signaling	0.048*								

α-synuclein stage 1-2 subjects and controls (4294 probe sets), resulted in 131 significantly altered probe sets between the transcriptome of the SN in Braak 1-2 and Braak 5-6 stages compared to controls, indicating that alterations of the same molecular mechanisms occur in iLBD and PD. The top deregulated pathways are involved in cellular proliferation and include molecular mechanisms of cancer (BH-FDR=0.000019), colorectal cancer metastasis signaling (BH-FDR=0.000074), gap junction signaling (BH-FDR=0.000074) and actin cytoskeleton signaling (BH-FDR=0.00010). In addition, we found previously identified pathways from other studies, which were not altered in PD in our study, to be altered between Braak α-synuclein stage 1-2 subjects and controls. These pathways include PDGF signaling (BH-FDR=0.00012), estrogen-dependent breast cancer signaling (BH-FDR=0.00068), JAK/Stat signaling (BH-FDR=0.00055), IGF-1 signaling (BH-FDR=0.00089), glucocorticoid receptor signaling (BH-FDR=0.0017), VEGF Signaling (BH-FDR=0.0012) and BMP signaling pathway (BH-FDR=0.0025), suggesting that these pathways are altered in the earliest stages of the disease.

Between Braak α-synuclein stage 1-2 and Braak α-synuclein stage 3-4 (3084 probe sets), two pathways involved in immune response and protein translation were significantly altered: FLT_3 signaling in progenitor cells (BH-FDR=0.001) and EIF2 signaling (BH-FDR=0.009). Finally, in Braak α-synuclein stage 5-6 compared to 3-4 (6602 probe sets), we observed 4 pathways to be altered, dopamine-$DARPP_{32}$ feedback in cAMP signaling (BH-FDR=0.0065), thrombin signaling (BH-FDR=0.0065), cardiac β–adrenergic signaling (BH-FDR=0.0065) and CTLA4 signaling in cytotoxic L lymphocytes (BH-FDR=0.0068). Several pathways altered during the progression of disease, as defined by Braak 0-6, are involved in autophagy: these include EIF2 signaling and regulation of eIF4 and p70S6K signaling and mTOR signaling. The alterations of the elements of these pathways in Braak α-synuclein stage 1-2 compared to controls are displayed in figure 2. All pathways altered in Braak α-synuclein stage 1-2 compared to controls, Braak 3-4 compared to Braak 1-2, Braak 5-6 compared to Braak 3-4, and all the Braak groups compared to controls, are listed in supplementary table 3.5.

Gene expression changes related to immune response, axonal degeneration and endocytosis in the Braak α-synuclein stages 1-2

From the analyses described above, we learned that the most pronounced changes in gene expression occur in pathways related to inflammation and immune response, axonal degeneration and autophagy in early stage PD. With regard to inflammation and immune response, several pathways were altered in the Braak α-synuclein stages 1-2. These include HMGB1 signaling (BH-FDR=0.00015), which is a mediator of inflammation, CXCR2 signaling (BH-FDR=0.00054) and P2Y purigenic receptor signaling (BH-FDR=0.00056), which both are thought to mediate inflammation by cytokine signaling. Also GM-CSF signaling - which is considered to be part of the immune/inflammation cascade (BH-FDR=0.00058) is altered. Other pathways found in our dataset related to inflammation and immune response include thrombin signaling (BH-FDR=0.0012), B cell receptor signaling (BH-FDR=0.00051) and T cell receptor signaling (BH-FDR=0.0035). In addition, CTLA4 signaling in cytotoxic T lymphocytes was up regulated in Braak α-synuclein stage 1 and 2 (BH-FDR=0.0038). The MHC II class receptors were also up regulated, indicating a disturbance of the extracellular matrix. When we looked at altered probe sets, an up regulation in HLA-DQA1 (p=0.02, FC=2.26) and HLA-DRA (p=0.02, FC=2.66) and HLA-DRB1 (p=0.02, FC=1.92) was observed in Braak α-synuclein stage 1-2 compared to controls, but not in other stages of the pathological progression. In addition to immune activation, we observed changes in pathways linked to inflammation, such as Interleukin (IL)-2,3,4,8 and 14 signaling pathways in Braak α-synuclein stage 1- 2 (BH-FDR ranged between 0.001 and 0.09; see

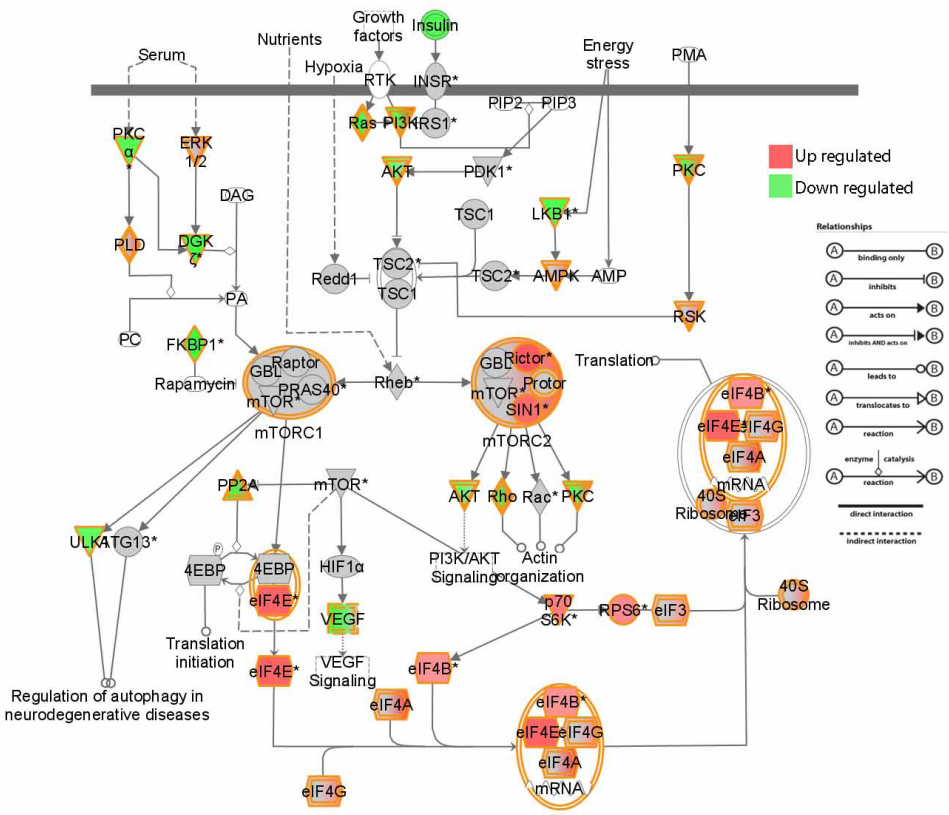

Figure 2. Alterations in elements of mTOR, EIF2 and EIF4 signaling pathways in Braak α-synuclein 1 and 2 compared to controls. Image generated using Ingenuity pathway analysis (IPA).

supplementary table 3.5).

In Braak α-synuclein stage 1-2, we observed a down regulation of pathways involved in cytoskeletal maintenance such as axonal guidance signaling (BH-FDR=0.00010), gap junction signaling (BH-FDR=0.000074), actin cytoskeleton signaling (BH-FDR=0.00010), RhoGDI signaling (BH-FDR=0.00056), protein kinase A signaling (BH-FDR=0.0028) and regulation of actin-based motility by Rho (BH-FDR=0.01). In the SN of donors with Braak α-synuclein stage 1-2, deregulated pathways related to dopamine functioning at the level of the synapse include dopamine-DARPP32 feedback in cAMP signaling (BH-FDR=0.000093). We observed no difference in expression level of α-synuclein (p=0.67) and the interactors of α-synuclein between Braak α-synuclein 1-2 compared to controls, but significant changes were observed for α-synuclein (p=0.001) and most of the interactors in PD compared to controls (table 3). When we focus on the anterograde transporter proteins, we observed a down regulation of kinesin light chain (KLC) (p=0.02, FC=-1.42) and kinesin family 20A (KIF20A) (p=0.02, FC=-1.17) in Braak α-synuclein stage 1-2 compared to controls. Among the pathways related to endocytosis, endocytosis mediated by clathrin (BH-FDR=0.000010) was down regulated and virus entry through endocytic pathways (BH-FDR=0.0079) was up regulated in Braak α-synuclein stage 1-2 compared to controls. In addition, markers for endosomes, such as transferrin (TF), early endosome antigen1 (EEA1) and member Ras oncogene family 4 (RAB4), were increased in subjects with Braak α-synuclein 1-2 compared to controls (table 4), but not in PD compared to controls.

Table 3. Alterations in expression levels of α-synuclein and known interactors of α-synuclein in Braak 1-2 and PD compared to controls.

	Braak α-synuclein 1-2 compared to control		Braak α-synuclein 5-6 compared to control	
Gene name	p-value	Fold change	p-value	Fold change
synaptotagmin II	$8.0*10^{-5}$	1.92	0.14	1.19
synaptophysin	$4.0*10^{-4}$	2.35	0.00	2.05
synapsin 3	0.02	1.45	0.89	1.02
synphilin 1	0.03	-1.19	0.01	-1.20
Complexin 2	0.04	-1.12	$9.0*10^{-4}$	-1.18
Synapsin 2	0.04	1.76	0.41	-1.20
Pra 1	0.13	1.26	0.19	-1.18
Syntaxin 1	0.15	-1.21	0.00	-1.76
GLUr1	0.22	-1.45	0.00	-2.23
Sptbn1	0.27	-1.30	0.03	1.59
Vamp2	0.39	-1.22	0.00	-1.91
Complexin 1	0.52	1.19	0.19	-1.36
Tubulin	0.56	-1.17	$3.0*10^{-3}$	-2.05
VMAT2	0.67	-1.40	0.03	-4.60
Snap25	0.79	1.07	0.03	-1.66
synapsin 1	0.82	-1.08	$3.0*10^{-3}$	-2.43
dynamin 1	0.92	-1.04	0.01	-2.44
α-synuclein	0.67	-1.12	$1.0*10^{-3}$	-2.34

Table 4. Alterations in expression levels of α-synuclein and known interactors of α-synuclein in Braak 1-2 and PD compared to controls.

		Braak α-synuclein 1-2 compared to control		Braak α-synuclein 5-6 compared to control	
Gene	**Gene symbol**	p-value	Fold change	p-value	Fold change
RAB4A, member RAS oncogene family	RAB4A	0.01	1.68	0.49	1.12
RAB5A, member RAS oncogene family	RAB5A	0.02	2.28	0.13	1.51
Ankyrin 2, neuronal	ANK2	0.01	2.11	0.20	1.33
Transferrin	TF	0.003	2.14	0.12	1.31
early endosome antigen 1	EEA1	0.02	1.32	0.07	1.19
early endosome antigen 1	EEA1	0.02	1.32	0.07	1.19

Validation

Correlation between microarray expression and qPCR expression data

We found a significant correlation between the microarray expression and the normalized gene expression calculated using Pfaffl for LAMP2 (r=0.71, p<0.01), GRM3 (r=0.81, p=0.01), FABP7

(r=0.84, p=0.01), HSPA8 (r=0.54, p=0.049), EIF4A2 (r=0.63, p=0.02) and SYPL1 (r=0.61, p=0.02).

In situ hybridization shows expression in glial and neuronal cells
LAMP2 expression is present only in glial cells in PD SN. EIF4A2 showed light expression in dopaminergic neurons in control and iLBD cases, and strong expression in glial cells in iLBD and PD donors. HSPA8 showed strong expression in the dopaminergic neurons in all groups and increased number of positive glial cells in PD cases compared to iLBDs (supplementary figure 3.1).

Discussion

In summary, the transcriptome of post-mortem SN tissue of donors with Braak α-synuclein stages 0 to 6 revealed a consistent deregulation of pathways related to autophagy and protein synthesis, including EIF2 signaling, mTOR signaling and regulation of eIF4 and p70S6K signaling during the progression of PD pathology. When focusing specifically on Braak α-synuclein 1-2 compared to controls, the transcriptome analysis revealed changes in pathways linked to immune response and axonal degeneration, including B cell receptor signaling, protein kinase A signaling and axonal guidance signaling. In addition, in Braak α-synuclein 1-2 stages, we observed a down regulation of clathrin-mediated endocytosis. These data indicate that endocytosis, inflammation and axonal function are compromised in the early stages of PD, prior to the presence of local α-synuclein pathology in the SN (5, 6), whereas EIF2 and mTOR signalling is impaired throughout disease progression in PD. A summary of the main transcriptional events and local pathology in the SN during disease progression in PD is given in figure 3.

In the present study, we used stringent inclusion and exclusion criteria, based on clinical diagnosis and comprehensive pathological assessment, for selecting controls, iLBD subjects and PD donors from a Dutch cohort recruited by the Netherlands Brain Bank and the department of Pathology of the VU University Medical Center. ILBD subjects and PD patients in which the distribution pattern of α-synuclein pathology was atypical at autopsy were excluded as well as donors with concomitant pathologies (5, 43, 44). The donors were matched based on age of death, gender, RIN, and tangle- and amyloid-β pathology. In this way, we were able to form a cohort of control, iLBD and PD donors, in which detected gene expression changes are most likely based on the presence of α-synuclein pathology, and limited variation caused by other factors.

Donors with Braak α-synuclein 1-2 compared to controls displayed a mild loss (~20%) of dopaminergic neurons (10, 38). The largest drop in neuronal loss was observed between Braak stages 3 and 4 and PD donors displayed ~60% loss in neuromelanin-containing neurons compared to controls (38). An increase in reactive microglia has been reported in the SN of end-stage PD patients (45, 46), and human imaging *in vivo* findings confirm that widespread microglial activation is associated with the pathological process in PD (47, 48). Recently, an increase of amoeboid microglial density was also reported in the OB of PD patients (49). These findings suggest that as the disease advances, the number of activated microglia increases in affected brain regions. In this study we have dissected the SN based on surrounding structures in all donors. As the ratio of glial to neuronal cell transcriptome levels is expected to rise with increasing Braak stages, pathway alterations may reflect the difference in composition of the lysate.

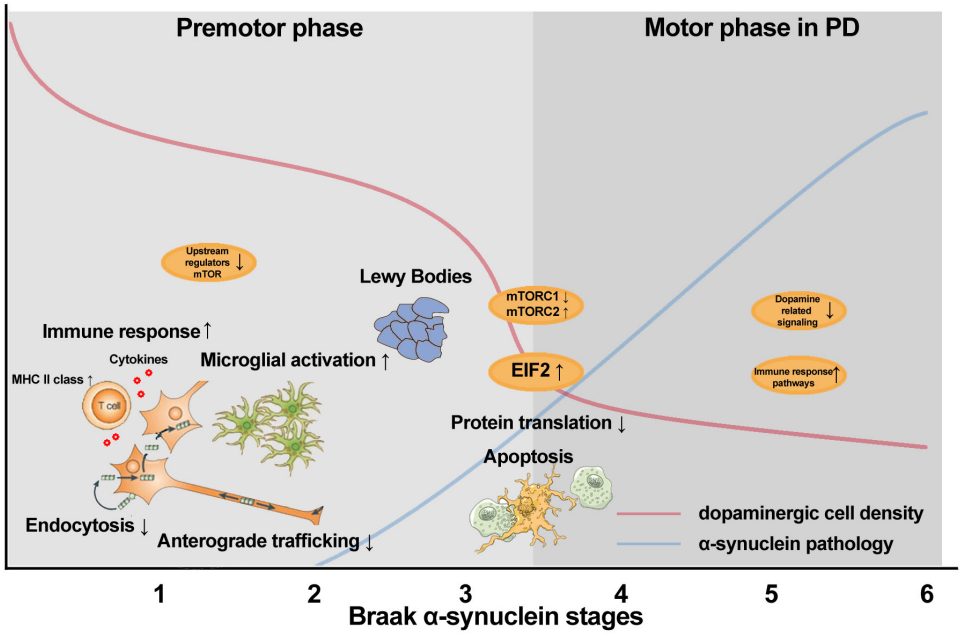

Figure 3. Schematic overview of processes involved in the progression of PD pathology. In Braak α-synuclein 1 and 2, minimal cell loss is observed along with decreased endocytosis and anterograde trafficking, and increased immune response and microglial activation. In addition, we see a down regulation in the upstream regulators in mTOR pathway. In Braak α-synuclein 3 and 4, a steep decline in cell loss and increase in α-synuclein pathology is observed together with indication for disturbed regulation of protein production and apoptosis of the dopaminergic cells. In Braak α-synuclein 5 and 6, cell loss is ~60% and local pathology increases per stage (38) and processes related to dopaminergic signaling and immune response are altered, due to the difference in cellular composition between the groups.

Elstner et al. (32) demonstrated that the differences in tissue processing and data generation can be overcome by focusing on pathway alterations. Here, we observed a large overlap between the pathways deregulated in end-stage PD and previously described datasets by others (19-29, 32), which indicates that the observed changes in gene expression profiles in the SN postmortem tissue are similar to those of other cohorts, even though different microarrays platforms were used. As our groups of controls and PD donors were pathologically and clinically very homogenous, we were also able to identify novel pathways, including signaling by rho family GTPases (BH-FDR=0.00032), RhoGDI Signaling and protein kinase A signaling. We were able to validate our data using qPCR using several probe sets which were present in pathways of interest.

Deregulation of mTOR and EIF2 signaling pathways during disease progression in PD

Several pathways were deregulated in the early pathological stages and remained altered in the later stages of PD in the SN, such as mTOR signaling, EIF2 signaling, and regulation of eIF4 and p70S6K signaling. mTOR and EIF2/EIF4 have previously been linked to PD in post-mortem transcriptome studies (25, 32), and mutations in the translation initiator EIF4G1 have recently been identified in familial PD (50). mTOR consist of two different sub-pathways; 1) the mTOR1 pathway results in the transient shutdown of protein translation through phosphorylation of the α-subunit of eukaryotic translation initiation factor, EIF2, which was up regulated in our dataset.

Rapamycin has been used in clinical trials (51, 52) and inhibits the activity of mTOR1. This results in an induction of autophagy, as demonstrated in a mice model for PD (53); 2) The other sub-pathway, mTOR2, promotes apoptosis and was up regulated in our dataset, suggested that the cells might be degenerating. These pathways are part of a network that relays metabolic signals to adaptive changes in protein translation and gene expression (54, 55), and our results indicate that metabolic change is an early event in the SN in PD. As these pathways are consistently deregulated in our dataset, even before the onset of motor symptoms, they might contain biomarker candidates that may aid in diagnosing PD at an earlier stage. The *in situ* hybridization showed that the expression of an important component in these pathways, EIF4A2, is expressed in neuromelanin containing neurons and glial cells whereas EIF4A2 is mainly expressed in glia at end-stage PD. This indicates that the alterations in mTOR and EIF2 signaling represent alterations in glial and neuronal pathways prior to the formation of aggregates in the SN. Moreover, a recent transcriptome study from Mutez and colleagues showed that deregulation of the EIF2 signaling pathway is evident in samples of peripheral blood mononuclear cells of genetic as well as sporadic PD patients compared age-matched healthy controls (56) providing further evidence for a key role of this pathway in both genetic and sporadic forms of PD.

Involvement of immune response during the progression of PD

Recently, it has been established that mutations in HLA-DR can cause familial PD or increase the risk of developing PD (57). In our dataset, we also observed an up regulation of several HLA genes in the early pathological stages, but not in the later stages. We demonstrated that GM-CSF Signaling, thrombin signaling, B cell receptor signaling, CTLA4 signaling in cytotoxic T lymphocytes and T cell receptor signaling were altered. These findings point towards a key role for deficient immune responses in the early stages of PD, where limited cell loss is present. Alterations in these pathways might be triggered by oxidative stress or abnormal forms of α-synuclein (reviewed in (58)). In later stages 5 and 6, we observed only up regulated B cell receptor signaling. As there is a large decrease in dopaminergic cells in end-stage PD, the up regulation in immune response related pathways might be an effect of the increased glial to neurons ratio observed in the SN tissue during disease progression.

Autophagy and axonal dysfunction in the early stages of PD pathology

In PD, there is an accumulation of autophagosomes, and mitochondria and microtubule-directed traffic might be the main players in the regulation of autophagy in PD (59). In Braak α-synuclein stage 1-2, we observed an up regulation of genes related to endosomes, suggesting accumulation of endosomes, possibly including autophagosomes. In addition, pathways related to endocytosis were deregulated, as a probable protection mechanism against further accumulation of endosomes. LAMP2 is a lysosomal protein and involved in chaperone mediated autophagy (60). We observed an up regulation in LAMP2 expression with increasing Braak stages, which we confirmed using qPCR, and *in situ* hybridization showed that there is a strong expression of LAMP2 in glial cells in PD. These data and the regulation of mTOR in the early stages of PD pathology suggest that autophagy is deregulated in the early pathological stages, and might play a role in α-synuclein aggregation in the SN in elderly. No alterations in mitochondrial dysfunction have been identified in the transcriptome of Braak α-synuclein 1-2 donors, which indicates that mitochondrial dysfunction might be a later event in the pathogenesis of PD.

The most significant deregulated pathways in Braak α-synuclein stages 1-2 are involved in cytoskeleton stability and maintenance. We observed that axonal guidance signaling, actin cytoskeleton signaling and regulation of actin-based motility by Rho are down regulated in the

early stages of PD pathology. This suggests that axonal dysfunction might contribute to the cell death cascade, as limited dopaminergic loss has been observed in these stages (10, 38). Our data confirm that synaptic dysfunction is involved in the pathogenesis of PD (33) and support the "dying-back" hypothesis, which postulates an initial dysfunction at the level of the synapse and/or axonal transport disruption, prior to neuronal loss.

Changes in α-synuclein mRNA levels were subtle, and due to the low levels of endogenous α-synuclein and large biological variability, it might not be possible to observe alterations in transcriptome levels of α-synuclein and its interactors in the early Braak stages in a relatively small sample size. When we focused on PD compared to controls, we observed a significant decline in transcriptome levels of α-synuclein and its interactors such as vesicular monoamine transporter 2 (VMAT2), synapsin 1, dynamin1 and tubulin, which is in line with other studies (33). An explanation for the axonal dysfunction might be that the misfolded state of α-synuclein disrupts anterograde transport of proteins to the synapse (61, 62). We observed a decrease in the anterograde transporters (KHC and KLC) in Braak α-synuclein 1- 2, whereas in advanced PD (Braak α-synuclein 5-6) dynein, a retrograde transporter, was affected. We were able to find similar changes in axonal transport motor proteins as Chu et al. (63), who investigated known axonal transport proteins, such as kinesins and dynein, in a rat model for over expression of α-synuclein. This may implicate that even though mRNA levels of α-synuclein are not changing in Braak α-synuclein 1-2 compared to controls, the transport of α-synuclein to the synapse might be disturbed.

To summarize, the deregulated pathways indicate that axonal guidance signaling is compromised. No alterations in mRNA levels of α-synuclein and its interactors were observed in Braak stages 1-2, but a disturbance in anterograde trafficking might result in reduced synaptic functioning.

To conclude, transcriptome analysis revealed that mTOR and EIF2 signaling are deregulated in the SN throughout the progression of PD pathology. Prior to the presence of α-synuclein aggregates, molecular mechanisms involved in axonal dysfunction, immune response and disturbed endocytosis may play a role in the neuronal cell death and the formation of protein aggregates in PD. Specific elements of these pathways and cellular processes may hold the key to altering the disease progression in PD.

Acknowledgments

We thank the Netherlands Brain Bank (Amsterdam, the Netherlands), especially Michiel Kooreman and Inge Huitinga, for providing excellent post-mortem human brain tissue, and Wouter Kamphorst for neuropathological evaluation of the donors. We are grateful to all patients and controls that donated their brains.

Funding

This work was funded by Prinses Beatrix Spierfonds and International Parkinson fonds (IPF).

References

1. Greffard S, Verny M, Bonnet AM, et al. Motor score of the Unified Parkinson Disease Rating Scale as a good predictor of Lewy body-associated neuronal loss in the substantia nigra. Arch Neurol 2006 Apr;63:584-588.
2. Spillantini MG, Schmidt ML, Lee VM, Trojanowski JQ, Jakes R, Goedert M. Alpha-synuclein in Lewy bodies. Nature 1997 Aug 28;388:839-840.
3. Alafuzoff I, Ince PG, Arzberger T, et al. Staging/typing of Lewy body related alpha-synuclein pathology: a study of the BrainNet Europe Consortium. Acta Neuropathol 2009 Jun;117:635-652.
4. Braak H, Braak E. Neuropathological stageing of Alzheimer-related changes. Acta Neuropathol 1991;82:239-259.
5. Braak H, Del Tredici K, Rub U, De Vos RA, Jansen Steur EN, Braak E. Staging of brain pathology related to sporadic Parkinson's disease. Neurobiol Aging 2003 Mar;24:197-211.
6. Braak H, Bohl JR, Muller CM, Rub U, De Vos RA, Del Tredici K. Stanley Fahn Lecture 2005: The staging procedure for the inclusion body pathology associated with sporadic Parkinson's disease reconsidered. Mov Disord 2006 Dec;21:2042-2051.
7. Wolters EC, Braak H. Parkinson's disease: premotor clinico-pathological correlations. J Neural Transm Suppl 2006;309-319.
8. Hawkes CH, Del Tredici K, Braak H. A timeline for Parkinson's disease. Parkinsonism Relat Disord 2010 Feb;16:79-84.
9. DelleDonne A, Klos KJ, Fujishiro H, et al. Incidental Lewy body disease and preclinical Parkinson disease. Arch Neurol 2008 Aug;65:1074-1080.
10. Milber JM, Noorigian JV, Morley JF, et al. Lewy pathology is not the first sign of degeneration in vulnerable neurons in Parkinson disease. Neurology 2012 Nov 14.
11. Dickson DW, Uchikado H, Fujishiro H, Tsuboi Y. Evidence in favor of Braak staging of Parkinson's disease. Mov Disord 2010;25 Suppl 1:S78-S82.
12. Halliday GM, McCann H. Human-based studies on alpha-synuclein deposition and relationship to Parkinson's disease symptoms. Exp Neurol 2008 Jan;209:12-21.
13. Kingsbury AE, Bandopadhyay R, Silveira-Moriyama L, et al. Brain stem pathology in Parkinson's disease: an evaluation of the Braak staging model. Mov Disord 2010 Nov 15;25:2508-2515.
14. Zaccai J, Brayne C, McKeith I, Matthews F, Ince PG. Patterns and stages of alpha-synucleinopathy: Relevance in a population-based cohort. Neurology 2008 Mar 25;70:1042-1048.
15. Sundal C, Fujioka S, Uitti RJ, Wszolek ZK. Autosomal dominant Parkinson's disease. Parkinsonism Relat Disord 2012 Jan;18 Suppl 1:S7-10.
16. Simon-Sanchez J, van Hilten JJ, van de WB, et al. Genome-wide association study confirms extant PD risk loci among the Dutch. Eur J Hum Genet 2011 Jun;19:655-661.
17. Hamza TH, Zabetian CP, Tenesa A, et al. Common genetic variation in the HLA region is associated with late-onset sporadic Parkinson's disease. Nat Genet 2010 Sep;42:781-785.
18. Rochet JC, Hay BA, Guo M. Molecular insights into Parkinson's disease. Prog Mol Biol Transl Sci 2012;107:125-188.
19. Bossers K, Meerhoff G, Balesar R, et al. Analysis of gene expression in Parkinson's disease: possible involvement of neurotrophic support and axon guidance in dopaminergic cell death. Brain Pathol 2009 Jan;19:91-107.
20. Cantuti-Castelvetri I, Keller-McGandy C, Bouzou B, et al. Effects of gender on nigral gene expression and parkinson

disease. Neurobiol Dis 2007 Jun;26:606-614.
21. Grunblatt E, Mandel S, Jacob-Hirsch J, et al. Gene expression profiling of parkinsonian substantia nigra pars compacta; alterations in ubiquitin-proteasome, heat shock protein, iron and oxidative stress regulated proteins, cell adhesion/cellular matrix and vesicle trafficking genes. J Neural Transm 2004 Dec;111:1543-1573.
22. Hauser MA, Li YJ, Xu H, et al. Expression profiling of substantia nigra in Parkinson disease, progressive supranuclear palsy, and frontotemporal dementia with parkinsonism. Arch Neurol 2005 Jun;62:917-921.
23. Miller RM, Kiser GL, Kaysser-Kranich TM, Lockner RJ, Palaniappan C, Federoff HJ. Robust dysregulation of gene expression in substantia nigra and striatum in Parkinson's disease. Neurobiol Dis 2006 Feb;21:305-313.
24. Moran LB, Duke DC, Deprez M, Dexter DT, Pearce RK, Graeber MB. Whole genome expression profiling of the medial and lateral substantia nigra in Parkinson's disease. Neurogenetics 2006 Mar;7:1-11.
25. Simunovic F, Yi M, Wang Y, et al. Gene expression profiling of substantia nigra dopamine neurons: further insights into Parkinson's disease pathology. Brain 2009 Jul;132:1795-1809.
26. Sutherland GT, Matigian NA, Chalk AM, et al. A cross-study transcriptional analysis of Parkinson's disease. PLoS One 2009;4:e4955.
27. Vogt IR, Lees AJ, Evert BO, Klockgether T, Bonin M, Wullner U. Transcriptional changes in multiple system atrophy and Parkinson's disease putamen. Exp Neurol 2006 Jun;199:465-478.
28. Zhang Y, James M, Middleton FA, Davis RL. Transcriptional analysis of multiple brain regions in Parkinson's disease supports the involvement of specific protein processing, energy metabolism, and signaling pathways, and suggests novel disease mechanisms. Am J Med Genet B Neuropsychiatr Genet 2005 Aug 5;137B:5-16.
29. Duke DC, Moran LB, Pearce RK, Graeber MB. The medial and lateral substantia nigra in Parkinson's disease: mRNA profiles associated with higher brain tissue vulnerability. Neurogenetics 2007 Apr;8:83-94.
30. Botta-Orfila T, Sanchez-Pla A, Fernandez M, Carmona F, Ezquerra M, Tolosa E. Brain transcriptomic profiling in idiopathic and LRRK2-associated Parkinson's disease. Brain Res 2012 Jul 23;1466:152-157.
31. Botta-Orfila T, Tolosa E, Gelpi E, et al. Microarray expression analysis in idiopathic and LRRK2-associated Parkinson's disease. Neurobiol Dis 2012 Jan;45:462-468.
32. Elstner M, Morris CM, Heim K, et al. Expression analysis of dopaminergic neurons in Parkinson's disease and aging links transcriptional dysregulation of energy metabolism to cell death. Acta Neuropathol 2011 Jul;122:75-86.
33. Pienaar IS, Burn D, Morris C, Dexter D. Synaptic protein alterations in Parkinson's disease. Mol Neurobiol 2012 Feb;45:126-143.
34. Exner N, Lutz AK, Haass C, Winklhofer KF. Mitochondrial dysfunction in Parkinson's disease: molecular mechanisms and pathophysiological consequences. EMBO J 2012 Jul 18;31:3038-3062.
35. Alafuzoff I, Arzberger T, Al-Sarraj S, et al. Staging of neurofibrillary pathology in Alzheimer's disease: a study of the BrainNet Europe Consortium. Brain Pathol 2008 Oct;18:484-496.
36. Alafuzoff I, Thal DR, Arzberger T, et al. Assessment of beta-amyloid deposits in human brain: a study of the BrainNet Europe Consortium. Acta Neuropathol 2009 Mar;117:309-320.
37. Schmitz C, Hof PR. Design-based stereology in neuroscience. Neuroscience

2005;130:813-831.
38. Dijkstra AA, Voorn P, Berendse HW, et al. Stage-dependent nigral neuronal loss in incidental Lewy body and Parkinson's disease. 2014.
39. Edgar R, Domrachev M, Lash AE. Gene Expression Omnibus: NCBI gene expression and hybridization array data repository. Nucleic Acids Res 2002 Jan 1;30:207-210.
40. Benjamini Y, Hochberg Y. Controlling the false discovery rate: a practical and powerful approach to multiple testing., 1 ed Journal of the Royal Statistical Society, 1995:289-300.
41. Pfaffl MW. A new mathematical model for relative quantification in real-time RT-PCR. Nucleic Acids Res 2001 May 1;29:e45.
42. Lesnick TG, Papapetropoulos S, Mash DC, et al. A genomic pathway approach to a complex disease: axon guidance and Parkinson disease. PLoS Genet 2007 Jun;3:e98.
43. Jellinger KA. A critical evaluation of current staging of alpha-synuclein pathology in Lewy body disorders. Biochim Biophys Acta 2009 Jul;1792:730-740.
44. Frigerio R, Fujishiro H, Ahn TB, et al. Incidental Lewy body disease: do some cases represent a preclinical stage of dementia with Lewy bodies? Neurobiol Aging 2011 May;32:857-863.
45. McGeer PL, Itagaki S, Boyes BE, McGeer EG. Reactive microglia are positive for HLA-DR in the substantia nigra of Parkinson's and Alzheimer's disease brains. Neurology 1988 Aug;38:1285-1291.
46. Mogi M, Harada M, Kondo T, et al. Interleukin-1 beta, interleukin-6, epidermal growth factor and transforming growth factor-alpha are elevated in the brain from parkinsonian patients. Neurosci Lett 1994 Oct 24;180:147-150.
47. Gerhard A, Pavese N, Hotton G, et al. In vivo imaging of microglial activation with [11C](R)-PK11195 PET in idiopathic Parkinson's disease. Neurobiol Dis 2006 Feb;21:404-412.
48. Ouchi Y, Yagi S, Yokokura M, Sakamoto M. Neuroinflammation in the living brain of Parkinson's disease. Parkinsonism Relat Disord 2009 Dec;15 Suppl 3:S200-S204.
49. Doorn KJ, Goudriaan A, Blits-Huizinga C, et al. Increased Amoeboid Microglial Density in the Olfactory Bulb of Parkinson's and Alzheimer's Patients. Brain Pathol 2013 Aug 23.
50. Chartier-Harlin MC, Dachsel JC, Vilarino-Guell C, et al. Translation initiator EIF4G1 mutations in familial Parkinson disease. Am J Hum Genet 2011 Sep 9;89:398-406.
51. Rodriguez AE, Palacios I, Rodriguez-Granillo AM, et al. Comparison of cost-effectiveness of oral rapamycin plus bare-metal stents versus first generation of drug-eluting stents (from the Randomized Oral Rapamycin in Argentina [ORAR] 3 trial). Am J Cardiol 2014 Mar 1;113:815-821.
52. Liesveld JL, O'Dwyer K, Walker A, et al. A phase I study of decitabine and rapamycin in relapsed/refractory AML. Leuk Res 2013 Dec;37:1622-1627.
53. Liu K, Shi N, Sun Y, Zhang T, Sun X. Therapeutic effects of rapamycin on MPTP-induced Parkinsonism in mice. Neurochem Res 2013 Jan;38:201-207.
54. Bishop NA, Lu T, Yankner BA. Neural mechanisms of ageing and cognitive decline. Nature 2010 Mar 25;464:529-535.
55. Hock MB, Kralli A. Transcriptional control of mitochondrial biogenesis and function. Annu Rev Physiol 2009;71:177-203.
56. Mutez E, Nkiliza A, Belarbi K, et al. Involvement of the immune system, endocytosis and EIF2 signaling in both genetically determined and sporadic forms of Parkinson's disease. Neurobiol Dis 2014 Mar;63:165-170.
57. Hamza TH, Zabetian CP, Tenesa A, et al. Common genetic variation in the HLA

region is associated with late-onset sporadic Parkinson's disease. Nat Genet 2010 Sep;42:781-785.
58. Hirsch EC, Hunot S. Neuroinflammation in Parkinson's disease: a target for neuroprotection? Lancet Neurol 2009 Apr;8:382-397.
59. Arduino DM, Esteves AR, Cardoso SM. Mitochondria drive autophagy pathology via microtubule disassembly: a new hypothesis for Parkinson disease. Autophagy 2013 Jan;9:112-114.
60. Orenstein SJ, Kuo SH, Tasset I, et al. Interplay of LRRK2 with chaperone-mediated autophagy. Nat Neurosci 2013 Apr;16:394-406.
61. Saha AR, Hill J, Utton MA, et al. Parkinson's disease alpha-synuclein mutations exhibit defective axonal transport in cultured neurons. J Cell Sci 2004 Mar 1;117:1017-1024.
62. Yang ML, Hasadsri L, Woods WS, George JM. Dynamic transport and localization of alpha-synuclein in primary hippocampal neurons. Mol Neurodegener 2010;5:9.
63. Chu Y, Morfini GA, Langhamer LB, He Y, Brady ST, Kordower JH. Alterations in axonal transport motor proteins in sporadic and experimental Parkinson's disease. Brain 2012 Jul;135:2058-2073.

Supplementary data

Supplementary table 3.1. Detailed clinical and pathological characteristics of donors included in the study.

NBB	Clinical diagnosis	Pathological diagnosis	Braak stage (T,A,S)	Gender (M/F)	Age (years)	PMD (hrs)	pH of CSF	RIN	qPCR
2000-031	Control	Control	2,b,0	F	77	9:15	n/a	8.1	*
2006-037	Control	Control	0,0,0	M	66	7:45	6.70	7.4	*
2000-032	Control	Control	1,a,0	F	78	6:30	7.02	7.9	
2003-002	Control	Control	1,0,0	M	60	7:44	n/a	6.5	*
1990-038	Control	Control	0,-,0	F	83	8:00	6.37	6.0	
VUPATH C	Control	Control	1,0,0	M	81	<10:00	n/a	7.2	*
2007-082	Control	Control	2,0,0	M	81	7:55	6.23	7.0	
1996-084	Control	Control	2,0,0	F	78	7:30	6.60	6.5	
2007-056	Control	iLBD	2,b,2	M	79	9:00	6.15	7.1	
2001-033	Control	iLBD	1,c,4	M	75	6:20	6.18	6.3	*
2001-069	Control	iLBD	1,a,1	F	68	5:45	6.97	5.8	
2002-012	Control	iLBD	1,a,4	M	87	4:45	7.60	7.5	*
2004-033	Control	iLBD	1,0,3	F	82	7:00	6.66	7.9	*
2005-049	Control	iLBD	2,-,2	F	86	6:25	6.39	6.8	*
2005-063	Control	iLBD	2,0,3	F	93	4:00	6.64	6.3	*
2006-008	Delirant	iLBD	2,a,1	F	85	4:40	6.71	6.6	
2009-056	PD	PD	1,0,4	M	74	10:48	n/a	6.2	
2009-095	Control	iLBD	1,a,3	F	71	7:40	6.31	7.7	
2010-013	Control	ILBD	0,0,3	M	70	6:15	6.45	7.5	
VUPATH IC1	Control	iLBD	0,0,1	M	79	<10:00	n/a	7.2	
2004-080	PD	PD	1,a,6	M	71	5:50	6.27	6.9	
2006-030	PD	PDDEM	1,c,5	F	80	5:15	6.31	7.8	*
2006-040	PDDEM	PDDEM	0,0,5	F	81	6:05	6.38	6.9	*
2006-002	PD	PD	2,b,5	F	84	7:25	6.85	7.8	
2007-031	PD	PD	1,0,6	M	61	7:35	6.98	7.2	*
2008-080	PD	PD	1,b,6	M	80	6:35	6.15	7.2	
2005-045	PDDEM	PDDEM	2,b,6	F	87	5:25	6.44	7.8	
2008-089	PD	PDDEM	1,0,6	M	84	9:00	6.66	7.2	*

T=tangle; A=amyloid beta; S=alpha-synuclein; M/F=male/female; CSF=cerebrospinal fluid; NBB=Netherlands Brain Bank; SVU=Departement of pathology VU; NDC=non-demented control; PD=Parkinson's disease; iLBD=incidental Lewy body disease; PDDEM=Parkinson with dementia. *= included in qPCR validation;n/a not available.

Supplementary table 3.2. Targets for qPCR and the properties of the created primers

Gene name	Affymetrix probe ID	Accession number	Primer sequence	Tm °C	UPL probe number	Amplicon length
LAMP2	203041_s_at	NM_002294.2	fwd: AAT-GTG-ACA-CAA-GGA-AAG-TAT-TCT-AC	58	24	122
			rev: ATA-AGC-CAG-CAA-CAC-TAG-AAT			
GRM3	205814_s_at	NM_000840.2	fwd: ACA-TAC-TCT-CAG-TCC-TCT-GC	60	77	97
			rev: GCA-ATT-CAC-AAT-CAC-AGA-GAT-GA			
FABP7	205029_s_at	NM_001446.3	fwd: CTC-TCA-GCA-CAT-TCA-AGA-ACA-C	60	7	198
			rev: CCA-TCC-AGG-CTA-ACA-ACA-GA			
SYPL1	201259_s_at	NM_006754.3	fwd: TAT-TGA-TGA-ACT-TCC-GCC-TTG-TA	56	21	117
			rev: CCA-GAG-TAT-CAT-ATT-TAG-AAA-GCC-A			
EIF4A2	200912_s_at	NM_001967.3	fwd: ATA TTC ACA GAA TTG GCA GAG GG	57	25	158
			rev: GGA ATT AAA TAA GGT CAG CCA CAT T			
HSPA8	210338_s_at	NM_006597.3	fwd: CAACCCTGATGAAGCTGTTG	60	46	101
			rev: GTGACATCCAAGAGCAGCAA			
RPL27	200025_s_at	NM_000988.3	fwd: CAA-TCA-CCT-AAT-GCC-CAC-AAG	60	15	129
			rev: CTT-CAA-ACT-TGA-CCT-TGG-CC			
RPS13	200018_at	NM_001017	fwd: CAC-TTG-GTT-GAA-GTT-GAC-ATC-T	57	68	111
			rev: CTT-GTG-CAA-CAC-CAT-GTG-AAT			

Supplementary table 3.3. Primers for *in situ* hybridization. Hybridization temperature for all primers was 60°C

Gene name	Affymetrix probe ID	Primer sequence	probelengts (BP)
LAMP2	203041_s_at	T3: aat taa ccc tca cta aag gAA TGT GAC ACA AGG AAA GTA TTC TAC AG	474
		T7: taa tac gac tca cta tag gAA GGC ATA CTT CAA GGT TAG GAT CAA A	
EIF4A2	1555996_s_at	T3: aat taa ccc tca cta aag gTC GCG GGA TTG ATG TGC AA	472
		T7: taa tac gac tca cta tag gGA AAG AAA GAT TTT ACA GAC CCC AT	
HSPA8	210338_s_at	T3: aat taa ccc tca cta aag gCA CTC CTC TTT CCC TTG GTA T	557
		T7: taa tac gac tca cta tag gCA AGC CAG TTG ATA ATT TCA TTA CAC	

Supplementary table 3.4. Genes with altered expression level in the SN of PD donors compared to controls (BH-FDR<0.05, Fold change ±1.50)

Probeset ID	Gene Title	Gene Symbol	p-value	Fold change
204006_s_at	Fc fragment of IgG, low affinity IIIa, receptor (CD16a) /// Fc fragment of IgG,	FCGR3A /// FCGR3B	$1.89*10^{-3}$	4.35
200800_s_at	heat shock 70kDa protein 1A /// heat shock 70kDa protein 1B	HSPA1A /// HSPA1B	$1.74*10^{-3}$	3.38
231029_at	coagulation factor V (proaccelerin, labile factor)	F5	$9.51*10^{-4}$	2.90
228143_at	ceruloplasmin (ferroxidase)	CP	$4.22*10^{-4}$	2.82
1569854_at	---	---	$9.98*10^{-4}$	2.79
201617_x_at	caldesmon 1	CALD1	$1.01*10^{-3}$	2.73
209301_at	carbonic anhydrase II	CA2	$2.92*10^{-5}$	2.72
204472_at	GTP binding protein overexpressed in skeletal muscle	GEM	$1.01*10^{-3}$	2.70
231513_at	---	---	$4.86*10^{-4}$	2.67
206898_at	cadherin 19, type 2	CDH19	$2.61*10^{-4}$	2.62
215071_s_at	histone cluster 1, H2ac	HIST1H2AC	$2.87*10^{-5}$	2.62
211571_s_at	versican	VCAN	$7.05*10^{-4}$	2.62
213156_at	---	---	$2.14*10^{-4}$	2.61
1552619_a_at	anillin, actin binding protein	ANLN	$4.71*10^{-5}$	2.56
221210_s_at	N-acetylneuraminate pyruvate lyase (dihydrodipicolinate synthase)	NPL	$4.01*10^{-6}$	2.56
215646_s_at	versican	VCAN	$1.31*10^{-3}$	2.55
1557481_a_at	chromosome 21 open reading frame 131	C21orf131	$1.50*10^{-4}$	2.54
201718_s_at	erythrocyte membrane protein band 4.1-like 2	EPB41L2	$2.27*10^{-3}$	2.51
238735_at	---	---	$1.36*10^{-4}$	2.46
204719_at	ATP-binding cassette, sub-family A (ABC1), member 8	ABCA8	$1.76*10^{-4}$	2.43
203041_s_at	lysosomal-associated membrane protein 2	LAMP2	$5.29*10^{-7}$	2.42
205934_at	phospholipase C-like 1	PLCL1	$1.63*10^{-6}$	2.40
232297_at	---	---	$5.57*10^{-4}$	2.40
1558111_at	muscleblind-like (Drosophila)	MBNL1	$1.25*10^{-3}$	2.38
1553027_a_at	kelch-like 4 (Drosophila)	KLHL4	$2.44*10^{-4}$	2.34
212546_s_at	FRY-like	FRYL	$2.84*10^{-6}$	2.34
227921_at	---	---	$8.53*10^{-5}$	2.33
208358_s_at	UDP glycosyltransferase 8	UGT8	$1.41*10^{-3}$	2.32
205609_at	angiopoietin 1	ANGPT1	$1.04*10^{-3}$	2.30
219728_at	myotilin	MYOT	$7.30*10^{-4}$	2.29
226498_at	fms-related tyrosine kinase 1 (vascular endothelial growth factor/ vascular perme	FLT1	$3.44*10^{-4}$	2.29
226094_at	phosphoinositide-3-kinase, class 2, alpha polypeptide	PIK3C2A	$1.67*10^{-3}$	2.28
228956_at	UDP glycosyltransferase 8	UGT8	$1.75*10^{-4}$	2.27
218566_s_at	cysteine and histidine-rich domain (CHORD)-containing 1	CHORDC1	$1.12*10^{-3}$	2.26
203042_at	lysosomal-associated membrane protein 2	LAMP2	$4.68*10^{-5}$	2.23
1568812_at	---	---	$3.58*10^{-4}$	2.22
217487_x_at	folate hydrolase (prostate-specific membrane antigen) 1	FOLH1	$1.53*10^{-3}$	2.20
212177_at	splicing factor, arginine/serine-rich 18	SFRS18	$7.16*10^{-4}$	2.19
1553613_s_at	forkhead box C1	FOXC1	$1.19*10^{-3}$	2.19
1554260_a_at	FRY-like	FRYL	$2.28*10^{-4}$	2.19
213418_at	heat shock 70kDa protein 6 (HSP70B')	HSPA6	$8.76*10^{-4}$	2.18
207238_s_at	protein tyrosine phosphatase, receptor type, C	PTPRC	$9.77*10^{-4}$	2.17
206100_at	carboxypeptidase M	CPM	$9.54*10^{-4}$	2.15
230741_at	---	---	$3.02*10^{-4}$	2.14
1553142_at	chromosome 13 open reading frame 31	C13orf31	$1.92*10^{-3}$	2.13
209576_at	guanine nucleotide binding protein (G protein), alpha inhibiting activity polype	GNAI1	$1.05*10^{-4}$	2.13
222473_s_at	erbb2 interacting protein	ERBB2IP	$3.71*10^{-5}$	2.12
205923_at	reelin	RELN	$1.01*10^{-3}$	2.12
226002_at	GRB2-associated binding protein 1	GAB1	$6.87*10^{-6}$	2.11
204036_at	lysophosphatidic acid receptor 1	LPAR1	$1.74*10^{-4}$	2.10
203553_s_at	mitogen-activated protein kinase kinase kinase kinase 5	MAP4K5	$8.94*10^{-5}$	2.10
230589_at	---	---	$1.28*10^{-4}$	2.10
204774_at	ecotropic viral integration site 2A	EVI2A	$7.82*10^{-5}$	2.09
207112_s_at	GRB2-associated binding protein 1	GAB1	$6.28*10^{-4}$	2.09
217985_s_at	bromodomain adjacent to zinc finger domain, 1A	BAZ1A	$1.75*10^{-3}$	2.09
201843_s_at	EGF-containing fibulin-like extracellular matrix protein 1	EFEMP1	$1.55*10^{-4}$	2.09
220026_at	chloride channel accessory 4	CLCA4	$8.66*10^{-4}$	2.08
233655_s_at	HAUS augmin-like complex, subunit 6	HAUS6	$1.08*10^{-4}$	2.08
1559776_at	---	---	$8.14*10^{-6}$	2.08
205105_at	mannosidase, alpha, class 2A, member 1	MAN2A1	$8.05*10^{-5}$	2.06
216920_s_at	TCR gamma alternate reading frame protein ///T cell receptor gamma constant 2	TARP ///TRGC2	$1.23*10^{-3}$	2.06
243940_at	teashirt zinc finger homeobox 2	TSHZ2	$6.46*10^{-4}$	2.05
201259_s_at	synaptophysin-like 1	SYPL1	$4.33*10^{-4}$	2.05
209257_s_at	structural maintenance of chromosomes 3	SMC3	$1.67*10^{-3}$	2.04
213385_at	chimerin (chimaerin) 2	CHN2	$1.15*10^{-4}$	2.04
208925_at	claudin domain containing 1	CLDND1	$3.24*10^{-4}$	2.04
1553530_a_at	integrin, beta 1 (fibronectin receptor, beta polypeptide, antigen CD29 includes	ITGB1	$1.22*10^{-3}$	2.03
213397_x_at	ribonuclease, RNase A family, 4	RNASE4	$1.18*10^{-3}$	2.03
218706_s_at	GRAM domain containing 3	GRAMD3	$1.60*10^{-3}$	2.03
219882_at	tubulin tyrosine ligase-like family, member 7	TTLL7	$7.99*10^{-4}$	2.03
223343_at	membrane-spanning 4-domains, subfamily A, member 7	MS4A7	$2.18*10^{-3}$	2.03
218340_s_at	ubiquitin-like modifier activating enzyme 6	UBA6	$1.38*10^{-3}$	2.02
206135_at	suppression of tumorigenicity 18 (breast carcinoma) (zinc finger protein)	ST18	$5.30*10^{-4}$	2.02
222608_s_at	anillin, actin binding protein	ANLN	$3.56*10^{-5}$	2.02
1555564_a_at	complement factor I	CFI	$7.35*10^{-4}$	2.02
1558233_s_at	activating transcription factor 1	ATF1	$7.30*10^{-4}$	2.02
201858_s_at	serglycin	SRGN	$1.51*10^{-3}$	2.02
232523_at	multiple EGF-like-domains 10	MEGF10	$8.12*10^{-7}$	2.02
221895_at	motile sperm domain containing 2	MOSPD2	$2.14*10^{-4}$	2.01
205158_at	ribonuclease, RNase A family, 4	RNASE4	$5.72*10^{-5}$	1.99

Probeset ID	Gene Title	Gene Symbol	p-value	Fold change
205608_s_at	angiopoietin 1	ANGPT1	$1.18*10^{-3}$	1.99
236517_at	multiple EGF-like-domains 10	MEGF10	$2.61*10^{-4}$	1.98
204037_at	lysophosphatidic acid receptor 1	LPAR1	$8.41*10^{-4}$	1.98
212397_at	radixin	RDX	$7.62*10^{-7}$	1.98
235465_at	family with sequence similarity 123A	FAM123A	$7.10*10^{-4}$	1.98
230206_at	Dedicator of cytokinesis 5	DOCK5	$4.75*10^{-4}$	1.98
1552275_s_at	PX domain containing serine/threonine kinase	PXK	$1.07*10^{-3}$	1.97
206245_s_at	influenza virus NS1A binding protein	IVNS1ABP	$1.82*10^{-5}$	1.97
212263_at	quaking homolog, KH domain RNA binding (mouse)	QKI	$6.92*10^{-5}$	1.97
1555807_a_at	myelin oligodendrocyte glycoprotein	MOG	$1.69*10^{-3}$	1.97
203300_x_at	adaptor-related protein complex 1, sigma 2 subunit	AP1S2	$1.18*10^{-3}$	1.96
213362_at	protein tyrosine phosphatase, receptor type, D	PTPRD	$9.53*10^{-4}$	1.96
203481_at	family with sequence similarity 178, member A	FAM178A	$1.95*10^{-5}$	1.96
210839_s_at	ectonucleotide pyrophosphatase/phosphodiesterase 2	ENPP2	$1.17*10^{-4}$	1.96
202514_at	discs, large homolog 1 (Drosophila)	DLG1	$5.33*10^{-4}$	1.96
220892_s_at	phosphoserine aminotransferase 1	PSAT1	$1.64*10^{-3}$	1.95
1556658_a_at	---	---	$1.17*10^{-3}$	1.95
201426_s_at	vimentin	VIM	$1.40*10^{-3}$	1.95
201752_s_at	adducin 3 (gamma)	ADD3	$2.23*10^{-3}$	1.95
225998_at	GRB2-associated binding protein 1	GAB1	$3.22*10^{-5}$	1.95
226844_at	MOB1, Mps One Binder kinase activator-like 2B (yeast)	MOBKL2B	$1.17*10^{-4}$	1.95
233609_at	Protein tyrosine phosphatase, receptor type, K	PTPRK	$1.80*10^{-4}$	1.95
201146_at	nuclear factor (erythroid-derived 2)-like 2	NFE2L2	$2.04*10^{-6}$	1.94
225406_at	twisted gastrulation homolog 1 (Drosophila)	TWSG1	$9.25*10^{-6}$	1.94
228937_at	chromosome 13 open reading frame 31	C13orf31	$2.35*10^{-3}$	1.94
221646_s_at	zinc finger, DHHC-type containing 11	ZDHHC11	$1.10*10^{-3}$	1.93
205814_at	glutamate receptor, metabotropic 3	GRM3	$8.54*10^{-5}$	1.93
201399_s_at	translocation associated membrane protein 1	TRAM1	$1.40*10^{-3}$	1.93
203824_at	tetraspanin 8	TSPAN8	$4.52*10^{-4}$	1.92
201847_at	lipase A, lysosomal acid, cholesterol esterase	LIPA	$1.68*10^{-5}$	1.92
205404_at	hydroxysteroid (11-beta) dehydrogenase 1	HSD11B1	$9.93*10^{-4}$	1.92
226109_at	chromosome 21 open reading frame 91	C21orf91	$1.94*10^{-3}$	1.92
204620_s_at	versican	VCAN	$6.18*10^{-5}$	1.92
206011_at	caspase 1, apoptosis-related cysteine peptidase (interleukin 1, beta, convertase	CASP1	$2.21*10^{-3}$	1.92
208442_s_at	ataxia telangiectasia mutated	ATM	$3.93*10^{-4}$	1.92
202604_x_at	ADAM metallopeptidase domain 10	ADAM10	$1.28*10^{-3}$	1.91
226250_at	---	---	$1.46*10^{-4}$	1.91
201842_s_at	EGF-containing fibulin-like extracellular matrix protein 1	EFEMP1	$4.99*10^{-4}$	1.91
212036_s_at	pinin, desmosome associated protein	PNN	$1.55*10^{-6}$	1.91
1567214_a_at	pinin, desmosome associated protein	PNN	$1.22*10^{-4}$	1.91
206030_at	aspartoacylase (Canavan disease)	ASPA	$7.56*10^{-5}$	1.91
228190_at	ATG4 autophagy related 4 homolog C (S. cerevisiae) /// Ctr9, Paf1/RNA polymerase	ATG4C /// CTR9	$5.31*10^{-5}$	1.91
201024_x_at	eukaryotic translation initiation factor 5B	EIF5B	$2.10*10^{-3}$	1.91
241681_at	---	---	$1.56*10^{-3}$	1.90
215806_x_at	TCR gamma alternate reading frame protein /// T cell receptor gamma constant 2	TARP /// TRGC2	$1.00*10^{-3}$	1.90
227620_at	solute carrier family 44, member 1	SLC44A1	$1.97*10^{-4}$	1.90
232896_at	Erbb2 interacting protein	ERBB2IP	$8.10*10^{-4}$	1.90
231098_at	---	---	$1.58*10^{-3}$	1.90
220924_s_at	solute carrier family 38, member 2	SLC38A2	$3.00*10^{-4}$	1.90
204160_s_at	ectonucleotide pyrophosphatase/phosphodiesterase 4 (putative function)	ENPP4	$6.19*10^{-5}$	1.90
213182_x_at	cyclin-dependent kinase inhibitor 1C (p57, Kip2)	CDKN1C	$9.51*10^{-4}$	1.89
241859_at	phospholipase C-like 1	PLCL1	$7.09*10^{-4}$	1.89
218614_at	chromosome 12 open reading frame 35	C12orf35	$4.95*10^{-6}$	1.88
221760_at	Mannosidase, alpha, class 1A, member 1	MAN1A1	$6.10*10^{-4}$	1.88
227481_at	CNKSR family member 3	CNKSR3	$1.31*10^{-4}$	1.88
202663_at	WAS/WASL interacting protein family, member 1	WIPF1	$7.92*10^{-4}$	1.87
213605_s_at	hypothetical LOC100272216 /// hypothetical protein LOC100292101	LOC100272216 /// LOC100292101	$1.63*10^{-3}$	1.87
209529_at	phosphatidic acid phosphatase type 2C	PPAP2C	$1.26*10^{-3}$	1.87
1556283_s_at	FGFR1 oncogene partner 2	FGFR1OP2	$1.70*10^{-5}$	1.87
209290_s_at	nuclear factor I/B	NFIB	$5.57*10^{-4}$	1.87
238558_at	---	---	$4.01*10^{-5}$	1.86
205669_at	neural cell adhesion molecule 2	NCAM2	$4.27*10^{-5}$	1.86
227565_at	---	---	$1.51*10^{-3}$	1.86
227121_at	---	---	$1.28*10^{-3}$	1.86
210588_x_at	heterogeneous nuclear ribonucleoprotein H3 (2H9)	HNRNPH3	$4.32*10^{-7}$	1.86
224358_s_at	membrane-spanning 4-domains, subfamily A, member 7	MS4A7	$2.41*10^{-3}$	1.86
206765_at	potassium inwardly-rectifying channel, subfamily J, member 2	KCNJ2	$1.64*10^{-3}$	1.86
235308_at	zinc finger and BTB domain containing 20	ZBTB20	$2.02*10^{-3}$	1.85
218041_x_at	solute carrier family 38, member 2	SLC38A2	$2.99*10^{-4}$	1.85
232997_at	---	---	$4.75*10^{-4}$	1.85
221731_x_at	versican	VCAN	$3.93*10^{-4}$	1.85
242669_at	Ubiquitin-fold modifier 1	UFM1	$2.20*10^{-3}$	1.84
1553720_a_at	family with sequence similarity 123A	FAM123A	$2.14*10^{-3}$	1.84
202973_x_at	family with sequence similarity 13, member A	FAM13A	$1.66*10^{-3}$	1.84
211450_s_at	mutS homolog 6 (E. coli)	MSH6	$1.33*10^{-3}$	1.84
202341_s_at	tripartite motif-containing 2	TRIM2	$2.42*10^{-3}$	1.84
235925_at	Transcription factor 12	TCF12	$6.24*10^{-4}$	1.83
232383_at	transcription factor EC	TFEC	$1.10*10^{-3}$	1.83
207108_s_at	Nipped-B homolog (Drosophila)	NIPBL	$1.12*10^{-3}$	1.82
220770_s_at	chromosome 5 open reading frame 54	C5orf54	$5.84*10^{-4}$	1.82
204204_at	solute carrier family 31 (copper transporters), member 2	SLC31A2	$3.51*10^{-4}$	1.82
1552703_s_at	caspase recruitment domain family, member 16 /// caspase 1, apoptosis-related cy	CARD16 /// CASP1	$2.00*10^{-3}$	1.82
209130_at	synaptosomal-associated protein, 23kDa	SNAP23	$5.72*10^{-5}$	1.82

Supplementary table 3.4 (continued)

Probeset ID	Gene Title	Gene Symbol	p-value	Fold change
234923_at	GTPase activating Rap/RanGAP domain-like 1	GARNL1	$6.49*10^{-4}$	1.82
244414_at	---	---	$1.79*10^{-4}$	1.82
229133_s_at	zinc finger protein 397	ZNF397	$1.27*10^{-3}$	1.82
243046_at	---	---	$1.26*10^{-3}$	1.82
226625_at	transforming growth factor, beta receptor III	TGFBR3	$2.65*10^{-4}$	1.81
209348_s_at	v-maf musculoaponeurotic fibrosarcoma oncogene homolog (avian)	MAF	$1.97*10^{-3}$	1.81
210178_x_at	FUS interacting protein (serine/arginine-rich) 1	FUSIP1	$1.97*10^{-4}$	1.81
222585_x_at	lysine-rich coiled-coil 1	KRCC1	$1.01*10^{-3}$	1.81
223260_s_at	polymerase (DNA directed) kappa	POLK	$2.23*10^{-3}$	1.81
205433_at	butyrylcholinesterase	BCHE	$2.21*10^{-3}$	1.81
209289_at	nuclear factor I/B	NFIB	$8.90*10^{-4}$	1.81
202662_s_at	inositol 1,4,5-triphosphate receptor, type 2	ITPR2	$2.30*10^{-3}$	1.80
220941_s_at	chromosome 21 open reading frame 91	C21orf91	$2.21*10^{-3}$	1.80
229114_at	GRB2-associated binding protein 1	GAB1	$1.69*10^{-4}$	1.79
217047_s_at	family with sequence similarity 13, member A	FAM13A	$4.92*10^{-4}$	1.79
207983_s_at	stromal antigen 2	STAG2	$5.23*10^{-4}$	1.79
232024_at	GTPase, IMAP family member 2	GIMAP2	$1.43*10^{-4}$	1.79
225946_at	Ras association (RalGDS/AF-6) domain family (N-terminal) member 8	RASSF8	$2.68*10^{-4}$	1.79
207896_s_at	deleted in lung and esophageal cancer 1	DLEC1	$6.80*10^{-4}$	1.79
217834_s_at	synaptotagmin binding, cytoplasmic RNA interacting protein	SYNCRIP	$1.05*10^{-4}$	1.79
239432_at	hypothetical LOC379025	FLJ31306	$2.42*10^{-3}$	1.78
219534_x_at	cyclin-dependent kinase inhibitor 1C (p57, Kip2)	CDKN1C	$1.29*10^{-3}$	1.78
230135_at	---	---	$1.39*10^{-3}$	1.78
228454_at	ligand dependent nuclear receptor corepressor	LCOR	$1.09*10^{-3}$	1.78
243020_at	---	---	$1.61*10^{-3}$	1.78
223300_s_at	coiled-coil domain containing 82	CCDC82	$1.31*10^{-3}$	1.78
206571_s_at	mitogen-activated protein kinase kinase kinase kinase 4	MAP4K4	$1.11*10^{-4}$	1.77
202085_at	tight junction protein 2 (zona occludens 2)	TJP2	$5.42*10^{-4}$	1.77
222146_s_at	transcription factor 4	TCF4	$4.59*10^{-4}$	1.77
209022_at	stromal antigen 2	STAG2	$2.09*10^{-5}$	1.77
242263_at	Transmembrane emp24 protein transport domain containing 5	TMED5	$9.27*10^{-4}$	1.77
227627_at	serum/glucocorticoid regulated kinase family, member 3	SGK3	$4.71*10^{-5}$	1.77
228485_s_at	solute carrier family 44, member 1	SLC44A1	$1.02*10^{-3}$	1.77
221899_at	NEDD4 binding protein 2-like 2	N4BP2L2	$4.93*10^{-4}$	1.77
214709_s_at	kinectin 1 (kinesin receptor)	KTN1	$3.64*10^{-5}$	1.77
218401_s_at	zinc finger protein 281	ZNF281	$3.66*10^{-4}$	1.76
226899_at	unc-5 homolog B (C. elegans)	UNC5B	$1.39*10^{-3}$	1.76
213016_at	bobby sox homolog (Drosophila)	BBX	$2.88*10^{-4}$	1.76
217865_at	ring finger protein 130	RNF130	$1.11*10^{-4}$	1.76
207127_s_at	heterogeneous nuclear ribonucleoprotein H3 (2H9)	HNRNPH3	$5.75*10^{-6}$	1.76
227227_at	---	---	$2.28*10^{-3}$	1.76
209168_at	glycoprotein M6B	GPM6B	$1.99*10^{-5}$	1.76
210438_x_at	TROVE domain family, member 2	TROVE2	$2.75*10^{-5}$	1.76
211419_s_at	chimerin (chimaerin) 2	CHN2	$2.22*10^{-3}$	1.76
210858_x_at	ataxia telangiectasia mutated	ATM	$1.20*10^{-4}$	1.76
235238_at	SHC (Src homology 2 domain containing) family, member 4	SHC4	$2.70*10^{-4}$	1.76
234645_at	---	---	$1.19*10^{-4}$	1.76
202527_s_at	SMAD family member 4	SMAD4	$1.07*10^{-3}$	1.76
237885_at	---	---	$1.52*10^{-3}$	1.75
211967_at	transmembrane protein 123	TMEM123	$6.04*10^{-4}$	1.75
234118_at	---	---	$2.61*10^{-4}$	1.75
224595_at	solute carrier family 44, member 1	SLC44A1	$1.37*10^{-3}$	1.75
226252_at	---	---	$8.25*10^{-4}$	1.75
229430_at	chromosome 8 open reading frame 46	C8orf46	$1.55*10^{-4}$	1.75
213158_at	---	---	$2.08*10^{-3}$	1.74
231911_at	ermin, ERM-like protein	ERMN	$5.99*10^{-4}$	1.74
212386_at	transcription factor 4	TCF4	$1.50*10^{-3}$	1.74
228216_at	---	---	$1.07*10^{-3}$	1.74
205603_s_at	diaphanous homolog 2 (Drosophila)	DIAPH2	$1.32*10^{-3}$	1.74
209307_at	SWAP switching B-cell complex 70kDa subunit	SWAP70	$2.25*10^{-5}$	1.74
201719_s_at	erythrocyte membrane protein band 4.1-like 2	EPB41L2	$5.64*10^{-5}$	1.74
202664_at	WAS/WASL interacting protein family, member 1	WIPF1	$5.85*10^{-4}$	1.74
224596_at	solute carrier family 44, member 1	SLC44A1	$7.35*10^{-5}$	1.74
203753_at	transcription factor 4	TCF4	$1.23*10^{-3}$	1.74
214541_s_at	quaking homolog, KH domain RNA binding (mouse)	QKI	$1.48*10^{-3}$	1.73
230831_at	FERM domain containing 5	FRMD5	$4.53*10^{-5}$	1.73
200723_s_at	cell cycle associated protein 1	CAPRIN1	$7.47*10^{-5}$	1.73
229273_at	sal-like 1 (Drosophila)	SALL1	$7.21*10^{-4}$	1.73
225707_at	ADP-ribosylation-like factor 6 interacting protein 6	ARL6IP6	$1.23*10^{-4}$	1.73
224955_at	TEA domain family member 1 (SV40 transcriptional enhancer factor)	TEAD1	$4.58*10^{-4}$	1.73
244050_at	protein tyrosine phosphatase-like A domain containing 2	PTPLAD2	$1.29*10^{-3}$	1.73
225810_at	myotubularin related protein 10	MTMR10	$1.19*10^{-5}$	1.73
213850_s_at	splicing factor, arginine/serine-rich 2, interacting protein	SFRS2IP	$9.87*10^{-4}$	1.73
64883_at	motile sperm domain containing 2	MOSPD2	$5.75*10^{-4}$	1.73
225613_at	microtubule associated serine/threonine kinase family member 4	MAST4	$5.35*10^{-4}$	1.73
212542_s_at	pleckstrin homology domain interacting protein	PHIP	$2.88*10^{-4}$	1.73
210110_x_at	heterogeneous nuclear ribonucleoprotein H3 (2H9)	HNRNPH3	$5.46*10^{-6}$	1.73
227180_at	ELOVL family member 7, elongation of long chain fatty acids (yeast)	ELOVL7	$2.67*10^{-4}$	1.73
211671_s_at	nuclear receptor subfamily 3, group C, member 1 (glucocorticoid receptor)	NR3C1	$3.54*10^{-4}$	1.72
213376_at	zinc finger and BTB domain containing 1	ZBTB1	$1.75*10^{-5}$	1.72
226022_at	SAM and SH3 domain containing 1	SASH1	$1.59*10^{-3}$	1.72
222103_at	activating transcription factor 1	ATF1	$2.16*10^{-3}$	1.72
201865_x_at	nuclear receptor subfamily 3, group C, member 1 (glucocorticoid receptor)	NR3C1	$2.92*10^{-4}$	1.72
203910_at	Rho GTPase activating protein 29	ARHGAP29	$1.15*10^{-3}$	1.72
212800_at	syntaxin 6	STX6	$1.40*10^{-4}$	1.72
202506_at	sperm specific antigen 2	SSFA2	$3.73*10^{-4}$	1.72
202889_x_at	microtubule-associated protein 7	MAP7	$1.38*10^{-3}$	1.72
202173_s_at	vascular endothelial zinc finger 1	VEZF1	$9.40*10^{-4}$	1.72

Probeset ID	Gene Title	Gene Symbol	p-value	Fold change
224571_at	interferon regulatory factor 2 binding protein 2	IRF2BP2	$3.19*10^{-5}$	1.72
212387_at	transcription factor 4	TCF4	$1.56*10^{-3}$	1.72
212368_at	zinc finger protein 292	ZNF292	$3.54*10^{-4}$	1.71
219525_at	solute carrier family 47, member 1	SLC47A1	$1.21*10^{-3}$	1.71
216894_x_at	cyclin-dependent kinase inhibitor 1C (p57, Kip2)	CDKN1C	$1.99*10^{-3}$	1.71
212548_s_at	FRY-like	FRYL	$6.03*10^{-5}$	1.71
239233_at	coiled-coil domain containing 88A	CCDC88A	$1.87*10^{-3}$	1.71
225095_at	Serine palmitoyltransferase, long chain base subunit 2	SPTLC2	$3.53*10^{-4}$	1.71
243952_at	---	---	$5.38*10^{-4}$	1.71
236157_at	RNA binding motif protein 4	RBM4	$1.41*10^{-3}$	1.71
224662_at	kinesin family member 5B	KIF5B	$2.39*10^{-5}$	1.71
213005_s_at	KN motif and ankyrin repeat domains 1	KANK1	$7.12*10^{-4}$	1.71
229315_at	---	---	$2.26*10^{-3}$	1.71
225619_at	SLAIN motif family, member 1	SLAIN1	$2.78*10^{-4}$	1.71
228807_at	---	---	$6.39*10^{-4}$	1.70
218303_x_at	lysine-rich coiled-coil 1	KRCC1	$6.17*10^{-5}$	1.70
1557239_at	bobby sox homolog (Drosophila)	BBX	$1.17*10^{-3}$	1.70
227561_at	discoidin domain receptor tyrosine kinase 2	DDR2	$1.11*10^{-3}$	1.70
201976_s_at	myosin X	MYO10	$1.39*10^{-3}$	1.70
224761_at	guanine nucleotide binding protein (G protein), alpha 13	GNA13	$4.31*10^{-5}$	1.70
1554482_a_at	SAR1 homolog B (S. cerevisiae)	SAR1B	$2.14*10^{-5}$	1.70
209875_s_at	secreted phosphoprotein 1	SPP1	$1.09*10^{-4}$	1.70
223058_at	family with sequence similarity 107, member B	FAM107B	$6.14*10^{-4}$	1.70
1554479_a_at	caspase recruitment domain family, member 8	CARD8	$6.43*10^{-5}$	1.70
201051_at	acidic (leucine-rich) nuclear phosphoprotein 32 family, member A	ANP32A	$7.58*10^{-4}$	1.70
202265_at	BMI1 polycomb ring finger oncogene	BMI1	$8.69*10^{-5}$	1.70
202603_at	---	---	$8.24*10^{-6}$	1.70
218181_s_at	mitogen-activated protein kinase kinase kinase kinase 4	MAP4K4	$7.12*10^{-4}$	1.70
209285_s_at	chromosome 3 open reading frame 63	C3orf63	$1.53*10^{-3}$	1.70
219158_s_at	NMDA receptor regulated 1	NARG1	$5.15*10^{-4}$	1.69
222662_at	protein phosphatase 1, regulatory (inhibitor) subunit 3B	PPP1R3B	$1.84*10^{-3}$	1.69
1556657_at	---	---	$7.85*10^{-4}$	1.69
212077_at	caldesmon 1	CALD1	$8.28*10^{-4}$	1.69
226464_at	chromosome 3 open reading frame 58	C3orf58	$6.59*10^{-4}$	1.69
201301_s_at	annexin A4	ANXA4	$2.31*10^{-6}$	1.69
201991_s_at	kinesin family member 5B	KIF5B	$3.94*10^{-4}$	1.69
229533_x_at	zinc finger protein 680	ZNF680	$1.29*10^{-3}$	1.69
224764_at	Rho GTPase activating protein 21	ARHGAP21	$1.66*10^{-4}$	1.69
228415_at	adaptor-related protein complex 1, sigma 2 subunit	AP1S2	$3.40*10^{-4}$	1.69
207735_at	ring finger protein 125	RNF125	$6.49*10^{-4}$	1.69
217941_s_at	erbb2 interacting protein	ERBB2IP	$1.28*10^{-3}$	1.69
1556598_at	cyclic AMP-regulated phosphoprotein, 21 kD	ARPP-21	$2.07*10^{-3}$	1.69
230795_at	---	---	$2.30*10^{-3}$	1.69
226711_at	forkhead box N2	FOXN2	$9.27*10^{-5}$	1.69
213044_at	Rho-associated, coiled-coil containing protein kinase 1	ROCK1	$6.60*10^{-5}$	1.68
221530_s_at	basic helix-loop-helix family, member e41	BHLHE41	$6.17*10^{-4}$	1.68
225850_at	SFT2 domain containing 1	SFT2D1	$1.06*10^{-4}$	1.68
211922_s_at	catalase	CAT	$5.10*10^{-4}$	1.68
242181_at	---	---	$2.01*10^{-3}$	1.68
227428_at	GA binding protein transcription factor, alpha subunit 60kDa	GABPA	$1.15*10^{-3}$	1.68
212195_at	interleukin 6 signal transducer (gp130, oncostatin M receptor)	IL6ST	$1.38*10^{-5}$	1.68
202195_s_at	transmembrane emp24 protein transport domain containing 5	TMED5	$7.95*10^{-4}$	1.68
227249_at	NudE nuclear distribution gene E homolog 1 (A. nidulans)	NDE1	$4.97*10^{-4}$	1.68
203038_at	protein tyrosine phosphatase, receptor type, K	PTPRK	$1.11*10^{-4}$	1.68
210555_s_at	nuclear factor of activated T-cells, cytoplasmic, calcineurin-dependent 3	NFATC3	$1.22*10^{-3}$	1.68
212785_s_at	La ribonucleoprotein domain family, member 7	LARP7	$1.77*10^{-4}$	1.68
226331_at	bobby sox homolog (Drosophila)	BBX	$1.45*10^{-4}$	1.68
208990_s_at	heterogeneous nuclear ribonucleoprotein H3 (2H9)	HNRNPH3	$2.48*10^{-6}$	1.68
215157_x_at	poly(A) binding protein, cytoplasmic 1	PABPC1	$5.69*10^{-4}$	1.68
212852_s_at	TROVE domain family, member 2	TROVE2	$1.17*10^{-4}$	1.68
242403_at	---	---	$4.16*10^{-4}$	1.67
217627_at	zinc finger protein 573	ZNF573	$7.27*10^{-4}$	1.67
230264_s_at	adaptor-related protein complex 1, sigma 2 subunit	AP1S2	$1.66*10^{-3}$	1.67
204899_s_at	Sin3A-associated protein, 30kDa	SAP30	$1.01*10^{-3}$	1.67
224866_at	fatty acyl CoA reductase 1	FAR1	$7.83*10^{-4}$	1.67
242229_at	N-acyl phosphatidylethanolamine phospholipase D	NAPEPLD	$2.21*10^{-3}$	1.67
204215_at	chromosome 7 open reading frame 23	C7orf23	$3.27*10^{-4}$	1.67
213618_at	ArfGAP with RhoGAP domain, ankyrin repeat and PH domain 2	ARAP2	$9.12*10^{-4}$	1.67
203845_at	K(lysine) acetyltransferase 2B	KAT2B	$7.95*10^{-4}$	1.67
203066_at	carbohydrate (N-acetylgalactosamine 4-sulfate 6-O) sulfotransferase 15	CHST15	$6.87*10^{-4}$	1.67
209283_at	crystallin, alpha B	CRYAB	$1.86*10^{-3}$	1.67
228574_at	Transmembrane and tetratricopeptide repeat containing 2	TMTC2	$1.15*10^{-3}$	1.67
213070_at	phosphoinositide-3-kinase, class 2, alpha polypeptide	PIK3C2A	$5.22*10^{-4}$	1.67
201432_at	catalase	CAT	$5.76*10^{-4}$	1.66
202679_at	Niemann-Pick disease, type C1	NPC1	$3.36*10^{-4}$	1.66
200915_x_at	kinectin 1 (kinesin receptor)	KTN1	$1.95*10^{-4}$	1.66
218738_s_at	ring finger protein 138	RNF138	$4.07*10^{-5}$	1.66
1557804_at	---	---	$1.88*10^{-3}$	1.66
208986_at	transcription factor 12	TCF12	$4.17*10^{-4}$	1.66
214522_x_at	histone cluster 1, H2ad /// histone cluster 1, H3d	HIST1H2AD /// HIST1H3D	$1.93*10^{-3}$	1.66
209267_s_at	solute carrier family 39 (zinc transporter), member 8	SLC39A8	$4.66*10^{-4}$	1.66
226177_at	glycolipid transfer protein	GLTP	$9.93*10^{-4}$	1.66
204373_s_at	centrosomal protein 350kDa	CEP350	$1.46*10^{-3}$	1.66
210493_s_at	microfibrillar-associated protein 3-like	MFAP3L	$9.26*10^{-4}$	1.65
227367_at	solute carrier organic anion transporter family, member 3A1	SLCO3A1	$9.54*10^{-4}$	1.65
209471_s_at	farnesyltransferase, CAAX box, alpha	FNTA	$1.10*10^{-3}$	1.65
224600_at	CGG triplet repeat binding protein 1	CGGBP1	$2.03*10^{-3}$	1.65
204566_at	protein phosphatase 1D magnesium-dependent, delta isoform	PPM1D	$4.09*10^{-4}$	1.65

Supplementary table 3.4 (continued)

Probeset ID	Gene Title	Gene Symbol	p-value	Fold change
223699_at	carnosine dipeptidase 1 (metallopeptidase M20 family)	CNDP1	2.23*10-3	1.65
214578_s_at	Rho-associated, coiled-coil containing protein kinase 1	ROCK1	2.24*10-3	1.65
223135_s_at	bobby sox homolog (Drosophila)	BBX	1.78*10-4	1.65
233080_s_at	PRP40 pre-mRNA processing factor 40 homolog A (S. cerevisiae)	PRPF40A	1.69*10-3	1.65
203138_at	histone acetyltransferase 1	HAT1	5.16*10-4	1.65
205383_s_at	zinc finger and BTB domain containing 20	ZBTB20	8.53*10-4	1.65
231729_s_at	calcyphosine	CAPS	1.61*10-3	1.65
218643_s_at	cysteine-rich PDZ-binding protein	CRIPT	6.73*10-5	1.65
237803_x_at	---	---	2.34*10-3	1.65
221808_at	RAB9A, member RAS oncogene family	RAB9A	3.93*10-6	1.65
117_at	heat shock 70kDa protein 6 (HSP70B')	HSPA6	1.58*10-4	1.65
225340_s_at	cell cycle associated protein 1	CAPRIN1	4.73*10-6	1.65
229442_at	chromosome 18 open reading frame 54	C18orf54	1.53*10-3	1.65
222122_s_at	THO complex 2	THOC2	1.78*10-4	1.65
225924_at	folliculin interacting protein 2	FNIP2	9.33*10-4	1.64
200791_s_at	IQ motif containing GTPase activating protein 1	IQGAP1	9.22*10-4	1.64
225626_at	phosphoprotein associated with glycosphingolipid microdomains 1	PAG1	1.18*10-3	1.64
205961_s_at	PC4 and SFRS1 interacting protein 1	PSIP1	1.14*10-3	1.64
217954_s_at	PHD finger protein 3	PHF3	1.17*10-3	1.64
213974_at	ADAMTS-like 3	ADAMTSL3	2.18*10-3	1.64
203310_at	syntaxin binding protein 3	STXBP3	5.35*10-4	1.64
201779_s_at	ring finger protein 13	RNF13	1.12*10-3	1.64
213463_s_at	family with sequence similarity 149, member B1	FAM149B1	4.56*10-4	1.64
201200_at	cellular repressor of E1A-stimulated genes 1	CREG1	1.82*10-4	1.64
225785_at	hypothetical protein LOC100289942 /// receptor accessory protein 3	LOC100289942 /// REEP3	8.75*10-4	1.64
225932_s_at	heterogeneous nuclear ribonucleoprotein A2/B1	HNRNPA2B1	7.84*10-4	1.64
226020_s_at	disabled homolog 1 (Drosophila) /// OMA1 homolog, zinc metallopeptidase (S. cere	DAB1 /// OMA1	5.01*10-4	1.64
226265_at	glutamine and serine rich 1	QSER1	1.69*10-3	1.63
202890_at	microtubule-associated protein 7	MAP7	2.82*10-4	1.63
226695_at	paired related homeobox 1	PRRX1	2.06*10-3	1.63
212530_at	NIMA (never in mitosis gene a)-related kinase 7	NEK7	1.40*10-3	1.63
208228_s_at	fibroblast growth factor receptor 2	FGFR2	7.03*10-4	1.63
228095_at	PHD finger protein 14	PHF14	1.22*10-3	1.63
220305_at	mitochondrial antiviral signaling protein	MAVS	2.03*10-3	1.63
211538_s_at	heat shock 70kDa protein 2	HSPA2	8.02*10-4	1.63
208015_at	SMAD family member 1	SMAD1	1.38*10-3	1.63
211833_s_at	BCL2-associated X protein	BAX	1.08*10-3	1.63
206893_at	sal-like 1 (Drosophila)	SALL1	1.11*10-3	1.63
1563497_at	ubiquitin specific peptidase 25	USP25	3.40*10-5	1.63
205618_at	proline rich Gla (G-carboxyglutamic acid) 1	PRRG1	9.56*10-4	1.62
200921_s_at	B-cell translocation gene 1, anti-proliferative	BTG1	7.45*10-5	1.62
212192_at	potassium channel tetramerisation domain containing 12	KCTD12	7.45*10-5	1.62
212096_s_at	mitochondrial tumor suppressor 1	MTUS1	3.31*10-4	1.62
202174_s_at	pericentriolar material 1	PCM1	7.25*10-6	1.62
209476_at	thioredoxin-related transmembrane protein 1	TMX1	1.81*10-4	1.62
227692_at	guanine nucleotide binding protein (G protein), alpha inhibiting activity polype	GNAI1	1.45*10-3	1.62
215501_s_at	dual specificity phosphatase 10	DUSP10	1.78*10-4	1.62
221652_s_at	chromosome 12 open reading frame 11	C12orf11	3.43*10-4	1.62
235074_at	sprouty-related, EVH1 domain containing 1	SPRED1	7.59*10-4	1.62
203962_s_at	nebulette	NEBL	1.84*10-3	1.62
222805_at	mannosidase, endo-alpha	MANEA	5.94*10-4	1.61
203313_s_at	TGFB-induced factor homeobox 1	TGIF1	9.74*10-4	1.61
200764_s_at	catenin (cadherin-associated protein), alpha 1, 102kDa	CTNNA1	7.08*10-5	1.61
216274_s_at	SEC11 homolog A (S. cerevisiae)	SEC11A	4.31*10-4	1.61
213056_at	FERM domain containing 4B	FRMD4B	1.20*10-3	1.61
232008_s_at	bobby sox homolog (Drosophila)	BBX	2.12*10-3	1.61
225524_at	anthrax toxin receptor 2	ANTXR2	2.34*10-4	1.61
219229_at	solute carrier organic anion transporter family, member 3A1	SLCO3A1	1.94*10-3	1.61
202412_s_at	ubiquitin specific peptidase 1	USP1	1.43*10-3	1.61
1552519_at	activin A receptor, type IC	ACVR1C	1.38*10-3	1.61
208523_x_at	histone cluster 1, H2bi	HIST1H2BI	2.60*10-6	1.61
216988_s_at	protein tyrosine phosphatase type IVA, member 2	PTP4A2	1.90*10-3	1.61
233329_s_at	lysine-rich coiled-coil 1	KRCC1	1.87*10-3	1.61
212907_at	Solute carrier family 30 (zinc transporter), member 1	SLC30A1	6.21*10-4	1.61
232724_at	membrane-spanning 4-domains, subfamily A, member 6A	MS4A6A	1.54*10-3	1.60
202656_s_at	SERTA domain containing 2	SERTAD2	2.91*10-4	1.60
225275_at	EGF-like repeats and discoidin I-like domains 3	EDIL3	8.27*10-5	1.60
217952_x_at	PHD finger protein 3	PHF3	7.54*10-6	1.60
230998_at	---	---	1.39*10-3	1.60
228732_at	---	---	2.18*10-3	1.60
223047_at	CKLF-like MARVEL transmembrane domain containing 6	CMTM6	7.18*10-5	1.60
208741_at	Sin3A-associated protein, 18kDa	SAP18	2.21*10-4	1.60
222580_at	zinc finger protein 644	ZNF644	2.63*10-4	1.60
225479_at	leucine rich repeat containing 58	LRRC58	8.20*10-4	1.60
203072_at	myosin IE	MYO1E	1.88*10-4	1.60
218319_at	pellino homolog 1 (Drosophila)	PELI1	1.98*10-3	1.60
200704_at	lipopolysaccharide-induced TNF factor	LITAF	4.77*10-4	1.59
228711_at	zinc finger protein 37A	ZNF37A	8.83*10-4	1.59
225997_at	MOB1, Mps One Binder kinase activator-like 1A (yeast)	MOBKL1A	3.87*10-4	1.59
226642_s_at	NudC domain containing 2	NUDCD2	1.80*10-4	1.59
224740_at	chromosome 5 open reading frame 43	C5orf43	8.54*10-5	1.59
216640_s_at	protein disulfide isomerase family A, member 6	PDIA6	1.28*10-3	1.59
208627_s_at	Y box binding protein 1	YBX1	1.25*10-3	1.59
212719_at	PH domain and leucine rich repeat protein phosphatase 1	PHLPP1	1.04*10-3	1.58
221958_s_at	G protein-coupled receptor 177	GPR177	4.92*10-4	1.58
201589_at	structural maintenance of chromosomes 1A	SMC1A	7.10*10-4	1.58
202171_at	vascular endothelial zinc finger 1	VEZF1	4.47*10-4	1.58
234987_at	---	---	1.81*10-3	1.58

Probeset ID	Gene Title	Gene Symbol	p-value	Fold change
212328_at	LIM and calponin homology domains 1	LIMCH1	$3.08*10^{-5}$	1.58
218640_s_at	pleckstrin homology domain containing, family F (with FYVE domain) member 2	PLEKHF2	$1.66*10^{-3}$	1.58
238906_s_at	ras homolog gene family, member J	RHOJ	$8.77*10^{-4}$	1.58
225927_at	mitogen-activated protein kinase kinase kinase 1	MAP3K1	$9.30*10^{-5}$	1.58
201987_at	mediator complex subunit 13	MED13	$6.46*10^{-4}$	1.58
212482_at	required for meiotic nuclear division 5 homolog A (S. cerevisiae)	RMND5A	$2.37*10^{-4}$	1.58
212783_at	retinoblastoma binding protein 6	RBBP6	$1.76*10^{-3}$	1.58
217725_x_at	SERPINE1 mRNA binding protein 1	SERBP1	$1.95*10^{-4}$	1.58
233656_s_at	vacuolar protein sorting 54 homolog (S. cerevisiae)	VPS54	$3.63*10^{-4}$	1.58
202363_at	sparc/osteonectin, cwcv and kazal-like domains proteoglycan (testican) 1	SPOCK1	$1.50*10^{-3}$	1.58
201726_at	ELAV (embryonic lethal, abnormal vision, Drosophila)-like 1 (Hu antigen R)	ELAVL1	$1.30*10^{-3}$	1.58
226460_at	folliculin interacting protein 2	FNIP2	$7.01*10^{-5}$	1.58
222233_s_at	DNA cross-link repair 1C (PSO2 homolog, S. cerevisiae)	DCLRE1C	$1.78*10^{-3}$	1.58
213103_at	StAR-related lipid transfer (START) domain containing 13	STARD13	$1.46*10^{-4}$	1.58
225921_at	ninein (GSK3B interacting protein)	NIN	$3.35*10^{-4}$	1.58
212179_at	splicing factor, arginine/serine-rich 18	SFRS18	$1.98*10^{-3}$	1.58
223289_s_at	ubiquitin specific peptidase 38	USP38	$2.21*10^{-3}$	1.58
200934_at	DEK oncogene	DEK	$2.14*10^{-4}$	1.58
210466_s_at	SERPINE1 mRNA binding protein 1	SERBP1	$9.05*10^{-5}$	1.57
218713_at	NMDA receptor regulated 2	NARG2	$2.19*10^{-4}$	1.57
224690_at	chromosome 20 open reading frame 108	C20orf108	$6.38*10^{-4}$	1.57
235484_at	protein prenyltransferase alpha subunit repeat containing 1	PTAR1	$8.60*10^{-4}$	1.57
1556200_a_at	chromosome 10 open reading frame 90	C10orf90	$3.25*10^{-4}$	1.57
1556599_s_at	cyclic AMP-regulated phosphoprotein, 21 kD	ARPP-21	$1.46*10^{-3}$	1.57
212807_s_at	sortilin 1	SORT1	$3.00*10^{-4}$	1.57
227416_s_at	zinc finger CCHC-type and RNA binding motif 1	ZCRB1	$1.75*10^{-4}$	1.57
1554895_a_at	rhomboid, veinlet-like 2 (Drosophila)	RHBDL2	$7.92*10^{-4}$	1.57
1559881_s_at	zinc finger protein 12	ZNF12	$2.03*10^{-3}$	1.57
230226_s_at	lysine (K)-specific demethylase 5A	KDM5A	$2.30*10^{-4}$	1.57
219024_at	pleckstrin homology domain containing, family A (phosphoinositide binding specif	PLEKHA1	$1.61*10^{-3}$	1.57
222182_s_at	CCR4-NOT transcription complex, subunit 2	CNOT2	$6.39*10^{-4}$	1.57
206095_s_at	FUS interacting protein (serine/arginine-rich) 1	FUSIP1	$7.16*10^{-4}$	1.57
222566_at	suppressor of variegation 4-20 homolog 1 (Drosophila)	SUV420H1	$7.96*10^{-4}$	1.57
204011_at	sprouty homolog 2 (Drosophila)	SPRY2	$1.52*10^{-3}$	1.57
200821_at	lysosomal-associated membrane protein 2	LAMP2	$8.32*10^{-4}$	1.56
224818_at	sortilin 1	SORT1	$7.28*10^{-5}$	1.56
205117_at	fibroblast growth factor 1 (acidic)	FGF1	$4.27*10^{-4}$	1.56
200971_s_at	stress-associated endoplasmic reticulum protein 1	SERP1	$2.05*10^{-4}$	1.56
226280_at	---	---	$1.01*10^{-3}$	1.56
229799_s_at	neural cell adhesion molecule 1	NCAM1	$1.42*10^{-3}$	1.56
218254_s_at	SAR1 homolog B (S. cerevisiae)	SAR1B	$4.06*10^{-4}$	1.56
216231_s_at	beta-2-microglobulin	B2M	$5.71*10^{-4}$	1.56
226579_at	---	---	$1.69*10^{-3}$	1.56
209392_at	ectonucleotide pyrophosphatase/phosphodiesterase 2	ENPP2	$1.09*10^{-3}$	1.55
206989_s_at	splicing factor, arginine/serine-rich 2, interacting protein	SFRS2IP	$1.84*10^{-3}$	1.55
212138_at	PDS5, regulator of cohesion maintenance, homolog A (S. cerevisiae)	PDS5A	$1.77*10^{-4}$	1.55
201034_at	adducin 3 (gamma)	ADD3	$4.95*10^{-4}$	1.55
201866_s_at	nuclear receptor subfamily 3, group C, member 1 (glucocorticoid receptor)	NR3C1	$1.93*10^{-4}$	1.55
218450_at	heme binding protein 1	HEBP1	$7.39*10^{-5}$	1.55
212289_at	ankyrin repeat domain 12	ANKRD12	$2.14*10^{-3}$	1.55
202303_x_at	SWI/SNF related, matrix associated, actin dependent regulator of chromatin, subf	SMARCA5	$1.56*10^{-4}$	1.55
200872_at	S100 calcium binding protein A10	S100A10	$1.26*10^{-3}$	1.55
214812_s_at	MOB1, Mps One Binder kinase activator-like 1B (yeast)	MOBKL1B	$8.59*10^{-5}$	1.55
240113_at	---	---	$7.21*10^{-4}$	1.55
201152_s_at	muscleblind-like (Drosophila)	MBNL1	$2.62*10^{-4}$	1.55
222401_s_at	transmembrane protein 50A	TMEM50A	$1.06*10^{-4}$	1.55
213050_at	cordon-bleu homolog (mouse)	COBL	$1.12*10^{-3}$	1.55
204544_at	Hermansky-Pudlak syndrome 5	HPS5	$1.71*10^{-3}$	1.55
238133_at	---	---	$7.37*10^{-4}$	1.55
209213_at	carbonyl reductase 1	CBR1	$5.16*10^{-4}$	1.55
212828_at	synaptojanin 2	SYNJ2	$2.33*10^{-3}$	1.55
232563_at	zinc finger protein 684	ZNF684	$2.02*10^{-3}$	1.55
212418_at	E74-like factor 1 (ets domain transcription factor)	ELF1	$2.94*10^{-4}$	1.55
205292_s_at	heterogeneous nuclear ribonucleoprotein A2/B1	HNRNPA2B1	$1.06*10^{-6}$	1.55
226423_at	progestin and adipoQ receptor family member VIII	PAQR8	$7.53*10^{-4}$	1.54
215823_x_at	similar to poly(A) binding protein, cytoplasmic 1	PABPC1 /// PABPC3 /// RLIM	$1.78*10^{-3}$	1.54
201845_s_at	RING1 and YY1 binding protein	RYBP	$1.78*10^{-3}$	1.54
212469_at	Nipped-B homolog (Drosophila)	NIPBL	$2.03*10^{-5}$	1.54
208113_x_at	poly(A) binding protein, cytoplasmic 3	PABPC3	$1.66*10^{-3}$	1.54
226041_at	N-acyl phosphatidylethanolamine phospholipase D	NAPEPLD	$2.04*10^{-3}$	1.54
201363_s_at	influenza virus NS1A binding protein	IVNS1ABP	$2.11*10^{-3}$	1.54
212730_at	synemin, intermediate filament protein	SYNM	$9.78*10^{-4}$	1.54
224893_at	atlastin GTPase 3	ATL3	$3.57*10^{-4}$	1.54
227699_at	chromosome 14 open reading frame 149	C14orf149	$3.52*10^{-4}$	1.54
225849_s_at	SFT2 domain containing 1	SFT2D1	$8.64*10^{-6}$	1.54
212522_at	phosphodiesterase 8A	PDE8A	$2.38*10^{-3}$	1.54
218490_s_at	zinc finger protein 302	ZNF302	$5.54*10^{-4}$	1.54
212977_at	chemokine (C-X-C motif) receptor 7	CXCR7	$2.17*10^{-3}$	1.54
225133_at	Kruppel-like factor 3 (basic)	KLF3	$3.90*10^{-4}$	1.54
212640_at	protein tyrosine phosphatase-like (proline instead of catalytic arginine), membe	PTPLB	$2.36*10^{-3}$	1.53

Supplementary table 3.4 (continued)

Probeset ID	Gene Title	Gene Symbol	p-value	Fold change
228220_at	FCH domain only 2	FCHO2	$2.22*10^{-4}$	1.53
208454_s_at	plasma glutamate carboxypeptidase	PGCP	$1.99*10^{-4}$	1.53
226230_at	SMEK homolog 2, suppressor of mek1 (Dictyostelium)	SMEK2	$1.02*10^{-3}$	1.53
201290_at	SEC11 homolog A (S. cerevisiae)	SEC11A	$2.50*10^{-5}$	1.53
212202_s_at	transmembrane protein 87A	TMEM87A	$3.52*10^{-5}$	1.53
201567_s_at	golgi autoantigen, golgin subfamily a, 4	GOLGA4	$2.10*10^{-3}$	1.53
205073_at	cytochrome P450, family 2, subfamily J, polypeptide 2	CYP2J2	$1.84*10^{-4}$	1.53
216756_at	---	---	$2.30*10^{-4}$	1.53
210840_s_at	IQ motif containing GTPase activating protein 1	IQGAP1	$1.82*10^{-3}$	1.53
208579_x_at	H2B histone family, member S /// histone cluster 1, H2bk	H2BFS /// HIST1H2BK	$3.66*10^{-4}$	1.53
236780_at	---	---	$1.96*10^{-3}$	1.53
212521_s_at	phosphodiesterase 8A	PDE8A	$5.26*10^{-4}$	1.53
203552_at	mitogen-activated protein kinase kinase kinase kinase 5	MAP4K5	$1.67*10^{-3}$	1.53
213165_at	centrosomal protein 350kDa	CEP350	$2.35*10^{-3}$	1.53
212672_at	ataxia telangiectasia mutated	ATM	$9.92*10^{-5}$	1.53
217947_at	CKLF-like MARVEL transmembrane domain containing 6	CMTM6	$4.96*10^{-4}$	1.53
212534_at	zinc finger protein 24	ZNF24	$1.70*10^{-5}$	1.53
223087_at	enoyl Coenzyme A hydratase domain containing 1	ECHDC1	$3.92*10^{-4}$	1.52
212796_s_at	TBC1 domain family, member 2B	TBC1D2B	$6.37*10^{-4}$	1.52
234340_at	---	---	$1.85*10^{-4}$	1.52
221858_at	TBC1 domain family, member 12	TBC1D12	$8.05*10^{-4}$	1.52
226153_s_at	CCR4-NOT transcription complex, subunit 6-like	CNOT6L	$2.24*10^{-4}$	1.52
225394_s_at	zinc finger CCHC-type and RNA binding motif 1	ZCRB1	$1.42*10^{-4}$	1.52
202258_s_at	NEDD4 binding protein 2-like 2	N4BP2L2	$7.08*10^{-5}$	1.52
227601_at	methyltransferase like 14	METTL14	$1.45*10^{-3}$	1.52
209007_s_at	chromosome 1 open reading frame 63	C10rf63	$1.20*10^{-3}$	1.52
208796_s_at	cyclin G1	CCNG1	$1.07*10^{-4}$	1.52
226148_at	zinc finger and BTB domain containing 44	ZBTB44	$1.37*10^{-3}$	1.52
202370_s_at	core-binding factor, beta subunit	CBFB	$2.74*10^{-4}$	1.52
233743_x_at	sphingosine-1-phosphate receptor 5	S1PR5	$1.80*10^{-3}$	1.52
222415_at	myeloid/lymphoid or mixed-lineage leukemia 3	MLL3	$1.65*10^{-3}$	1.52
212526_at	spastic paraplegia 20 (Troyer syndrome)	SPG20	$1.09*10^{-3}$	1.52
207486_x_at	chimerin (chimaerin) 2	CHN2	$1.17*10^{-3}$	1.51
1554149_at	claudin domain containing 1	CLDND1	$8.33*10^{-4}$	1.51
212616_at	chromodomain helicase DNA binding protein 9	CHD9	$3.10*10^{-4}$	1.51
210664_s_at	tissue factor pathway inhibitor (lipoprotein-associated coagulation inhibitor)	TFPI	$1.30*10^{-3}$	1.51
1566860_at	hypothetical protein LOC145663	LOC145663	$1.04*10^{-3}$	1.51
221230_s_at	AT rich interactive domain 4B (RBP1-like)	ARID4B	$1.79*10^{-3}$	1.51
217724_at	SERPINE1 mRNA binding protein 1	SERBP1	$1.67*10^{-5}$	1.51
209102_s_at	HMG-box transcription factor 1	HBP1	$6.46*10^{-4}$	1.51
227276_at	plexin domain containing 2	PLXDC2	$2.22*10^{-3}$	1.51
212251_at	metadherin	MTDH	$7.13*10^{-4}$	1.51
229312_s_at	G kinase anchoring protein 1	GKAP1	$1.75*10^{-3}$	1.51
201027_s_at	eukaryotic translation initiation factor 5B	EIF5B	$3.11*10^{-4}$	1.51
210844_x_at	catenin (cadherin-associated protein), alpha 1, 102kDa	CTNNA1	$5.53*10^{-5}$	1.51
211962_s_at	zinc finger protein 36, C3H type-like 1	ZFP36L1	$2.40*10^{-3}$	1.51
222720_x_at	chromosome 1 open reading frame 27	C10rf27	$1.12*10^{-4}$	1.51
236915_at	chromosome 4 open reading frame 47	C4orf47	$1.51*10^{-3}$	1.51
223027_at	sorting nexin 9	SNX9	$1.29*10^{-5}$	1.51
213027_at	TROVE domain family, member 2	TROVE2	$9.98*10^{-4}$	1.51
202194_at	transmembrane emp24 protein transport domain containing 5	TMED5	$1.48*10^{-3}$	1.51
203632_s_at	G protein-coupled receptor, family C, group 5, member B	GPRC5B	$2.60*10^{-5}$	1.51
209790_s_at	caspase 6, apoptosis-related cysteine peptidase	CASP6	$1.66*10^{-3}$	1.50
218040_at	PRP38 pre-mRNA processing factor 38 (yeast) domain containing B	PRPF38B	$1.53*10^{-4}$	1.50
200765_x_at	catenin (cadherin-associated protein), alpha 1, 102kDa	CTNNA1	$7.66*10^{-5}$	1.50
226329_s_at	MIT, microtubule interacting and transport, domain containing 1	MITD1	$1.74*10^{-3}$	1.50
217823_s_at	ubiquitin-conjugating enzyme E2, J1 (UBC6 homolog, yeast)	UBE2J1	$7.57*10^{-6}$	1.50
203556_at	zinc fingers and homeoboxes 2	ZHX2	$9.03*10^{-4}$	1.50
201362_at	influenza virus NS1A binding protein	IVNS1ABP	$8.18*10^{-4}$	1.50
207606_s_at	Rho GTPase activating protein 12	ARHGAP12	$1.69*10^{-3}$	1.50
202962_at	kinesin family member 13B	KIF13B	$7.38*10^{-4}$	1.50
216620_s_at	Rho guanine nucleotide exchange factor (GEF) 10	ARHGEF10	$1.51*10^{-3}$	1.50
225336_at	splicing factor, arginine/serine-rich 2, interacting protein	SFRS2IP	$1.26*10^{-4}$	1.50
225933_at	coiled-coil domain containing 137	CCDC137	$1.33*10^{-5}$	-1.50
206882_at	solute carrier family 1 (high affinity aspartate/glutamate transporter), member	SLC1A6	$1.01*10^{-3}$	-1.50
1570098_at	---	---	$9.31*10^{-4}$	-1.50
214162_at	hypothetical protein LOC284244	LOC284244	$2.22*10^{-3}$	-1.50
1563887_at	integrator complex subunit 4-like 1	INTS4L1	$7.54*10^{-5}$	-1.50
219706_at	chromosome 20 open reading frame 29	C20orf29	$1.84*10^{-5}$	-1.50
41660_at	cadherin, EGF LAG seven-pass G-type receptor 1 (flamingo homolog, Drosophila)	CELSR1	$7.92*10^{-8}$	-1.50
202513_s_at	protein phosphatase 2, regulatory subunit B', delta isoform	PPP2R5D	$2.83*10^{-6}$	-1.51
41397_at	zinc finger protein 821	ZNF821	$5.68*10^{-5}$	-1.51
203795_s_at	B-cell CLL/lymphoma 7A	BCL7A	$3.19*10^{-5}$	-1.51
222492_at	pyridoxal (pyridoxine, vitamin B6) kinase	PDXK	$1.17*10^{-3}$	-1.51
219301_s_at	contactin associated protein-like 2	CNTNAP2	$1.17*10^{-3}$	-1.51
223950_s_at	FLYWCH-type zinc finger 1	FLYWCH1	$4.75*10^{-5}$	-1.51
223382_s_at	zinc and ring finger 1	ZNRF1	$3.16*10^{-5}$	-1.51
219270_at	ChaC, cation transport regulator homolog 1 (E. coli)	CHAC1	$4.20*10^{-5}$	-1.51
823_at	chemokine (C-X3-C motif) ligand 1	CX3CL1	$1.74*10^{-3}$	-1.51
220952_s_at	pleckstrin homology domain containing, family A member 5	PLEKHA5	$2.07*10^{-3}$	-1.51
228595_at	hydroxysteroid (17-beta) dehydrogenase 1	HSD17B1	$7.53*10^{-5}$	-1.51
218944_at	pyrroline-5-carboxylate reductase-like	PYCRL	$7.50*10^{-5}$	-1.51
231194_at	sorting nexin 32	SNX32	$1.15*10^{-3}$	-1.51
222032_s_at	ubiquitin specific peptidase 7 (herpes virus-associated)	USP7	$2.17*10^{-3}$	-1.51
207239_s_at	PCTAIRE protein kinase 1	PCTK1	$1.76*10^{-3}$	-1.51
243345_at	---	---	$2.12*10^{-3}$	-1.51
212727_at	discs, large homolog 3 (Drosophila)	DLG3	$1.11*10^{-3}$	-1.51

Probeset ID	Gene Title	Gene Symbol	p-value	Fold change
222622_at	phosphoglycolate phosphatase	PGP	1.73*10-3	-1.51
225034_at	ST3 beta-galactoside alpha-2,3-sialyltransferase 1	ST3GAL1	3.56*10-4	-1.51
1553593_a_at	T-cell acute lymphocytic leukemia 2	TAL2	1.30*10-4	-1.51
205302_at	insulin-like growth factor binding protein 1	IGFBP1	2.36*10-3	-1.51
210547_x_at	islet cell autoantigen 1, 69kDa	ICA1	1.66*10-3	-1.51
200999_s_at	cytoskeleton-associated protein 4	CKAP4	1.45*10-3	-1.52
1554796_at	dipeptidyl-peptidase 6	DPP6	9.00*10-5	-1.52
1559910_at	---	---	8.42*10-4	-1.52
55093_at	chondroitin polymerizing factor 2	CHPF2	2.30*10-6	-1.52
223517_at	F-box protein 44	FBXO44	3.04*10-4	-1.52
230675_at	---	---	6.82*10-5	-1.52
233196_at	---	---	7.83*10-4	-1.52
202394_s_at	ATP-binding cassette, sub-family F (GCN20), member 3	ABCF3	1.80*10-3	-1.52
209237_s_at	solute carrier family 23 (nucleobase transporters), member 2	SLC23A2	2.20*10-3	-1.52
224186_s_at	ring finger protein 123	RNF123	2.53*10-4	-1.52
224864_at	steroid receptor RNA activator 1	SRA1	6.91*10-5	-1.52
224160_s_at	acyl-Coenzyme A dehydrogenase family, member 9	ACAD9	8.39*10-4	-1.52
237340_at	solute carrier family 26, member 8	SLC26A8	7.06*10-4	-1.52
219636_s_at	armadillo repeat containing 9	ARMC9	4.20*10-4	-1.52
1570125_at	---	---	3.59*10-4	-1.52
213408_s_at	phosphatidylinositol 4-kinase, catalytic	PI4KA	6.71*10-4	-1.52
223284_at	N-acetyltransferase 14 (GCN5-related, putative)	NAT14	8.02*10-4	-1.52
218910_at	anoctamin 10	ANO10	5.83*10-5	-1.52
227526_at	Cdon homolog (mouse)	CDON	1.01*10-3	-1.52
211348_s_at	CDC14 cell division cycle 14 homolog B (S. cerevisiae)	CDC14B	4.46*10-4	-1.52
219184_x_at	translocase of inner mitochondrial membrane 22 homolog (yeast)	TIMM22	1.28*10-3	-1.52
1554530_at	V-set and transmembrane domain containing 2A	VSTM2A	5.04*10-4	-1.52
1557248_at	Zinc finger protein 587	ZNF587	6.10*10-5	-1.52
239277_at	---	---	3.69*10-4	-1.53
219591_at	cell cycle exit and neuronal differentiation 1	CEND1	2.35*10-3	-1.53
220688_s_at	mRNA turnover 4 homolog (S. cerevisiae)	MRTO4	1.92*10-3	-1.53
219144_at	dual specificity phosphatase 26 (putative)	DUSP26	3.31*10-4	-1.53
223012_at	UBX domain protein 6	UBXN6	1.83*10-3	-1.53
205510_s_at	hypothetical protein FLJ10038	FLJ10038	8.22*10-4	-1.53
1569235_a_at	---	---	1.45*10-3	-1.53
235882_at	vacuolar protein sorting 53 homolog (S. cerevisiae)	VPS53	2.17*10-3	-1.53
233116_at	---	---	1.29*10-5	-1.53
220659_s_at	chromosome 7 open reading frame 43	C7orf43	4.26*10-6	-1.53
229771_at	---	---	5.35*10-6	-1.53
239286_at	---	---	8.70*10-4	-1.53
204209_at	phosphate cytidylyltransferase 1, choline, alpha	PCYT1A	7.87*10-5	-1.53
218887_at	mitochondrial ribosomal protein L2	MRPL2	3.27*10-4	-1.53
213608_s_at	SRR1 domain containing	SRRD	2.07*10-3	-1.53
1556082_a_at	---	---	4.84*10-4	-1.53
1556117_at	---	---	2.42*10-3	-1.54
218631_at	arginine vasopressin-induced 1	AVPI1	5.03*10-5	-1.54
223107_s_at	zinc finger, CCHC domain containing 17	ZCCHC17	2.39*10-3	-1.54
226456_at	chromosome 16 open reading frame 75	C16orf75	8.17*10-5	-1.54
226433_at	ring finger protein 157	RNF157	2.18*10-4	-1.54
209667_at	carboxylesterase 2 (intestine, liver)	CES2	1.29*10-3	-1.54
223756_at	KIAA1310	KIAA1310	7.72*10-5	-1.54
211677_x_at	cell adhesion molecule 3	CADM3	2.89*10-4	-1.54
229238_at	chromosome 17 open reading frame 97	C17orf97	3.41*10-5	-1.54
214773_x_at	TIP41, TOR signaling pathway regulator-like (S. cerevisiae)	TIPRL	1.04*10-4	-1.54
205271_s_at	cell cycle related kinase	CCRK	4.25*10-5	-1.54
224471_s_at	beta-transducin repeat containing	BTRC	1.16*10-3	-1.54
235431_s_at	pellino homolog 3 (Drosophila)	PELI3	2.66*10-4	-1.54
209256_s_at	PNAS-119	LOC100287552	5.32*10-4	-1.54
210879_s_at	RAB11 family interacting protein 5 (class I)	RAB11FIP5	1.94*10-3	-1.54
213198_at	activin A receptor, type IB	ACVR1B	1.12*10-4	-1.54
205050_s_at	mitogen-activated protein kinase 8 interacting protein 2	MAPK8IP2	4.31*10-4	-1.54
225238_at	musashi homolog 2 (Drosophila)	MSI2	1.57*10-3	-1.54
1554717_a_at	phosphodiesterase 4D, cAMP-specific (phosphodiesterase E3 dunce homolog, Drosoph	PDE4D	2.37*10-3	-1.54
228422_at	lipoma HMGIC fusion partner-like 4	LHFPL4	1.98*10-3	-1.54
232955_at	hypothetical LOC440200	FLJ41170	4.34*10-5	-1.54
222045_s_at	PDX1 C-terminal inhibiting factor 1	PCIF1	8.41*10-4	-1.54
232212_at	pleckstrin homology domain containing, family A (phosphoinositide binding specif	PLEKHA8	6.31*10-6	-1.55
206746_at	beaded filament structural protein 1, filensin	BFSP1	9.84*10-4	-1.55
225146_at	chromosome 9 open reading frame 25	C9orf25	1.41*10-5	-1.55
227326_at	matrix-remodelling associated 7	MXRA7	1.23*10-3	-1.55
226793_at	hypothetical LOC283267	LOC283267	2.21*10-3	-1.55
204488_at	dolichol kinase	DOLK	9.88*10-4	-1.55
202315_s_at	breakpoint cluster region	BCR	2.93*10-4	-1.55
226273_at	chloride channel 5	CLCN5	6.69*10-4	-1.55
219105_x_at	origin recognition complex, subunit 6 like (yeast)	ORC6L	1.36*10-3	-1.55
209407_s_at	deformed epidermal autoregulatory factor 1 (Drosophila)	DEAF1	1.94*10-3	-1.55
202801_at	protein kinase, cAMP-dependent, catalytic, alpha	PRKACA	1.78*10-4	-1.55
217925_s_at	chromosome 6 open reading frame 106	C6orf106	4.41*10-4	-1.55
219998_at	galectin-related protein	HSPC159	7.26*10-5	-1.55
205839_s_at	benzodiazapine receptor (peripheral) associated protein 1	BZRAP1	2.49*10-4	-1.55
203950_s_at	chloride channel 6	CLCN6	3.43*10-4	-1.55
215527_at	KH domain containing, RNA binding, signal transduction associated 2	KHDRBS2	9.70*10-5	-1.56
53991_at	DENN/MADD domain containing 2A	DENND2A	9.64*10-5	-1.56
1556361_s_at	ankyrin repeat domain 13C	ANKRD13C	1.19*10-3	-1.56
1561606_at	---	---	2.61*10-4	-1.56
242979_at	insulin receptor substrate 1	IRS1	1.26*10-4	-1.56
224212_s_at	protocadherin alpha 1	PCDHA1	9.82*10-4	-1.56
221953_s_at	hypothetical LOC729580	LOC729580	2.03*10-4	-1.56

Supplementary table 3.4 (continued)

Probeset ID	Gene Title	Gene Symbol	p-value	Fold change
64488_at	immunity-related GTPase family, Q	IRGQ	$2.43*10^{-3}$	-1.56
213216_at	OTU domain containing 3	OTUD3	$2.28*10^{-3}$	-1.56
215543_s_at	like-glycosyltransferase	LARGE	$2.06*10^{-3}$	-1.56
204763_s_at	guanine nucleotide binding protein (G protein), alpha activating activity polype	GNAO1	$9.07*10^{-5}$	-1.56
229884_s_at	mitochondrial ribosomal protein L2	MRPL2	$1.70*10^{-3}$	-1.56
229138_at	poly (ADP-ribose) polymerase family, member 11	PARP11	$2.20*10^{-3}$	-1.56
203965_at	ubiquitin specific peptidase 20	USP20	$2.46*10^{-5}$	-1.56
233587_s_at	signal-induced proliferation-associated 1 like 2	SIPA1L2	$1.69*10^{-3}$	-1.56
225739_at	RAB11 family interacting protein 4 (class II)	RAB11FIP4	$1.79*10^{-3}$	-1.56
203088_at	fibulin 5	FBLN5	$7.71*10^{-4}$	-1.57
219562_at	RAB26, member RAS oncogene family	RAB26	$2.33*10^{-3}$	-1.57
1562572_at	---	---	$2.19*10^{-3}$	-1.57
206690_at	amiloride-sensitive cation channel 1, neuronal	ACCN1	$8.92*10^{-4}$	-1.57
227778_at	HEAT repeat containing 7A	HEATR7A	$5.38*10^{-6}$	-1.57
1558021_at	Rab9 effector protein with kelch motifs	RABEPK	$1.60*10^{-5}$	-1.57
213266_at	Tubulin, gamma complex associated protein 4	TUBGCP4	$1.16*10^{-3}$	-1.57
214330_at	ATP synthase mitochondrial F1 complex assembly factor 2	ATPAF2	$1.08*10^{-3}$	-1.57
236716_at	---	---	$9.68*10^{-4}$	-1.57
219907_at	fibroblast growth factor receptor substrate 3	FRS3	$1.28*10^{-4}$	-1.57
49077_at	protein phosphatase methylesterase 1	PPME1	$3.35*10^{-4}$	-1.57
226451_at	ferredoxin 1-like	FDX1L	$2.38*10^{-3}$	-1.57
205253_at	pre-B-cell leukemia homeobox 1	PBX1	$2.07*10^{-3}$	-1.57
221273_s_at	ring finger protein 208	RNF208	$1.75*10^{-3}$	-1.57
223596_at	solute carrier family 12 (potassium/chloride transporters), member 6	SLC12A6	$4.24*10^{-4}$	-1.57
227644_at	regulating synaptic membrane exocytosis 4	RIMS4	$4.43*10^{-5}$	-1.57
213393_at	Major facilitator superfamily domain containing 9	MFSD9	$1.04*10^{-4}$	-1.58
205864_at	solute carrier family 7 (cationic amino acid transporter, y+ system), member 4	SLC7A4	$6.24*10^{-4}$	-1.58
235373_at	---	---	$1.06*10^{-3}$	-1.58
204483_at	enolase 3 (beta, muscle)	ENO3	$7.92*10^{-4}$	-1.58
210991_s_at	regulating synaptic membrane exocytosis 3	RIMS3	$4.10*10^{-4}$	-1.58
238753_at	frequenin homolog (Drosophila)	FREQ	$2.04*10^{-3}$	-1.58
239699_s_at	postmeiotic segregation increased 2-like 1 pseudogene /// postmeiotic segregatio	PMS2L1 /// PMS2L5	$5.21*10^{-4}$	-1.58
218019_s_at	pyridoxal (pyridoxine, vitamin B6) kinase	PDXK	$3.22*10^{-5}$	-1.58
205616_at	potassium voltage-gated channel, shaker-related subfamily, member 6	KCNA6	$3.83*10^{-4}$	-1.58
215052_at	FERM and PDZ domain containing 4	FRMPD4	$1.34*10^{-4}$	-1.58
240122_at	DIRAS family, GTP-binding RAS-like 2	DIRAS2	$8.64*10^{-5}$	-1.58
212662_at	poliovirus receptor	PVR	$8.03*10^{-4}$	-1.58
237086_at	Forkhead box A1	FOXA1	$7.75*10^{-4}$	-1.58
207393_at	hypocretin (orexin) receptor 2	HCRTR2	$2.03*10^{-3}$	-1.58
203407_at	periplakin	PPL	$1.75*10^{-4}$	-1.58
219440_at	retinoic acid induced 2	RAI2	$7.07*10^{-4}$	-1.58
1553300_a_at	diacylglycerol kinase, eta	DGKH	$2.07*10^{-3}$	-1.58
1554643_at	regulator of G-protein signaling 11	RGS11	$1.42*10^{-4}$	-1.58
201677_at	Chromosome 3 open reading frame 37	C3orf37	$1.29*10^{-4}$	-1.58
227999_at	PWWP domain containing 2B	PWWP2B	$1.13*10^{-5}$	-1.58
232126_at	---	---	$1.49*10^{-3}$	-1.58
219610_at	Rho-guanine nucleotide exchange factor	RGNEF	$4.77*10^{-5}$	-1.59
218812_s_at	ORAI calcium release-activated calcium modulator 2	ORAI2	$6.40*10^{-4}$	-1.59
230715_at	zinc finger protein 518B	ZNF518B	$1.21*10^{-4}$	-1.59
219046_s_at	PBX/knotted 1 homeobox 2	PKNOX2	$6.45*10^{-5}$	-1.59
210086_at	hairless homolog (mouse)	HR	$2.22*10^{-5}$	-1.59
218906_x_at	kinesin light chain 2	KLC2	$6.30*10^{-4}$	-1.59
205944_s_at	clathrin, heavy chain-like 1	CLTCL1	$1.20*10^{-5}$	-1.59
39650_s_at	pecanex-like 2 (Drosophila)	PCNXL2	$7.53*10^{-4}$	-1.59
213885_at	tripartite motif-containing 3	TRIM3	$3.57*10^{-4}$	-1.59
226605_at	diacylglycerol kinase, theta 110kDa	DGKQ	$1.50*10^{-3}$	-1.59
239832_at	---	---	$1.42*10^{-3}$	-1.59
207010_at	gamma-aminobutyric acid (GABA) A receptor, beta 1	GABRB1	$1.71*10^{-3}$	-1.59
240363_at	ankyrin 1, erythrocytic	ANK1	$1.37*10^{-4}$	-1.59
241759_at	---	---	$5.66*10^{-4}$	-1.59
1557103_a_at	lemur tyrosine kinase 3	LMTK3	$1.26*10^{-3}$	-1.59
231355_at	---	---	$1.82*10^{-7}$	-1.59
225969_at	alkB, alkylation repair homolog 6 (E. coli)	ALKBH6	$1.31*10^{-3}$	-1.59
227698_s_at	RAB40C, member RAS oncogene family	RAB40C	$6.78*10^{-5}$	-1.60
236638_at	family with sequence similarity 123C	FAM123C	$5.50*10^{-5}$	-1.60
221861_at	---	---	$1.82*10^{-5}$	-1.60
1554245_x_at	ADP-ribosylation factor-like 17 /// ADP-ribosylation factor-like 17 pseudogene 1	ARL17 /// ARL17P1	$5.04*10^{-5}$	-1.60
230025_at	gap junction protein, delta 3, 31.9kDa	GJD3	$3.21*10^{-7}$	-1.60
236726_at	regulator of G-protein signaling 6	RGS6	$1.25*10^{-3}$	-1.60
235948_at	ribosomal modification protein rimK-like family member A	RIMKLA	$1.08*10^{-3}$	-1.60
227872_at	polymerase (RNA) III (DNA directed) polypeptide A, 155kDa	POLR3A	$8.52*10^{-4}$	-1.60
243594_x_at	spire homolog 2 (Drosophila)	SPIRE2	$2.23*10^{-4}$	-1.60
217080_s_at	homer homolog 2 (Drosophila)	HOMER2	$6.62*10^{-4}$	-1.60
227704_at	chromosome 19 open reading frame 12	C19orf12	$2.23*10^{-3}$	-1.60
244183_x_at	protocadherin beta 3	PCDHB3	$1.11*10^{-3}$	-1.60
221538_s_at	plexin A1	PLXNA1	$2.03*10^{-4}$	-1.60
207593_at	ATP-binding cassette, sub-family G (WHITE), member 4	ABCG4	$5.06*10^{-4}$	-1.60
205331_s_at	receptor accessory protein 2	REEP2	$1.82*10^{-4}$	-1.60
206137_at	regulating synaptic membrane exocytosis 2	RIMS2	$1.97*10^{-3}$	-1.60
40273_at	sphingosine kinase 2	SPHK2	$6.32*10^{-5}$	-1.60
206106_at	mitogen-activated protein kinase 12	MAPK12	$1.88*10^{-5}$	-1.60
200734_s_at	ADP-ribosylation factor 3	ARF3	$1.76*10^{-3}$	-1.60
220795_s_at	brain-enriched guanylate kinase-associated homolog (rat)	BEGAIN	$4.31*10^{-5}$	-1.60
209334_s_at	proteasome (prosome, macropain) 26S subunit, non-ATPase, 9	PSMD9	$1.98*10^{-3}$	-1.60

Probeset ID	Gene Title	Gene Symbol	p-value	Fold change
241416_at	---	---	$9.97*10^{-6}$	-1.60
231835_at	chromosome 1 open reading frame 93	C1orf93	$2.23*10^{-3}$	-1.60
50965_at	RAB26, member RAS oncogene family	RAB26	$7.51*10^{-4}$	-1.60
49679_s_at	hypothetical LOC729580	LOC729580	$8.78*10^{-6}$	-1.60
221069_s_at	translational activator of mitochondrially encoded cytochrome c oxidase I	TACO1	$4.52*10^{-4}$	-1.60
221560_at	MAP/microtubule affinity-regulating kinase 4	MARK4	$1.16*10^{-5}$	-1.60
208632_at	ring finger protein 10	RNF10	$1.27*10^{-3}$	-1.60
236151_at	KIAA1853	KIAA1853	$1.24*10^{-3}$	-1.61
222852_at	chromosome 10 open reading frame 88	C10orf88	$1.20*10^{-3}$	-1.61
1570450_at	---	---	$8.14*10^{-4}$	-1.61
242694_at	IQ motif and Sec7 domain 3	IQSEC3	$1.14*10^{-3}$	-1.61
225788_at	chromosome 6 open reading frame 153	C6orf153	$1.50*10^{-3}$	-1.61
209345_s_at	phosphatidylinositol 4-kinase type 2 alpha	PI4K2A	$1.22*10^{-3}$	-1.61
213178_s_at	mitogen-activated protein kinase 8 interacting protein 3	MAPK8IP3	$1.94*10^{-5}$	-1.61
206846_s_at	histone deacetylase 6	HDAC6	$1.17*10^{-4}$	-1.61
201709_s_at	nipsnap homolog 1 (C. elegans)	NIPSNAP1	$9.31*10^{-4}$	-1.61
203031_s_at	uroporphyrinogen III synthase	UROS	$1.79*10^{-3}$	-1.61
49111_at	---	---	$6.14*10^{-5}$	-1.61
236200_at	---	---	$2.17*10^{-3}$	-1.61
228158_at	lymphocyte-specific protein 1 pseudogene /// lymphocyte-specific protein 1 pseud	LOC645166 /// LOC654342	$9.81*10^{-4}$	-1.61
215972_at	---	---	$9.43*10^{-4}$	-1.61
218208_at	PQ loop repeat containing 1	PQLC1	$1.50*10^{-4}$	-1.61
206213_at	wingless-type MMTV integration site family, member 10B	WNT10B	$8.02*10^{-5}$	-1.61
206078_at	kalirin, RhoGEF kinase	KALRN	$1.82*10^{-5}$	-1.61
1562834_at	---	---	$1.75*10^{-3}$	-1.61
203408_s_at	SATB homeobox 1	SATB1	$6.42*10^{-4}$	-1.61
205493_s_at	dihydropyrimidinase-like 4	DPYSL4	$6.99*10^{-4}$	-1.61
227497_at	SRY (sex determining region Y)-box 6	SOX6	$3.75*10^{-4}$	-1.62
212520_s_at	SWI/SNF related, matrix associated, actin dependent regulator of chromatin, subf	SMARCA4	$9.94*10^{-5}$	-1.62
206806_at	diacylglycerol kinase, iota	DGKI	$1.01*10^{-3}$	-1.62
220449_at	hypothetical protein MGC5566	MGC5566	$2.13*10^{-4}$	-1.62
228781_at	oligonucleotide/oligosaccharide-binding fold containing 1	OBFC1	$2.95*10^{-4}$	-1.62
213276_at	calcium/calmodulin-dependent protein kinase II beta	CAMK2B	$6.88*10^{-4}$	-1.62
227456_s_at	chromosome 6 open reading frame 136	C6orf136	$1.76*10^{-3}$	-1.62
223458_at	seizure related 6 homolog (mouse)-like 2	SEZ6L2	$1.74*10^{-3}$	-1.62
213011_s_at	triosephosphate isomerase 1	TPI1	$1.87*10^{-3}$	-1.62
219170_at	fibronectin type III and SPRY domain containing 1	FSD1	$1.54*10^{-3}$	-1.62
201269_s_at	NudC domain containing 3	NUDCD3	$6.94*10^{-6}$	-1.62
224476_s_at	mesoderm posterior 1 homolog (mouse)	MESP1	$2.87*10^{-4}$	-1.62
202913_at	Rho guanine nucleotide exchange factor (GEF) 11	ARHGEF11	$3.67*10^{-6}$	-1.62
207128_s_at	zinc finger protein 223	ZNF223	$1.56*10^{-4}$	-1.62
226125_at	---	---	$7.03*10^{-4}$	-1.62
222113_s_at	epidermal growth factor receptor pathway substrate 15-like 1	EPS15L1	$1.38*10^{-3}$	-1.62
226198_at	target of myb1-like 2 (chicken)	TOM1L2	$1.37*10^{-4}$	-1.62
57539_at	zinc finger, CCCH-type with G patch domain	ZGPAT	$1.85*10^{-4}$	-1.63
219365_s_at	CaM kinase-like vesicle-associated	CAMKV	$5.96*10^{-5}$	-1.63
222328_x_at	Maternally expressed 3 (non-protein coding)	MEG3	$1.13*10^{-4}$	-1.63
214110_s_at	---	---	$1.45*10^{-3}$	-1.63
204175_at	zinc finger protein 593	ZNF593	$2.09*10^{-3}$	-1.63
244113_at	---	---	$1.43*10^{-4}$	-1.63
217749_at	coatomer protein complex, subunit gamma	COPG	$1.36*10^{-3}$	-1.63
202424_at	mitogen-activated protein kinase kinase 2	MAP2K2	$1.12*10^{-3}$	-1.63
1570552_at	chromosome 18 open reading frame 50	C18orf50	$8.12*10^{-4}$	-1.63
236921_at	---	---	$2.31*10^{-3}$	-1.63
223367_at	DnaJ (Hsp40) homolog, subfamily C, member 30	DNAJC30	$1.62*10^{-3}$	-1.63
203162_s_at	katanin p80 (WD repeat containing) subunit B 1	KATNB1	$1.98*10^{-4}$	-1.63
212383_at	ATPase, H+ transporting, lysosomal Vo subunit a1	ATP6V0A1	$1.06*10^{-4}$	-1.64
1557176_a_at	chromosome 14 open reading frame 37	C14orf37	$2.24*10^{-3}$	-1.64
208320_at	calcium binding protein 1	CABP1	$1.88*10^{-3}$	-1.64
218560_s_at	jumonji domain containing 4	JMJD4	$4.23*10^{-5}$	-1.64
227185_at	hypothetical LOC643988	LOC643988	$8.12*10^{-4}$	-1.64
236142_at	Peptidylprolyl isomerase H (cyclophilin H)	PPIH	$1.04*10^{-3}$	-1.64
221657_s_at	ankyrin repeat and SOCS box-containing 6	ASB6	$1.93*10^{-4}$	-1.64
210341_at	myelin transcription factor 1	MYT1	$7.33*10^{-4}$	-1.64
209236_at	solute carrier family 23 (nucleobase transporters), member 2	SLC23A2	$1.12*10^{-3}$	-1.64
1552689_at	CASK interacting protein 1	CASKIN1	$5.82*10^{-5}$	-1.64
223603_at	ring finger protein 112	RNF112	$9.28*10^{-4}$	-1.64
219779_at	zinc finger homeobox 4	ZFHX4	$1.37*10^{-3}$	-1.64
235961_at	G protein-coupled receptor 161	GPR161	$2.58*10^{-5}$	-1.65
216672_s_at	myelin transcription factor 1-like	MYT1L	$2.37*10^{-4}$	-1.65
1554262_s_at	kelch-like 29 (Drosophila)	KLHL29	$1.31*10^{-5}$	-1.65
228804_at	DiGeorge syndrome critical region gene 5 (non-protein coding)	DGCR5	$2.94*10^{-4}$	-1.65
221261_x_at	melanoma antigen family D, 4 /// melanoma antigen family D, 4B	MAGED4 /// MAGED4B	$2.83*10^{-5}$	-1.65
222125_s_at	prolyl 4-hydroxylase, transmembrane (endoplasmic reticulum)	P4HTM	$1.55*10^{-3}$	-1.65
213834_at	IQ motif and Sec7 domain 3	IQSEC3	$6.27*10^{-5}$	-1.65
238815_at	leucine rich repeat transmembrane neuronal 1	LRRTM1	$2.28*10^{-3}$	-1.65
220584_at	hypothetical protein FLJ22184	FLJ22184	$1.14*10^{-5}$	-1.65
207219_at	zinc finger protein 643	ZNF643	$7.12*10^{-4}$	-1.65
1559072_a_at	extracellular leucine-rich repeat and fibronectin type III domain containing 2	ELFN2	$3.15*10^{-4}$	-1.65
213041_s_at	ATP synthase, H+ transporting, mitochondrial F1 complex, delta subunit	ATP5D	$1.40*10^{-3}$	-1.65
238682_at	coiled-coil domain containing 96	CCDC96	$2.01*10^{-4}$	-1.65
223313_s_at	melanoma antigen family D, 4 /// melanoma antigen family D, 4B	MAGED4 /// MAGED4B	$2.06*10^{-5}$	-1.65
43511_s_at	---	---	$2.23*10^{-5}$	-1.66
235746_s_at	phospholipase A2 receptor 1, 180kDa	PLA2R1	$1.79*10^{-3}$	-1.66

Supplementary table 3.4 (continued)

Probeset ID	Gene Title	Gene Symbol	p-value	Fold change
223874_at	actin-related Arp11	ARP11	$1.12*10^{-4}$	-1.66
215692_s_at	metallophosphoesterase domain containing 2	MPPED2	$1.86*10^{-4}$	-1.66
209003_at	solute carrier family 25 (mitochondrial carrier; oxoglutarate carrier), member 1	SLC25A11	$1.99*10^{-3}$	-1.66
230691_at	syntaxin 1B	STX1B	$1.19*10^{-3}$	-1.67
224878_at	ubiquitin family domain containing 1	UBFD1	$1.43*10^{-3}$	-1.67
1566138_at	---	---	$6.24*10^{-5}$	-1.67
204303_s_at	KIAA0427	KIAA0427	$3.82*10^{-5}$	-1.67
210227_at	discs, large (Drosophila) homolog-associated protein 2	DLGAP2	$8.32*10^{-4}$	-1.67
200697_at	hexokinase 1	HK1	$1.96*10^{-3}$	-1.67
233651_s_at	MPN domain containing	MPND	$5.92*10^{-4}$	-1.67
203151_at	microtubule-associated protein 1A	MAP1A	$1.86*10^{-4}$	-1.67
237995_at	RIMS binding protein 2	RIMBP2	$1.47*10^{-3}$	-1.67
1554181_at	sorting nexin 32	SNX32	$2.63*10^{-4}$	-1.67
235375_x_at	tetratricopeptide repeat domain 9B	TTC9B	$7.15*10^{-4}$	-1.67
204262_s_at	presenilin 2 (Alzheimer disease 4)	PSEN2	$2.04*10^{-4}$	-1.67
214180_at	mannosidase, alpha, class 1C, member 1	MAN1C1	$4.11*10^{-4}$	-1.67
223604_at	GTPase activating Rap/RanGAP domain-like 3	GARNL3	$1.42*10^{-3}$	-1.67
206818_s_at	cyclin M2	CNNM2	$7.70*10^{-5}$	-1.67
215785_s_at	cytoplasmic FMR1 interacting protein 2	CYFIP2	$5.94*10^{-5}$	-1.68
210364_at	sodium channel, voltage-gated, type II, beta	SCN2B	$3.15*10^{-4}$	-1.68
224611_s_at	DnaJ (Hsp40) homolog, subfamily C, member 5	DNAJC5	$3.32*10^{-4}$	-1.68
214140_at	solute carrier family 25 (mitochondrial carrier; Graves disease autoantigen), me	SLC25A16	$1.65*10^{-3}$	-1.68
214430_at	galactosidase, alpha	GLA	$1.61*10^{-3}$	-1.68
204099_at	SWI/SNF related, matrix associated, actin dependent regulator of chromatin, subf	SMARCD3	$1.31*10^{-5}$	-1.68
221921_s_at	cell adhesion molecule 3	CADM3	$1.71*10^{-4}$	-1.68
221995_s_at	---	---	$8.60*10^{-4}$	-1.68
205155_s_at	spectrin, beta, non-erythrocytic 2	SPTBN2	$6.14*10^{-4}$	-1.68
205318_at	kinesin family member 5A	KIF5A	$5.87*10^{-4}$	-1.68
205613_at	synaptotagmin XVII	SYT17	$3.51*10^{-4}$	-1.68
227394_at	neural cell adhesion molecule 1	NCAM1	$2.21*10^{-4}$	-1.68
219617_at	chromosome 2 open reading frame 34	C20rf34	$3.82*10^{-4}$	-1.68
210720_s_at	N-terminal EF-hand calcium binding protein 3	NECAB3	$7.92*10^{-6}$	-1.68
243452_at	hypothetical LOC646778	LOC646778	$2.75*10^{-4}$	-1.69
227229_at	vacuolar protein sorting 53 homolog (S. cerevisiae)	VPS53	$4.79*10^{-5}$	-1.69
40020_at	cadherin, EGF LAG seven-pass G-type receptor 3 (flamingo homolog, Drosophila)	CELSR3	$2.16*10^{-4}$	-1.69
212983_at	v-Ha-ras Harvey rat sarcoma viral oncogene homolog	HRAS	$5.26*10^{-4}$	-1.69
202752_x_at	solute carrier family 7 (cationic amino acid transporter, y+ system), member 8	SLC7A8	$4.95*10^{-5}$	-1.69
229100_s_at	translocase of inner mitochondrial membrane 22 homolog (yeast)	TIMM22	$1.98*10^{-4}$	-1.69
232003_at	PNMA-like 2	PNMAL2	$2.39*10^{-3}$	-1.69
229579_s_at	dispatched homolog 2 (Drosophila)	DISP2	$9.60*10^{-4}$	-1.69
215458_s_at	SMAD specific E3 ubiquitin protein ligase 1	SMURF1	$2.65*10^{-4}$	-1.69
210448_s_at	purinergic receptor P2X, ligand-gated ion channel, 5	P2RX5	$9.01*10^{-4}$	-1.69
216092_s_at	solute carrier family 7 (cationic amino acid transporter, y+ system), member 8	SLC7A8	$7.46*10^{-4}$	-1.69
226305_at	Ly6/neurotoxin 1	LYNX1	$6.77*10^{-4}$	-1.69
216149_at	leucine rich repeat containing 37, member B2	LRRC37B2	$2.09*10^{-5}$	-1.70
1553677_a_at	TIP41, TOR signaling pathway regulator-like (S. cerevisiae)	TIPRL	$2.31*10^{-3}$	-1.70
236775_s_at	---	---	$1.39*10^{-3}$	-1.70
1556764_s_at	---	---	$1.36*10^{-3}$	-1.70
229653_at	vacuolar protein sorting 53 homolog (S. cerevisiae)	VPS53	$1.17*10^{-5}$	-1.70
217841_s_at	protein phosphatase methylesterase 1	PPME1	$2.25*10^{-4}$	-1.70
219632_s_at	transient receptor potential cation channel, subfamily V, member 1	TRPV1	$2.40*10^{-3}$	-1.70
242173_at	---	---	$3.41*10^{-5}$	-1.70
211572_s_at	solute carrier family 23 (nucleobase transporters), member 2	SLC23A2	$2.14*10^{-3}$	-1.70
215789_s_at	adherens junctions associated protein 1	AJAP1	$1.10*10^{-3}$	-1.70
221901_at	KIAA1644	KIAA1644	$1.87*10^{-3}$	-1.70
39705_at	SIN3 homolog B, transcription regulator (yeast)	SIN3B	$6.97*10^{-4}$	-1.70
213174_at	tetratricopeptide repeat domain 9	TTC9	$9.30*10^{-4}$	-1.70
226930_at	fibronectin type III domain containing 1	FNDC1	$8.42*10^{-4}$	-1.71
201704_at	ectonucleoside triphosphate diphosphohydrolase 6 (putative function)	ENTPD6	$1.52*10^{-4}$	-1.71
211593_s_at	microtubule associated serine/threonine kinase 2	MAST2	$1.88*10^{-4}$	-1.71
1554283_at	CCR4 carbon catabolite repression 4-like (S. cerevisiae)	CCRN4L	$1.88*10^{-5}$	-1.71
209945_s_at	glycogen synthase kinase 3 beta	GSK3B	$1.04*10^{-4}$	-1.71
44040_at	F-box protein 41	FBXO41	$6.94*10^{-4}$	-1.71
228951_at	---	---	$1.26*10^{-5}$	-1.71
226034_at	---	---	$1.45*10^{-3}$	-1.71
227321_at	GATS, stromal antigen 3 opposite strand	GATS	$1.08*10^{-3}$	-1.71
230475_at	chromosome 15 open reading frame 59	C15orf59	$2.02*10^{-3}$	-1.71
218434_s_at	acetoacetyl-CoA synthetase	AACS	$1.08*10^{-4}$	-1.72
1556638_at	paired box 7	PAX7	$6.89*10^{-5}$	-1.72
202737_s_at	LSM4 homolog, U6 small nuclear RNA associated (S. cerevisiae)	LSM4	$3.69*10^{-4}$	-1.72
204629_at	parvin, beta	PARVB	$6.39*10^{-4}$	-1.72
220482_s_at	secretion regulating guanine nucleotide exchange factor	SERGEF	$1.73*10^{-3}$	-1.72
228741_s_at	hyperpolarization activated cyclic nucleotide-gated potassium channel 3	HCN3	$1.31*10^{-4}$	-1.72
47560_at	latrophilin 1	LPHN1	$6.27*10^{-4}$	-1.72
235219_at	chromosome 5 open reading frame 55	C5orf55	$9.27*10^{-5}$	-1.72
1552782_at	solute carrier family 44, member 5	SLC44A5	$1.53*10^{-3}$	-1.72
218537_at	host cell factor C1 regulator 1 (XPO1 dependent)	HCFC1R1	$1.69*10^{-4}$	-1.72
227498_at	SRY (sex determining region Y)-box 6	SOX6	$1.97*10^{-3}$	-1.72
1557112_a_at	vacuolar protein sorting 53 homolog (S. cerevisiae)	VPS53	$9.46*10^{-8}$	-1.72
65585_at	family with sequence similarity 86, member B1	FAM86B1	$1.76*10^{-3}$	-1.72
238605_at	nucleolar protein 4	NOL4	$3.40*10^{-4}$	-1.72

Probeset ID	Gene Title	Gene Symbol	p-value	Fold change
228165_at	chromosome 12 open reading frame 53	C12orf53	$1.07*10^{-3}$	-1.72
211471_s_at	RAB36, member RAS oncogene family	RAB36	$3.14*10^{-6}$	-1.72
212411_at	IMP4, U3 small nucleolar ribonucleoprotein, homolog (yeast)	IMP4	$3.55*10^{-4}$	-1.73
1568617_a_at	KIAA1543	KIAA1543	$6.01*10^{-4}$	-1.73
205325_at	phytanoyl-CoA 2-hydroxylase interacting protein	PHYHIP	$1.98*10^{-5}$	-1.73
228396_at	protein kinase, cGMP-dependent, type I	PRKG1	$1.92*10^{-3}$	-1.73
223024_at	adaptor-related protein complex 1, mu 1 subunit	AP1M1	$1.59*10^{-3}$	-1.73
236233_at	tripartite motif-containing 32	TRIM32	$2.51*10^{-4}$	-1.73
221708_s_at	unc-45 homolog A (C. elegans)	UNC45A	$2.03*10^{-4}$	-1.73
207693_at	calcium channel, voltage-dependent, beta 4 subunit	CACNB4	$2.28*10^{-3}$	-1.73
1556039_s_at	G protein-coupled receptor 173	GPR173	$1.30*10^{-5}$	-1.73
215235_at	spectrin, alpha, non-erythrocytic 1 (alpha-fodrin)	SPTAN1	$2.27*10^{-4}$	-1.73
1562074_a_at	unc-13 homolog C (C. elegans)	UNC13C	$1.45*10^{-4}$	-1.74
212360_at	adenosine monophosphate deaminase 2 (isoform L)	AMPD2	$5.11*10^{-5}$	-1.74
1564676_a_at	---	---	$9.25*10^{-5}$	-1.74
204695_at	cell division cycle 25 homolog A (S. pombe)	CDC25A	$2.06*10^{-3}$	-1.74
212358_at	CAP-GLY domain containing linker protein 3	CLIP3	$6.17*10^{-4}$	-1.74
1559061_at	hypothetical protein LOC253962	LOC253962	$4.51*10^{-7}$	-1.74
222584_at	misato homolog 1 (Drosophila)	MSTO1	$7.27*10^{-4}$	-1.74
241807_x_at	---	---	$1.65*10^{-3}$	-1.74
206655_s_at	glycoprotein Ib (platelet), beta polypeptide /// septin 5	GP1BB /// SEPT5	$6.02*10^{-5}$	-1.74
224505_s_at	phospholipase C, delta 4	PLCD4	$2.77*10^{-4}$	-1.74
207110_at	potassium inwardly-rectifying channel, subfamily J, member 12	KCNJ12	$1.65*10^{-3}$	-1.75
211483_x_at	calcium/calmodulin-dependent protein kinase II beta	CAMK2B	$2.01*10^{-3}$	-1.75
208968_s_at	cytokine induced apoptosis inhibitor 1	CIAPIN1	$1.36*10^{-3}$	-1.75
210290_at	zinc finger protein 174	ZNF174	$1.65*10^{-3}$	-1.75
205217_at	translocase of inner mitochondrial membrane 8 homolog A (yeast)	TIMM8A	$1.70*10^{-3}$	-1.75
214209_s_at	ATP-binding cassette, sub-family B (MDR/TAP), member 9	ABCB9	$1.31*10^{-3}$	-1.75
218856_at	tumor necrosis factor receptor superfamily, member 21	TNFRSF21	$6.28*10^{-4}$	-1.75
1557891_s_at	hypothetical protein LOC729178	LOC729178	$1.84*10^{-3}$	-1.75
1569453_a_at	hypothetical locus LOC692247	LOC692247	$7.68*10^{-5}$	-1.75
215134_at	phosphatidylinositol 4-kinase type 2 alpha	PI4K2A	$3.72*10^{-4}$	-1.75
1563110_at	---	---	$2.35*10^{-5}$	-1.75
235377_at	chromosome 6 open reading frame 142	C6orf142	$3.58*10^{-4}$	-1.76
220555_s_at	PDZ domain containing 7	PDZD7	$5.36*10^{-4}$	-1.76
213242_x_at	KIAA0284	KIAA0284	$1.27*10^{-3}$	-1.76
1558648_at	chromosome 15 open reading frame 57	C15orf57	$4.29*10^{-4}$	-1.76
1566219_at	hypothetical protein LOC338651	LOC338651	$2.07*10^{-4}$	-1.76
1556798_a_at	hypothetical protein LOC386597	LOC386597	$1.43*10^{-4}$	-1.76
201415_at	glutathione synthetase	GSS	$1.92*10^{-3}$	-1.76
213059_at	cAMP responsive element binding protein 3-like 1	CREB3L1	$8.10*10^{-5}$	-1.76
230977_at	nucleophosmin/nucleoplasmin 2	NPM2	$2.93*10^{-5}$	-1.76
55065_at	MAP/microtubule affinity-regulating kinase 4	MARK4	$9.79*10^{-6}$	-1.76
204729_s_at	syntaxin 1A (brain)	STX1A	$2.98*10^{-5}$	-1.76
201439_at	golgi-specific brefeldin A resistant guanine nucleotide exchange factor 1	GBF1	$4.13*10^{-5}$	-1.76
212444_at	---	---	$7.44*10^{-4}$	-1.76
212775_at	obscurin-like 1	OBSL1	$1.48*10^{-3}$	-1.77
240145_at	---	---	$7.98*10^{-4}$	-1.77
223586_at	aryl hydrocarbon receptor nuclear translocator-like 2	ARNTL2	$3.12*10^{-4}$	-1.77
226718_at	adhesion molecule with Ig-like domain 1	AMIGO1	$1.11*10^{-4}$	-1.77
233365_at	---	---	$2.07*10^{-3}$	-1.78
33736_at	stomatin (EPB72)-like 1	STOML1	$8.81*10^{-5}$	-1.78
231053_at	---	---	$2.29*10^{-5}$	-1.78
228845_at	phospholipase B domain containing 2	PLBD2	$2.87*10^{-4}$	-1.78
204000_at	guanine nucleotide binding protein (G protein), beta 5	GNB5	$9.77*10^{-5}$	-1.78
203402_at	potassium voltage-gated channel, shaker-related subfamily, beta member 2	KCNAB2	$4.44*10^{-4}$	-1.78
224612_s_at	DnaJ (Hsp40) homolog, subfamily C, member 5	DNAJC5	$8.63*10^{-4}$	-1.78
209352_s_at	SIN3 homolog B, transcription regulator (yeast)	SIN3B	$3.95*10^{-4}$	-1.78
225300_at	chromosome 15 open reading frame 23	C15orf23	$2.66*10^{-4}$	-1.78
237790_at	hypothetical protein FLJ33996	FLJ33996	$1.25*10^{-3}$	-1.78
235656_s_at	---	---	$5.15*10^{-4}$	-1.78
228632_at	---	---	$5.44*10^{-5}$	-1.78
1557098_s_at	highly accelerated region 1A (non-protein coding)	HAR1A	$6.03*10^{-4}$	-1.79
211043_s_at	clathrin, light chain (Lcb)	CLTB	$1.01*10^{-3}$	-1.79
204411_at	kinesin family member 21B	KIF21B	$2.05*10^{-4}$	-1.79
229267_at	---	---	$5.90*10^{-4}$	-1.79
1564220_a_at	---	---	$1.71*10^{-4}$	-1.79
224162_s_at	F-box protein 31	FBXO31	$1.35*10^{-5}$	-1.79
209211_at	Kruppel-like factor 5 (intestinal)	KLF5	$1.52*10^{-3}$	-1.79
1569372_at	---	---	$9.16*10^{-4}$	-1.80
44065_at	chromosome 12 open reading frame 52	C12orf52	$2.11*10^{-3}$	-1.80
209926_at	hypothetical protein LOC729991	LOC729991	$1.68*10^{-3}$	-1.80
235396_at	chromosome 22 open reading frame 25	C22orf25	$9.36*10^{-4}$	-1.80
228546_at	dipeptidyl-peptidase 6	DPP6	$8.77*10^{-4}$	-1.80
235719_at	cytochrome P450, family 4, subfamily V, polypeptide 2	CYP4V2	$5.06*10^{-4}$	-1.80
1561595_x_at	---	---	$3.05*10^{-4}$	-1.81
239303_at	---	---	$2.09*10^{-4}$	-1.81
236391_at	---	---	$3.80*10^{-6}$	-1.81
227217_at	WNK lysine deficient protein kinase 2	WNK2	$5.18*10^{-4}$	-1.81
237282_s_at	A kinase (PRKA) anchor protein 14	AKAP14	$4.55*10^{-4}$	-1.81
211106_at	---	---	$4.08*10^{-4}$	-1.81
219695_at	sphingomyelin phosphodiesterase 3, neutral membrane (neutral sphingomyelinase II	SMPD3	$3.22*10^{-5}$	-1.81
238012_at	Dipeptidyl-peptidase 7	DPP7	$6.81*10^{-4}$	-1.82
63305_at	PBX/knotted 1 homeobox 2	PKNOX2	$3.28*10^{-4}$	-1.82
243599_at	---	---	$1.48*10^{-6}$	-1.82
223715_at	BR serine/threonine kinase 2	BRSK2	$3.68*10^{-7}$	-1.82
216215_s_at	RNA binding motif protein 9	RBM9	$1.84*10^{-3}$	-1.82

Supplementary table 3.4 (continued)

Probeset ID	Gene Title	Gene Symbol	p-value	Fold change
203826_s_at	phosphatidylinositol transfer protein, membrane-associated 1	PITPNM1	$3.74*10^{-5}$	-1.82
233457_at	---	---	$7.41*10^{-4}$	-1.82
235474_at	---	---	$2.35*10^{-4}$	-1.82
1563181_a_at	---	---	$1.69*10^{-5}$	-1.83
205165_at	cadherin, EGF LAG seven-pass G-type receptor 3 (flamingo homolog, Drosophila)	CELSR3	$8.20*10^{-5}$	-1.83
244159_at	Hypothetical gene supported by BC008048	LOC440934	$9.69*10^{-4}$	-1.83
221792_at	RAB6B, member RAS oncogene family	RAB6B	$1.22*10^{-3}$	-1.83
218608_at	ATPase type 13A2	ATP13A2	$1.28*10^{-3}$	-1.83
217150_s_at	neurofibromin 2 (merlin)	NF2	$9.11*10^{-6}$	-1.83
227641_at	F-box and leucine-rich repeat protein 16	FBXL16	$1.94*10^{-3}$	-1.83
220041_at	phosphatidylinositol glycan anchor biosynthesis, class Z	PIGZ	$1.45*10^{-4}$	-1.83
244071_at	fibrillarin-like 1	FBLL1	$6.65*10^{-4}$	-1.83
212339_at	erythrocyte membrane protein band 4.1-like 1	EPB41L1	$5.74*10^{-4}$	-1.83
206046_at	ADAM metallopeptidase domain 23	ADAM23	$8.62*10^{-4}$	-1.83
215903_s_at	microtubule associated serine/threonine kinase 2	MAST2	$9.21*10^{-5}$	-1.84
231908_at	zinc finger, DHHC-type containing 18	ZDHHC18	$1.30*10^{-4}$	-1.84
224991_at	c-Maf-inducing protein	CMIP	$7.41*10^{-4}$	-1.84
227853_at	---	---	$1.38*10^{-3}$	-1.84
1555616_at	---	---	$6.36*10^{-5}$	-1.84
216924_s_at	dopamine receptor D2	DRD2	$3.07*10^{-4}$	-1.84
219522_at	four jointed box 1 (Drosophila)	FJX1	$2.11*10^{-3}$	-1.84
1554537_at	transmembrane protein 126B	TMEM126B	$7.88*10^{-5}$	-1.84
222841_s_at	translocase of inner mitochondrial membrane 22 homolog (yeast)	TIMM22	$3.73*10^{-4}$	-1.84
225073_at	periphilin 1	PPHLN1	$1.27*10^{-3}$	-1.84
218324_s_at	spermatogenesis associated, serine-rich 2	SPATS2	$9.15*10^{-4}$	-1.85
228354_at	MORN repeat containing 4	MORN4	$4.78*10^{-4}$	-1.85
223960_s_at	chromosome 16 open reading frame 5	C16orf5	$9.35*10^{-5}$	-1.85
1556797_at	hypothetical protein LOC386597	LOC386597	$1.81*10^{-6}$	-1.85
223385_at	cytochrome P450, family 2, subfamily S, polypeptide 1	CYP2S1	$3.56*10^{-4}$	-1.85
208806_at	chromodomain helicase DNA binding protein 3	CHD3	$1.48*10^{-4}$	-1.85
215790_at	adherens junctions associated protein 1	AJAP1	$5.75*10^{-5}$	-1.85
205918_at	solute carrier family 4, anion exchanger, member 3	SLC4A3	$1.99*10^{-3}$	-1.85
207081_s_at	phosphatidylinositol 4-kinase, catalytic, alpha	PI4KA	$1.11*10^{-3}$	-1.85
221880_s_at	family with sequence similarity 174, member B	FAM174B	$2.20*10^{-4}$	-1.85
222941_at	ubiquitin specific peptidase 46	USP46	$2.07*10^{-3}$	-1.86
208626_s_at	vesicle amine transport protein 1 homolog (T. californica)	VAT1	$3.45*10^{-4}$	-1.86
229890_at	proline-rich transmembrane protein 1	PRRT1	$4.40*10^{-4}$	-1.86
218547_at	dehydrodolichyl diphosphate synthase	DHDDS	$4.60*10^{-4}$	-1.86
235939_at	---	---	$5.76*10^{-5}$	-1.86
221696_s_at	serine/threonine/tyrosine kinase 1	STYK1	$7.91*10^{-4}$	-1.86
227392_at	nischarin	NISCH	$8.72*10^{-6}$	-1.87
228844_at	solute carrier family 13 (sodium-dependent citrate transporter), member 5	SLC13A5	$1.90*10^{-3}$	-1.87
204546_at	KIAA0513	KIAA0513	$2.43*10^{-3}$	-1.87
40472_at	lysophosphatidylcholine acyltransferase 4	LPCAT4	$1.29*10^{-3}$	-1.87
213078_x_at	lysophosphatidylcholine acyltransferase 4	LPCAT4	$7.22*10^{-4}$	-1.87
222995_s_at	rhomboid domain containing 2	RHBDD2	$1.49*10^{-3}$	-1.87
211006_s_at	potassium voltage-gated channel, Shab-related subfamily, member 1	KCNB1	$2.25*10^{-4}$	-1.87
242840_at	---	---	$2.22*10^{-3}$	-1.87
1557143_at	CUB and Sushi multiple domains 2	CSMD2	$1.61*10^{-3}$	-1.87
222171_s_at	PBX/knotted 1 homeobox 2	PKNOX2	$1.26*10^{-4}$	-1.88
1560296_at	---	---	$2.58*10^{-5}$	-1.88
1562403_a_at	solute carrier family 8 (sodium/calcium exchanger), member 3	SLC8A3	$1.41*10^{-3}$	-1.88
202042_at	histidyl-tRNA synthetase	HARS	$8.82*10^{-4}$	-1.88
215342_s_at	RAB GTPase activating protein 1-like	RABGAP1L	$1.69*10^{-3}$	-1.88
222350_at	---	---	$2.53*10^{-4}$	-1.88
231223_at	CUB and Sushi multiple domains 1	CSMD1	$1.26*10^{-3}$	-1.88
230241_at	---	---	$1.41*10^{-3}$	-1.89
223707_at	ribosomal protein L27a	RPL27A	$1.73*10^{-3}$	-1.89
222594_s_at	spermatogenesis associated, serine-rich 2	SPATS2	$1.55*10^{-3}$	-1.89
228205_at	transketolase	TKT	$3.42*10^{-5}$	-1.89
227365_at	ataxia, cerebellar, Cayman type	ATCAY	$2.13*10^{-4}$	-1.89
222298_at	---	---	$1.90*10^{-3}$	-1.89
205696_s_at	GDNF family receptor alpha 1	GFRA1	$7.38*10^{-4}$	-1.89
231104_at	tudor domain containing 5	TDRD5	$1.16*10^{-4}$	-1.89
215145_s_at	contactin associated protein-like 2	CNTNAP2	$2.03*10^{-3}$	-1.89
243894_at	solute carrier family 41, member 2	SLC41A2	$5.70*10^{-4}$	-1.89
236826_at	Tetratricopeptide repeat domain 39B	TTC39B	$2.43*10^{-3}$	-1.89
229202_at	---	---	$2.26*10^{-3}$	-1.90
1553371_at	EPH receptor A10	EPHA10	$8.72*10^{-4}$	-1.90
203114_at	Sjogren syndrome/scleroderma autoantigen 1	SSSCA1	$1.38*10^{-3}$	-1.90
236724_at	cripto, FRL-1, cryptic family 1	CFC1	$1.00*10^{-3}$	-1.90
235505_s_at	---	---	$1.47*10^{-3}$	-1.90
223822_at	sushi domain containing 4	SUSD4	$1.36*10^{-3}$	-1.91
228069_at	family with sequence similarity 54, member A	FAM54A	$9.38*10^{-4}$	-1.91
236448_at	unc-5 homolog A (C. elegans)	UNC5A	$1.03*10^{-3}$	-1.91
1555058_a_at	lysophosphatidylglycerol acyltransferase 1	LPGAT1	$2.24*10^{-3}$	-1.91
225033_at	ST3 beta-galactoside alpha-2,3-sialyltransferase 1	ST3GAL1	$1.44*10^{-3}$	-1.91
1554486_a_at	chromosome 6 open reading frame 114	C6orf114	$1.45*10^{-3}$	-1.91
206284_x_at	clathrin, light chain (Lcb)	CLTB	$4.22*10^{-4}$	-1.91
218938_at	F-box and leucine-rich repeat protein 15	FBXL15	$1.58*10^{-3}$	-1.91
203389_at	kinesin family member 3C	KIF3C	$1.86*10^{-3}$	-1.91
219461_at	p21 protein (Cdc42/Rac)-activated kinase 6	PAK6	$8.96*10^{-6}$	-1.92
239975_at	major histocompatibility complex, class II, DP beta 2 (pseudogene)	HLA-DPB2	$1.48*10^{-3}$	-1.92
206435_at	beta-1,4-N-acetyl-galactosaminyl transferase 1	B4GALNT1	$7.71*10^{-5}$	-1.92
202517_at	collapsin response mediator protein 1	CRMP1	$1.21*10^{-4}$	-1.92
232994_s_at	Rho-guanine nucleotide exchange factor	RGNEF	$4.55*10^{-4}$	-1.92
230706_s_at	calcium/calmodulin-dependent protein kinase II inhibitor 2	CAMK2N2	$9.04*10^{-4}$	-1.92
204974_at	RAB3A, member RAS oncogene family	RAB3A	$6.76*10^{-5}$	-1.93

Probeset ID	Gene Title	Gene Symbol	p-value	Fold change
206017_at	KIAA0319	KIAA0319	$9.68*10^{-4}$	-1.93
217287_s_at	transient receptor potential cation channel, subfamily C, member 6	TRPC6	$2.22*10^{-3}$	-1.93
230208_at	hyperpolarization activated cyclic nucleotide-gated potassium channel 4	HCN4	$1.07*10^{-4}$	-1.93
219928_s_at	calcium binding tyrosine-(Y)-phosphorylation regulated	CABYR	$1.50*10^{-3}$	-1.94
229715_at	Hypothetical protein DKFZp686O24166	DKFZp686O24166	$2.54*10^{-4}$	-1.94
235655_at	---	---	$2.05*10^{-3}$	-1.94
231406_at	ORAI calcium release-activated calcium modulator 2	ORAI2	$4.99*10^{-6}$	-1.94
221844_x_at	signal peptidase complex subunit 3 homolog (S. cerevisiae)	SPCS3	$7.05*10^{-4}$	-1.94
229883_at	glutamate receptor, ionotropic, N-methyl D-aspartate 2D	GRIN2D	$1.00*10^{-5}$	-1.94
229002_at	family with sequence similarity 69, member B	FAM69B	$3.38*10^{-4}$	-1.95
235758_at	paraneoplastic antigen like 6A	PNMA6A	$6.44*10^{-4}$	-1.95
210215_at	transferrin receptor 2	TFR2	$8.62*10^{-4}$	-1.95
204287_at	synaptogyrin 1	SYNGR1	$2.25*10^{-4}$	-1.95
240173_at	---	---	$1.79*10^{-3}$	-1.95
216047_x_at	seizure related 6 homolog (mouse)-like	SEZ6L	$1.94*10^{-4}$	-1.96
1555385_at	beta-1,4-N-acetyl-galactosaminyl transferase 1	B4GALNT1	$1.18*10^{-4}$	-1.96
1555774_at	zygote arrest 1	ZAR1	$1.91*10^{-3}$	-1.96
1556425_a_at	hypothetical protein LOC284219	LOC284219	$1.16*10^{-3}$	-1.96
212668_at	SMAD specific E3 ubiquitin protein ligase 1	SMURF1	$7.84*10^{-5}$	-1.96
238212_at	---	---	$2.09*10^{-3}$	-1.96
240089_at	---	---	$2.78*10^{-4}$	-1.97
229015_at	FP944	LOC286367	$1.77*10^{-3}$	-1.97
214914_at	family with sequence similarity 13, member C	FAM13C	$1.69*10^{-4}$	-1.97
205509_at	carboxypeptidase B1 (tissue)	CPB1	$1.12*10^{-3}$	-1.97
1569867_at	essential meiotic endonuclease 1 homolog 2 (S. pombe)	EME2	$5.89*10^{-5}$	-1.97
229253_at	thioesterase superfamily member 4	THEM4	$6.19*10^{-4}$	-1.97
219689_at	sema domain, immunoglobulin domain (Ig), short basic domain, secreted, (semaphor	SEMA3G	$1.41*10^{-3}$	-1.97
217838_s_at	Enah/Vasp-like	EVL	$6.55*10^{-5}$	-1.97
223901_at	synaptotagmin III	SYT3	$7.56*10^{-4}$	-1.98
202178_at	protein kinase C, zeta	PRKCZ	$5.94*10^{-4}$	-1.98
1556776_a_at	---	---	$1.08*10^{-3}$	-1.98
1557617_at	hypothetical LOC100189589	LOC100189589	$9.23*10^{-4}$	-1.99
1555908_at	family with sequence similarity 120A	FAM120A	$3.72*10^{-4}$	-1.99
206065_s_at	dihydropyrimidinase	DPYS	$1.81*10^{-4}$	-1.99
237933_at	---	---	$1.84*10^{-3}$	-1.99
217991_x_at	single stranded DNA binding protein 3	SSBP3	$1.16*10^{-3}$	-1.99
228825_at	prostaglandin reductase 1	PTGR1	$4.92*10^{-6}$	-1.99
1563638_at	family with sequence similarity 18, member A	FAM18A	$1.64*10^{-5}$	-2.00
1552803_a_at	stathmin 1	STMN1	$2.21*10^{-3}$	-2.00
205172_x_at	clathrin, light chain (Lcb)	CLTB	$2.08*10^{-3}$	-2.00
223574_x_at	protein phosphatase 2 (formerly 2A), regulatory subunit B, gamma isoform	PPP2R2C	$4.34*10^{-4}$	-2.00
217231_s_at	microtubule associated serine/threonine kinase 1	MAST1	$3.46*10^{-5}$	-2.01
235149_at	phosphoglucomutase 2-like 1	PGM2L1	$3.73*10^{-4}$	-2.01
205567_at	carbohydrate (keratan sulfate Gal-6) sulfotransferase 1	CHST1	$3.99*10^{-5}$	-2.01
226248_s_at	KIAA1324	KIAA1324	$4.67*10^{-6}$	-2.01
204505_s_at	erythrocyte membrane protein band 4.9 (dematin)	EPB49	$3.16*10^{-4}$	-2.01
244322_at	hypothetical LOC646329	hCG_2038586	$4.89*10^{-4}$	-2.01
213587_s_at	ATPase, H+ transporting V0 subunit e2	ATP6V0E2	$8.41*10^{-5}$	-2.01
205445_at	prolactin	PRL	$9.58*10^{-4}$	-2.02
1565937_a_at	LIM domain only 3 (rhombotin-like 2)	LMO3	$7.39*10^{-4}$	-2.02
219045_at	ras homolog gene family, member F (in filopodia)	RHOF	$9.30*10^{-5}$	-2.02
204922_at	chromosome 11 open reading frame 80	C11orf80	$1.42*10^{-4}$	-2.02
211894_x_at	seizure related 6 homolog (mouse)-like	SEZ6L	$5.63*10^{-4}$	-2.02
212699_at	secretory carrier membrane protein 5	SCAMP5	$7.07*10^{-4}$	-2.02
212148_at	pre-B-cell leukemia homeobox 1	PBX1	$2.00*10^{-3}$	-2.02
204424_s_at	LIM domain only 3 (rhombotin-like 2)	LMO3	$1.19*10^{-3}$	-2.03
226918_at	junctophilin 4	JPH4	$6.26*10^{-4}$	-2.03
244069_at	---	---	$8.86*10^{-5}$	-2.03
230163_at	GDNF family receptor alpha 1	GFRA1	$1.50*10^{-3}$	-2.03
230458_at	solute carrier family 45, member 1	SLC45A1	$2.60*10^{-5}$	-2.03
215153_at	nitric oxide synthase 1 (neuronal) adaptor protein	NOS1AP	$4.62*10^{-4}$	-2.03
203911_at	RAP1 GTPase activating protein	RAP1GAP	$7.74*10^{-4}$	-2.03
1568781_at	---	---	$5.76*10^{-4}$	-2.04
232983_s_at	secretion regulating guanine nucleotide exchange factor	SERGEF	$1.02*10^{-3}$	-2.04
206732_at	SLIT and NTRK-like family, member 3	SLITRK3	$9.98*10^{-5}$	-2.04
232416_at	bruno-like 5, RNA binding protein (Drosophila)	BRUNOL5	$5.28*10^{-5}$	-2.04
216286_at	---	---	$1.42*10^{-3}$	-2.05
227198_at	AF4/FMR2 family, member 3	AFF3	$1.18*10^{-3}$	-2.06
1556588_at	chromosome 15 open reading frame 37	C15orf37	$6.56*10^{-4}$	-2.06
226791_at	kinesin family member C2	KIFC2	$3.42*10^{-5}$	-2.06
218568_at	acylglycerol kinase	AGK	$9.38*10^{-4}$	-2.06
218625_at	neuritin 1	NRN1	$2.18*10^{-3}$	-2.06
234103_at	Potassium channel, subfamily T, member 2	KCNT2	$9.08*10^{-4}$	-2.06
1555310_a_at	p21 protein (Cdc42/Rac)-activated kinase 6	PAK6	$1.96*10^{-6}$	-2.07
219282_s_at	transient receptor potential cation channel, subfamily V, member 2	TRPV2	$9.21*10^{-4}$	-2.07
243704_at	---	---	$1.36*10^{-3}$	-2.07
45714_at	host cell factor C1 regulator 1 (XPO1 dependent)	HCFC1R1	$1.31*10^{-5}$	-2.07
1559172_at	---	---	$1.07*10^{-3}$	-2.07
219400_at	contactin associated protein 1	CNTNAP1	$5.71*10^{-4}$	-2.07
232735_at	ankyrin repeat domain 34A	ANKRD34A	$4.80*10^{-4}$	-2.07
210331_at	HECT, C2 and WW domain containing E3 ubiquitin protein ligase 1	HECW1	$2.65*10^{-7}$	-2.08
230988_at	---	---	$5.23*10^{-6}$	-2.08
244873_s_at	---	---	$6.59*10^{-4}$	-2.09
51158_at	family with sequence similarity 174, member B	FAM174B	$1.08*10^{-4}$	-2.09
227408_s_at	sorting nexin 25	SNX25	$1.39*10^{-3}$	-2.09
240709_at	seizure related 6 homolog (mouse)-like	SEZ6L	$3.11*10^{-4}$	-2.11
210270_at	regulator of G-protein signaling 6	RGS6	$2.38*10^{-5}$	-2.11

Supplementary table 3.4 (continued)

Probeset ID	Gene Title	Gene Symbol	p-value	Fold change
229487_at	early B-cell factor 1	EBF1	$6.45*10^{-5}$	-2.11
209981_at	cold shock domain containing C2, RNA binding	CSDC2	$1.52*10^{-6}$	-2.11
240304_s_at	transmembrane channel-like 5	TMC5	$2.05*10^{-4}$	-2.11
204604_at	PFTAIRE protein kinase 1	PFTK1	$1.18*10^{-3}$	-2.11
238878_at	aristaless related homeobox	ARX	$4.42*10^{-4}$	-2.11
214933_at	calcium channel, voltage-dependent, P/Q type, alpha 1A subunit	CACNA1A	$4.17*10^{-4}$	-2.12
207873_x_at	seizure related 6 homolog (mouse)-like	SEZ6L	$2.03*10^{-4}$	-2.12
1569868_s_at	essential meiotic endonuclease 1 homolog 2 (S. pombe)	EME2	$1.35*10^{-5}$	-2.12
1559194_a_at	C-type lectin domain family 4, member G pseudogene 1	CLEC4GP1	$4.31*10^{-4}$	-2.12
1556627_at	dystrophin related protein 2	DRP2	$1.60*10^{-3}$	-2.12
213439_x_at	RUN domain containing 3A	RUNDC3A	$6.90*10^{-5}$	-2.12
240083_at	---	---	$6.68*10^{-4}$	-2.12
238600_at	janus kinase and microtubule interacting protein 1	JAKMIP1	$1.32*10^{-3}$	-2.13
222549_at	claudin 1	CLDN1	$4.35*10^{-4}$	-2.14
206014_at	actin-like 6B	ACTL6B	$2.17*10^{-3}$	-2.14
215149_at	---	---	$4.35*10^{-4}$	-2.15
204945_at	protein tyrosine phosphatase, receptor type, N	PTPRN	$1.76*10^{-3}$	-2.15
228885_at	MAM domain containing 2	MAMDC2	$1.52*10^{-3}$	-2.15
239134_at	---	---	$2.09*10^{-5}$	-2.16
227760_at	insulin-like growth factor binding protein-like 1	IGFBPL1	$1.02*10^{-4}$	-2.16
34408_at	reticulon 2	RTN2	$8.24*10^{-5}$	-2.16
220091_at	solute carrier family 2 (facilitated glucose transporter), member 6	SLC2A6	$5.30*10^{-6}$	-2.16
232127_at	chloride channel 5	CLCN5	$7.84*10^{-4}$	-2.17
235781_at	calcium channel, voltage-dependent, N type, alpha 1B subunit	CACNA1B	$2.37*10^{-3}$	-2.17
204217_s_at	reticulon 2	RTN2	$4.32*10^{-5}$	-2.17
212559_at	protein kinase, cAMP-dependent, regulatory, type I, beta	PRKAR1B	$2.69*10^{-4}$	-2.17
200623_s_at	calmodulin 3 (phosphorylase kinase, delta)	CALM3	$1.08*10^{-3}$	-2.17
1569256_a_at	family with sequence similarity 43, member B	FAM43B	$4.07*10^{-4}$	-2.17
237240_at	---	---	$7.54*10^{-4}$	-2.18
227453_at	unc-13 homolog A (C. elegans)	UNC13A	$1.29*10^{-4}$	-2.18
232785_at	retrotransposon gag domain containing 1	RGAG1	$3.04*10^{-4}$	-2.18
1562687_x_at	---	---	$1.37*10^{-3}$	-2.18
216012_at	---	---	$8.06*10^{-4}$	-2.19
228554_at	progesterone receptor	PGR	$9.94*10^{-4}$	-2.19
215267_s_at	solute carrier family 8 (sodium/calcium exchanger), member 2	SLC8A2	$1.46*10^{-7}$	-2.20
223362_s_at	septin 3	3-Sep	$8.22*10^{-4}$	-2.21
59697_at	RAB15, member RAS onocogene family	RAB15	$2.96*10^{-4}$	-2.21
235251_at	---	---	$1.32*10^{-3}$	-2.22
235935_at	chromosome 6 open reading frame 154	C6orf154	$2.74*10^{-4}$	-2.22
222801_s_at	stromal antigen 3-like 4	STAG3L4	$1.10*10^{-3}$	-2.23
229942_at	basonuclin 2	BNC2	$3.74*10^{-4}$	-2.23
214104_at	G protein-coupled receptor 161	GPR161	$1.75*10^{-5}$	-2.23
228613_at	RAB11 family interacting protein 3 (class II)	RAB11FIP3	$1.34*10^{-4}$	-2.24
213965_s_at	chromodomain helicase DNA binding protein 5	CHD5	$1.36*10^{-5}$	-2.24
238654_at	hypothetical protein LOC147645	LOC147645	$6.06*10^{-4}$	-2.24
229088_at	ectonucleotide pyrophosphatase/phosphodiesterase 1	ENPP1	$1.56*10^{-3}$	-2.24
219300_s_at	contactin associated protein-like 2	CNTNAP2	$2.38*10^{-5}$	-2.24
236214_at	family with sequence similarity 71, member F1	FAM71F1	$3.56*10^{-5}$	-2.24
230010_at	KIAA1853	KIAA1853	$2.20*10^{-5}$	-2.25
1552895_a_at	cancer-testis SP-1	C210rf99	$1.15*10^{-4}$	-2.25
206528_at	transient receptor potential cation channel, subfamily C, member 6	TRPC6	$2.24*10^{-4}$	-2.25
244617_at	G protein-coupled receptor 26	GPR26	$2.32*10^{-3}$	-2.28
227816_at	netrin 1	NTN1	$1.08*10^{-4}$	-2.28
225735_at	ankyrin repeat domain 50	ANKRD50	$5.05*10^{-4}$	-2.29
223739_at	peptidyl arginine deiminase, type I	PADI1	$2.73*10^{-4}$	-2.29
218662_s_at	non-SMC condensin I complex, subunit G	NCAPG	$2.17*10^{-3}$	-2.30
225186_at	Ras association (RalGDS/AF-6) and pleckstrin homology domains 1	RAPH1	$1.75*10^{-3}$	-2.31
213636_at	KIAA1045	KIAA1045	$1.61*10^{-3}$	-2.32
229294_at	junctophilin 3	JPH3	$5.25*10^{-4}$	-2.32
211756_at	parathyroid hormone-like hormone	PTHLH	$6.08*10^{-4}$	-2.32
231300_at	chromosome 16 open reading frame 93	C16orf93	$6.67*10^{-4}$	-2.33
220327_at	vestigial like 3 (Drosophila)	VGLL3	$1.97*10^{-3}$	-2.34
204467_s_at	synuclein, alpha (non A4 component of amyloid precursor)	SNCA	$9.57*10^{-4}$	-2.34
229523_at	Two transmembrane domain family member A	TTMA	$1.51*10^{-3}$	-2.35
1564031_a_at	RELT-like 2	RELL2	$4.02*10^{-4}$	-2.35
230287_at	small G protein signaling modulator 1	SGSM1	$1.06*10^{-3}$	-2.36
209530_at	calcium channel, voltage-dependent, beta 3 subunit	CACNB3	$2.79*10^{-5}$	-2.37
231880_at	family with sequence similarity 40, member B	FAM40B	$2.38*10^{-3}$	-2.37
205391_x_at	ankyrin 1, erythrocytic	ANK1	$1.94*10^{-4}$	-2.37
238747_at	---	---	$1.74*10^{-3}$	-2.37
205914_s_at	glutamate receptor, ionotropic, N-methyl D-aspartate 1	GRIN1	$1.18*10^{-4}$	-2.37
223621_at	paraneoplastic antigen MA3	PNMA3	$5.96*10^{-4}$	-2.37
1565936_a_at	LIM domain only 3 (rhombotin-like 2)	LMO3	$2.52*10^{-4}$	-2.38
208352_x_at	ankyrin 1, erythrocytic	ANK1	$2.17*10^{-5}$	-2.38
221011_s_at	limb bud and heart development homolog (mouse)	LBH	$4.96*10^{-4}$	-2.39
242100_at	chondroitin sulfate synthase 3	CHSY3	$6.83*10^{-4}$	-2.40
227909_at	non-protein coding RNA 86 / non-protein coding RNA 87	NCRNA00086 / NCRNA00087	$3.15*10^{-4}$	-2.41
213943_at	twist homolog 1 (Drosophila)	TWIST1	$1.78*10^{-4}$	-2.41
229822_at	---	---	$4.23*10^{-4}$	-2.42
238378_at	---	---	$2.23*10^{-3}$	-2.43
230369_at	G protein-coupled receptor 161	GPR161	$1.32*10^{-3}$	-2.43
230552_at	hypothetical protein LOC100131606 / hypothetical protein LOC100134317 /	LOC100131606 / LOC100134317 /	$4.51*10^{-4}$	-2.45
228414_at	potassium large conductance calcium-activated channel, subfamily M, alpha member	KCNMA1	$4.87*10^{-4}$	-2.45
205389_s_at	ankyrin 1, erythrocytic	ANK1	$1.09*10^{-4}$	-2.45
240407_at	hypothetical LOC100126784	LOC100126784	$1.14*10^{-3}$	-2.45

Probeset ID	Gene Title	Gene Symbol	p-value	Fold change
233220_at	glutamate receptor, ionotropic, N-methyl-D-aspartate 3A	GRIN3A	$4.83*10^{-4}$	-2.45
232848_at	hCG1818123	hCG_1795283	$1.77*10^{-5}$	-2.45
206091_at	matrilin 3	MATN3	$5.34*10^{-4}$	-2.46
37566_at	KIAA1045	KIAA1045	$1.50*10^{-3}$	-2.46
213343_s_at	glycerophosphodiester phosphodiesterase domain containing 5	GDPD5	$5.90*10^{-7}$	-2.46
204730_at	regulating synaptic membrane exocytosis 3	RIMS3	$3.93*10^{-4}$	-2.46
215771_x_at	ret proto-oncogene	RET	$2.69*10^{-4}$	-2.46
226211_at	maternally expressed 3 (non-protein coding)	MEG3	$4.42*10^{-5}$	-2.47
240841_at	insulinoma-associated 2	INSM2	$4.73*10^{-6}$	-2.47
227618_at	---	---	$2.11*10^{-4}$	-2.47
237794_at	cancer-testis SP-1 / non-protein coding RNA 164	C210rf99 / NCRNA00164	$3.68*10^{-4}$	-2.47
229770_at	glycosyltransferase 1 domain containing 1	GLT1D1	$1.53*10^{-3}$	-2.48
241881_at	olfactory receptor, family 2, subfamily W, member 3	OR2W3	$1.62*10^{-4}$	-2.50
204586_at	bassoon (presynaptic cytomatrix protein)	BSN	$1.33*10^{-4}$	-2.50
228427_at	F-box protein 16	FBXO16	$2.55*10^{-4}$	-2.50
215161_at	calcium/calmodulin-dependent protein kinase IG	CAMK1G	$3.08*10^{-5}$	-2.51
223753_s_at	cripto, FRL-1, cryptic family 1 / cripto, FRL-1, cryptic family 1B	CFC1 / CFC1B	$1.05*10^{-3}$	-2.51
206590_x_at	dopamine receptor D2	DRD2	$3.03*10^{-5}$	-2.52
228882_at	tubby homolog (mouse)	TUB	$1.90*10^{-3}$	-2.52
206196_s_at	RUN domain containing 3A	RUNDC3A	$1.23*10^{-3}$	-2.54
208353_x_at	ankyrin 1, erythrocytic	ANK1	$3.29*10^{-5}$	-2.54
207360_s_at	neurotensin receptor 1 (high affinity)	NTSR1	$2.55*10^{-5}$	-2.55
205030_at	fatty acid binding protein 7, brain	FABP7	$1.81*10^{-3}$	-2.55
232856_at	Leucine rich repeat containing 55	LRRC55	$1.65*10^{-4}$	-2.57
231348_s_at	LIM domain only 3 (rhombotin-like 2)	LMO3	$2.77*10^{-4}$	-2.58
231261_at	cation channel, sperm-associated, gamma	CATSPERG	$2.96*10^{-4}$	-2.58
1557638_at	---	---	$7.06*10^{-5}$	-2.58
227399_at	vestigial like 3 (Drosophila)	VGLL3	$7.71*10^{-4}$	-2.58
235952_at	---	---	$1.63*10^{-4}$	-2.59
207087_x_at	ankyrin 1, erythrocytic	ANK1	$1.19*10^{-5}$	-2.59
220131_at	FXYD domain containing ion transport regulator 7	FXYD7	$1.53*10^{-4}$	-2.61
1557545_s_at	ring finger protein 165	RNF165	$6.44*10^{-6}$	-2.61
237131_at	chromosome 1 open reading frame 230	C10rf230	$6.19*10^{-4}$	-2.62
213869_x_at	Thy-1 cell surface antigen	THY1	$1.88*10^{-3}$	-2.62
210380_s_at	calcium channel, voltage-dependent, T type, alpha 1G subunit	CACNA1G	$1.23*10^{-4}$	-2.63
210103_s_at	forkhead box A2	FOXA2	$2.89*10^{-4}$	-2.64
204667_at	forkhead box A1	FOXA1	$1.18*10^{-3}$	-2.66
222482_at	similar to single stranded DNA binding protein 3 / hypothetical LOC100131851 /	LOC100131851 //SSBP3	$8.14*10^{-5}$	-2.66
210682_at	lactoperoxidase	LPO	$1.77*10^{-5}$	-2.66
213997_at	family with sequence similarity 189, member A1	FAM189A1	$3.60*10^{-5}$	-2.67
213358_at	KIAA0802	KIAA0802	$1.14*10^{-3}$	-2.67
240869_at	---	---	$4.10*10^{-5}$	-2.67
235836_at	matrix-remodelling associated 7	MXRA7	$1.41*10^{-3}$	-2.68
242705_x_at	similar to hCG1981348	LOC100289219	$6.20*10^{-4}$	-2.70
205879_x_at	ret proto-oncogene	RET	$1.65*10^{-4}$	-2.71
205538_at	coronin, actin binding protein, 2A	CORO2A	$5.28*10^{-4}$	-2.71
32502_at	glycerophosphodiester phosphodiesterase domain containing 5	GDPD5	$1.49*10^{-6}$	-2.73
205968_at	potassium voltage-gated channel, delayed-rectifier, subfamily S, member 3	KCNS3	$5.90*10^{-4}$	-2.74
223885_at	calneuron 1	CALN1	$2.67*10^{-4}$	-2.74
206774_at	FERM and PDZ domain containing 1	FRMPD1	$6.93*10^{-5}$	-2.75
233602_at	---	---	$4.23*10^{-4}$	-2.76
238617_at	---	---	$5.36*10^{-4}$	-2.77
208463_at	gamma-aminobutyric acid (GABA) A receptor, alpha 4	GABRA4	$1.41*10^{-4}$	-2.77
229103_at	wingless-type MMTV integration site family, member 3	WNT3	$6.92*10^{-4}$	-2.78
232426_at	synaptic vesicle glycoprotein 2B	SV2B	$5.68*10^{-4}$	-2.79
1554355_a_at	sialic acid acetylesterase	SIAE	$5.34*10^{-4}$	-2.79
216938_x_at	dopamine receptor D2	DRD2	$2.45*10^{-4}$	-2.82
209325_s_at	regulator of G-protein signaling 16	RGS16	$4.74*10^{-4}$	-2.83
212992_at	AHNAK nucleoprotein 2	AHNAK2	$1.33*10^{-3}$	-2.83
235182_at	isthmin 1 homolog (zebrafish)	ISM1	$8.21*10^{-5}$	-2.89
206232_s_at	UDP-Gal:betaGlcNAc beta 1,4- galactosyltransferase, polypeptide 6	B4GALT6	$1.39*10^{-3}$	-2.90
231766_s_at	collagen, type XII, alpha 1	COL12A1	$9.06*10^{-4}$	-2.90
236013_at	calcium channel, voltage-dependent, R type, alpha 1E subunit	CACNA1E	$1.77*10^{-3}$	-2.92
203108_at	G protein-coupled receptor, family C, group 5, member A	GPRC5A	$1.21*10^{-5}$	-2.94
213036_x_at	ATPase, Ca++ transporting, ubiquitous	ATP2A3	$2.83*10^{-4}$	-2.96
236901_at	---	---	$1.49*10^{-3}$	-2.97
230596_at	---	---	$1.17*10^{-3}$	-2.98
242998_at	retinol dehydrogenase 12 (all-trans/9-cis/11-cis)	RDH12	$2.21*10^{-4}$	-3.03
229626_at	chromosome 12 open reading frame 68	C12orf68	$3.55*10^{-4}$	-3.04
243806_at	---	---	$7.01*10^{-4}$	-3.05
209324_s_at	regulator of G-protein signaling 16	RGS16	$3.77*10^{-4}$	-3.05
233506_at	---	---	$1.25*10^{-3}$	-3.07
214745_at	phospholipase C, eta 1	PLCH1	$1.20*10^{-4}$	-3.09
233482_at	---	---	$7.04*10^{-4}$	-3.09
1552694_at	solute carrier family 2 (facilitated glucose transporter), member 13	SLC2A13	$1.99*10^{-3}$	-3.10
1561615_s_at	solute carrier family 8 (sodium/calcium exchanger), member 1	SLC8A1	$4.30*10^{-4}$	-3.12
230698_at	calneuron 1	CALN1	$2.84*10^{-4}$	-3.13
227177_at	coronin, actin binding protein, 2A	CORO2A	$1.19*10^{-3}$	-3.14
217250_s_at	chromodomain helicase DNA binding protein 5	CHD5	$3.27*10^{-4}$	-3.18
34726_at	calcium channel, voltage-dependent, beta 3 subunit	CACNB3	$1.40*10^{-4}$	-3.18
227875_at	kelch-like 13 (Drosophila)	KLHL13	$1.74*10^{-3}$	-3.22
232443_at	hypothetical LOC441052	LOC441052	$1.60*10^{-4}$	-3.22
235600_at	---	---	$1.09*10^{-3}$	-3.24
228101_at	amyloid beta (A4) precursor protein-binding, family A, member 1	APBA1	$6.74*10^{-4}$	-3.25
207869_s_at	calcium channel, voltage-dependent, T type, alpha 1G subunit	CACNA1G	$2.12*10^{-3}$	-3.28
239881_at	---	---	$5.66*10^{-4}$	-3.29
208427_s_at	ELAV (embryonic lethal, abnormal vision, Drosophila)-like 2 (Hu antigen B)	ELAVL2	$7.51*10^{-4}$	-3.35

Supplementary table 3.4 (continued)

Probeset ID	Gene Title	Gene Symbol	p-value	Fold change
204621_s_at	nuclear receptor subfamily 4, group A, member 2	NR4A2	$1.80*10^{-3}$	-3.42
204723_at	sodium channel, voltage-gated, type III, beta	SCN3B	$2.35*10^{-3}$	-3.43
205390_s_at	ankyrin 1, erythrocytic	ANK1	$1.01*10^{-4}$	-3.48
244675_at	regulator of G-protein signaling 8	RGS8	$1.23*10^{-3}$	-3.55
1568868_at	cytochrome P450, family 27, subfamily C, polypeptide 1	CYP27C1	$8.75*10^{-4}$	-3.58
206502_s_at	insulinoma-associated 1	INSM1	$2.31*10^{-3}$	-3.62
1552695_a_at	solute carrier family 2 (facilitated glucose transporter), member 13	SLC2A13	$1.58*10^{-3}$	-3.67
205747_at	cerebellin 1 precursor	CBLN1	$1.36*10^{-3}$	-3.70
207195_at	contactin 6	CNTN6	$4.35*10^{-4}$	-3.73
219414_at	calsyntenin 2	CLSTN2	$1.83*10^{-4}$	-3.76
207522_s_at	ATPase, Ca++ transporting, ubiquitous	ATP2A3	$4.13*10^{-4}$	-3.84
1553357_at	hypothetical LOC158696	LOC158696	$3.60*10^{-4}$	-4.01
229084_at	contactin 4	CNTN4	$1.10*10^{-3}$	-4.13
229580_at	---	---	$2.28*10^{-3}$	-4.27
1553865_a_at	G protein-coupled receptor 26	GPR26	$1.67*10^{-3}$	-4.37
1560676_at	seven in absentia homolog 3 (Drosophila)	SIAH3	$2.32*10^{-4}$	-4.82
226847_at	follistatin	FST	$4.63*10^{-4}$	-5.03
231341_at	solute carrier family 35, member D3	SLC35D3	$3.03*10^{-4}$	-10.66

3

Supplementary table 3.5. Altered molecular pathways based on 4 groups (control, Braak 1-2, Braak 3-4, and Braak 5-6) analysis: comparisons among all consecutive pathological groups, and between all pathological groups and controls (B-H p-value displayed).

Ingenuity pathway	all groups	Braak α-synuclein 1-2 compared to controls	Braak α-synuclein 3-4 compared to 1-2	Braak α-synuclein 5-6 compared to 3-4	Braak α-synuclein 3-4 compared to controls	Braak α-synuclein 5-6 compared to controls
EIF2 Signaling	$4.68*10^{-7}$	$1.82*10^{-2}$	$8.91*10^{-3}$	0.51	$3,16*10^{-17}$	$3.16*10^{-4}$
Breast Cancer Regulation by Stathmin1	$5.13*10^{-5}$	$1.07*10^{-3}$	0.11	$1.20*10^{-2}$	0.29	$1.29*10^{-3}$
Regulation of eIF4 and p70S6K Signaling	$1.45*10^{-4}$	$1.00*10^{-3}$	$2.95*10^{-2}$	0.31	$7.41*10^{-5}$	$6.17*10^{-3}$
Dopamine-DARPP32 Feedback in cAMP Signaling	$1.82*10^{-4}$	$9.33*10^{-5}$	0,20	$6.46*10^{-3}$	0.51	$1.86*10^{-3}$
mTOR Signaling	$1.95*10^{-4}$	$1.02*10^{-4}$	$6.46*10^{-2}$	0.30	$1.38*10^{-4}$	$5.25*10^{-3}$
Protein Kinase A Signaling	$5.25*10^{-4}$	$2.75*10^{-3}$	$2.95*10^{-2}$	$5.01*10^{-2}$	0.22	$2.57*10^{-3}$
Signaling by Rho Family GTPases	$5.37*10^{-4}$	$9.33*10^{-5}$	$2.95*10^{-2}$	0.11	0.11	$3.16*10^{-4}$
Molecular Mechanisms of Cancer	$2.14*10^{-3}$	$1.95*10^{-5}$	$1.02*10^{-3}$	0.10	0.36	$2.75*10^{-2}$
Role of NFAT in Cardiac Hypertrophy	$2.14*10^{-3}$	$9.33*10^{-4}$	$2.34*10^{-2}$	$1.15*10^{-2}$	0.30	$2.57*10^{-3}$
B Cell Receptor Signaling	$3.24*10^{-3}$	$5.13*10^{-4}$	$1.58*10^{-2}$	$1.41*10^{-2}$	0.36	$1.86*10^{-3}$
Huntington's Disease Signaling	$3.80*10^{-3}$	$1.02*10^{-4}$	$4.07*10^{-2}$	0,20	0.30	$1.86*10^{-2}$
PI3K/AKT Signaling	$3.89*10^{-3}$	$1.38*10^{-3}$	$8.71*10^{-2}$	$3.98*10^{-2}$	0.71	$3.16*10^{-4}$
RhoGDI Signaling	$3.89*10^{-3}$	$5.62*10^{-4}$	0.23	0.22	0.30	$7.24*10^{-4}$
Axonal Guidance Signaling	$4.57*10^{-3}$	$1.02*10^{-4}$	$4.17*10^{-2}$	0.27	0.54	$1.82*10^{-2}$
GNRH Signaling	$4.90*10^{-3}$	$1.38*10^{-3}$	$2.95*10^{-2}$	0.17	0.22	$2.95*10^{-2}$
CCR3 Signaling in Eosinophils	$6.17*10^{-3}$	$1.62*10^{-3}$	$2.95*10^{-2}$	$7.59*10^{-2}$	0.24	0.13
Gap Junction Signaling	$6.17*10^{-3}$	$7.41*10^{-5}$	0.16	0.34	0.52	$1.82*10^{-2}$
RhoA Signaling	$6.76*10^{-3}$	$1.23*10^{-4}$	$6.92*10^{-2}$	0.32	0.35	$1.35*10^{-2}$
Insulin Receptor Signaling	$7.24*10^{-3}$	$1.02*10^{-3}$	$6.46*10^{-2}$	$3.98*10^{-2}$	0.77	$5.37*10^{-2}$
Thrombin Signaling	$7.76*10^{-3}$	$1.20*10^{-3}$	$5.75*10^{-2}$	$6.46*10^{-3}$	0.26	$4.47*10^{-2}$
Nitric Oxide Signaling in the Cardiovascular System	$9.33*10^{-3}$	$1.70*10^{-3}$	$6.03*10^{-2}$	$7.08*10^{-2}$	0.68	0.27
Ephrin Receptor Signaling	$1.38*10^{-2}$	$2.82*10^{-4}$	$5.25*10^{-2}$	$5.01*10^{-2}$	0.43	$2.75*10^{-2}$
HGF Signaling	$1.45*10^{-2}$	$5.01*10^{-4}$	$2.95*10^{-2}$	0.30	0.52	$4.79*10^{-2}$
HIF1α Signaling	$1.45*10^{-2}$	$8.91*10^{-3}$	$2.95*10^{-2}$	0.30	0.52	$4.79*10^{-2}$
Semaphorin Signaling in Neurons	$1.70*10^{-2}$	$9.12*10^{-3}$	0.19	0.30	$2.29*10^{-2}$	$6.17*10^{-2}$
CREB Signaling in Neurons	$1.74*10^{-2}$	$6.46*10^{-3}$	0.11	$1.41*10^{-2}$	0.42	0.14

Ingenuity pathway	all groups	Braak α-synuclein 1-2 compared to controls	Braak α-synuclein 3-4 compared to 1-2	Braak α-synuclein 5-6 compared to 3-4	Braak α-synuclein 3-4 compared to controls	Braak α-synuclein 5-6 compared to controls
Phospholipase C Signaling	$1.78*10^{-2}$	$2.95*10^{-3}$	$5.25*10^{-2}$	$7.08*10^{-2}$	0.78	$4.07*10^{-3}$
SAPK/JNK Signaling	$1.78*10^{-2}$	$6.46*10^{-4}$	0.10	0.16	0.38	$2.95*10^{-2}$
PTEN Signaling	$2.34*10^{-2}$	$8.91*10^{-4}$	$1.58*10^{-2}$	$7.08*10^{-2}$	0.65	$9.55*10^{-4}$
Renin-Angiotensin Signaling	$2.45*10^{-2}$	$1.02*10^{-4}$	$2.95*10^{-2}$	0.15	0.35	$7.59*10^{-2}$
Rac Signaling	$2.45*10^{-2}$	$1.02*10^{-4}$	$7.08*10^{-2}$	$9.55*10^{-2}$	0.08	$2.69*10^{-3}$
Angiopoietin Signaling	$2.45*10^{-2}$	$8.51*10^{-5}$	$7.59*10^{-2}$	$6.03*10^{-2}$	0.50	0.12
Neuregulin Signaling	$2.45*10^{-2}$	$1.20*10^{-3}$	$7.76*10^{-2}$	0.16	0.67	$7.24*10^{-2}$
CXCR4 Signaling	$2.45*10^{-2}$	$5.37*10^{-4}$	0.10	$7.41*10^{-2}$	0.39	$1.51*10^{-2}$
p70S6K Signaling	$2.45*10^{-2}$	$6.31*10^{-4}$	0.31	$9.55*10^{-2}$	0.63	$1.91*10^{-2}$
Relaxin Signaling	$2.75*10^{-2}$	$9.33*10^{-3}$	0.27	$3.98*10^{-2}$	0.35	0.10
HER-2 Signaling in Breast Cancer	$2.95*10^{-2}$	$1.05*10^{-3}$	$4.47*10^{-2}$	$7.41*10^{-2}$	0.76	0.13
Actin Cytoskeleton Signaling	$2.95*10^{-2}$	$1.02*10^{-4}$	$6.17*10^{-2}$	0.24	0.26	$6.92*10^{-2}$
CTLA4 Signaling in Cytotoxic T Lymphocytes	$2.95*10^{-2}$	$3.80*10^{-3}$	0.11	$6.76*10^{-3}$	0.52	$2.75*10^{-2}$
Regulation of Actin-based Motility by Rho	$2.95*10^{-2}$	$1.00*10^{-2}$	0.64	0.41	0.13	$7.76*10^{-2}$
Amyloid Processing	$3.16*10^{-2}$	$6.46*10^{-3}$	$4.17*10^{-2}$	0.43	0.35	0.15
IL-3 Signaling	$3.89*10^{-2}$	$6.17*10^{-4}$	$3.80*10^{-2}$	0.13	0.78	0.20
NGF Signaling	$3.89*10^{-2}$	$2.24*10^{-3}$	$5.37*10^{-2}$	0.10	0.38	$1.82*10^{-2}$
FAK Signaling	$3.89*10^{-2}$	$1.02*10^{-4}$	$5.75*10^{-2}$	0.22	0.20	0.12
Virus Entry via Endocytic Pathways	$3.89*10^{-2}$	$7.94*10^{-3}$	0.15	0.21	0.61	$1.91*10^{-2}$
Production of Nitric Oxide and Reactive Oxygen Species in Macrophages	$3.89*10^{-2}$	$8.91*10^{-4}$	0.22	0.24	0.61	0.11
Role of NFAT in Regulation of the Immune Response	$3.89*10^{-2}$	$6.17*10^{-4}$	0.31	0.15	0.59	$2.95*10^{-2}$
ILK Signaling	$4.47*10^{-2}$	$1.70*10^{-3}$	0.11	0.26	0.78	$3.63*10^{-2}$
Telomerase Signaling	$4.47*10^{-2}$	$8.91*10^{-4}$	0.15	0.20	0.50	$2.95*10^{-2}$
Ceramide Signaling	$4.47*10^{-2}$	$1.58*10^{-3}$	0.45	$7.41*10^{-2}$	0.77	$2.95*10^{-2}$
ERK/MAPK Signaling	$4.68*10^{-2}$	$1.02*10^{-3}$	0.13	0.10	0.52	$4.57*10^{-2}$
Agrin Interactions at Neuromuscular Junction	$5.01*10^{-2}$	$2.34*10^{-3}$	$2.95*10^{-2}$	0.57	0.22	$7.76*10^{-2}$
LPS-stimulated MAPK Signaling	$5.01*10^{-2}$	$2.95*10^{-3}$	$4.07*10^{-2}$	0.11	0.36	0.14
Acute Myeloid Leukemia Signaling	$5.01*10^{-2}$	$1.20*10^{-3}$	$6.92*10^{-2}$	0.11	0.72	0.20
Prolactin Signaling	$5.01*10^{-2}$	$8.51*10^{-4}$	0.20	0.20	0.79	0.48
G Beta Gamma Signaling	$5.01*10^{-2}$	$6.92*10^{-3}$	0.38	0.16	0.65	0.03
Cardiac Hypertrophy Signaling	$6.17*10^{-2}$	$1.78*10^{-3}$	$7.94*10^{-2}$	0.12	0.50	0.13
Cardiac β-adrenergic Signaling	$6.17*10^{-2}$	$3.31*10^{-3}$	$7.94*10^{-2}$	$6.50*10^{-3}$	0.50	0.13
IL-8 Signaling	$6.76*10^{-2}$	$2.75*10^{-3}$	$6.92*10^{-2}$	$7.59*10^{-2}$	0.54	0.11
IGF-1 Signaling	$6.76*10^{-2}$	$8.91*10^{-4}$	0.10	$7.41*10^{-2}$	0.54	0.12
AMPK Signaling	$7.41*10^{-2}$	$9.33*10^{-3}$	0.14	0.16	0.65	0.13
Estrogen Receptor Signaling	$7.59*10^{-2}$	$1.58*10^{-3}$	0.14	0.32	0.75	0.24
Germ Cell-Sertoli Cell Junction Signaling	$8.13*10^{-2}$	$1.45*10^{-3}$	0.33	0.53	0.29	$3.55*10^{-2}$
Pancreatic Adenocarcinoma Signaling	$8.71*10^{-2}$	$1.23*10^{-4}$	$5.25*10^{-3}$	0.66	0.54	0.24

Supplementary table 3.5 (continued)

Ingenuity pathway	all groups	Braak α-synuclein 1-2 compared to controls	Braak α-synuclein 3-4 compared to 1-2	Braak α-synuclein 5-6 compared to 3-4	Braak α-synuclein 3-4 compared to controls	Braak α-synuclein 5-6 compared to controls
RANK Signaling in Osteoclasts	$8.71*10^{-2}$	$1.00*10^{-2}$	$2.34*10^{-2}$	0.10	0.73	0.15
GM-CSF Signaling	$8.71*10^{-2}$	$5.75*10^{-4}$	$4.27*10^{-2}$	0.08	0.62	0.15
CNTF Signaling	$8.71*10^{-2}$	$6.92*10^{-4}$	$5.01*10^{-2}$	0.15	0.76	0.27
Non-Small Cell Lung Cancer Signaling	$8.71*10^{-2}$	$8.91*10^{-4}$	$5.13*10^{-2}$	0.10	0.73	0.23
Role of Tissue Factor in Cancer	$8.71*10^{-2}$	$5.62*10^{-4}$	0.23	0.17	0.77	0.30
IL-4 Signaling	$8.71*10^{-2}$	$8.91*10^{-4}$	0.38	0.15	0.67	0.23
RAR Activation	$8.71*10^{-2}$	$2.09*10^{-3}$	0.39	0.46	0.73	$8.13*10^{-2}$
HMGB1 Signaling	$9.12*10^{-2}$	$1.48*10^{-4}$	0.12	0.21	0.72	0.25
Human Embryonic Stem Cell Pluripotency	$9.12*10^{-2}$	$7.76*10^{-3}$	0.34	0.21	0.72	0.66
Aldosterone Signaling in Epithelial Cells	0.10	$9.33*10^{-4}$	0.40	0.45	0.51	0.26
Glioma Signaling	0.11	$6.76*10^{-4}$	$6.31*10^{-2}$	$7.08*10^{-2}$	0.61	0.17
Fcγ Receptor-mediated Phagocytosis in Macrophages and Monocytes	0.11	$1.45*10^{-3}$	0.24	0.44	0.78	$6.76*10^{-3}$
Prostate Cancer Signaling	0.11	$5.75*10^{-4}$	$4.07*10^{-2}$	0.23	0.78	$8.32*10^{-2}$
VEGF Signaling	0.11	$1.20*10^{-3}$	$7.76*10^{-2}$	0.32	0.61	0.37
fMLP Signaling in Neutrophils	0.11	$4.37*10^{-4}$	0.26	$9.77*10^{-2}$	0.78	0.14
Androgen Signaling	0.11	$8.91*10^{-3}$	0.28	0.23	0.76	0.37
Corticotropin Releasing Hormone Signaling	0.11	$3.24*10^{-3}$	0.41	0.24	0.75	0.23
NRF2-mediated Oxidative Stress Response	0.11	$4.07*10^{-3}$	$2.63*10^{-2}$	0.33	0.29	0.37
Chronic Myeloid Leukemia Signaling	0.11	$5.62*10^{-4}$	$2.34*10^{-2}$	$9.55*10^{-2}$	0.79	$3.02*10^{-2}$
Cdc42 Signaling	0.12	$4.47*10^{-4}$	$3.89*10^{-2}$	0.16	0.51	0.10
Tight Junction Signaling	0.12	$1.58*10^{-3}$	0.46	0.29	0.77	0.02
Chemokine Signaling	0.13	$6.17*10^{-3}$	$6.17*10^{-2}$	0.14	0.08	0.41
Integrin Signaling	0.13	$1.23*10^{-4}$	0.16	0.31	0.54	$5.01*10^{-2}$
Renal Cell Carcinoma Signaling	0.13	$1.38*10^{-3}$	0.31	0.10	0.30	0.41
Cholecystokinin/Gastrin-mediated Signaling	0.13	$1.38*10^{-3}$	$8.71*10^{-2}$	0.39	0.76	0.24
Neurotrophin/TRK Signaling	0.17	$2.95*10^{-3}$	$4.68*10^{-2}$	0.17	0.76	0.36
NF-αB Activation by Viruses	0.17	$6.46*10^{-3}$	$4.68*10^{-2}$	0.17	0.76	0.36
FGF Signaling	0.17	$5.62*10^{-4}$	$6.92*10^{-2}$	0.10	0.79	0.65
IL-15 Signaling	0.17	$5.50*10^{-4}$	$8.71*10^{-2}$	0.19	0.78	0.34
Thrombopoietin Signaling	0.18	$6.76*10^{-4}$	$5.75*10^{-2}$	0.16	0.80	0.48
Endometrial Cancer Signaling	0.18	$3.89*10^{-3}$	$4.68*10^{-2}$	0.11	0.78	0.28
EGF Signaling	0.18	$2.75*10^{-3}$	$2.95*10^{-2}$	0.18	0.76	0.54
P2Y Purigenic Receptor Signaling Pathway	0.18	$5.62*10^{-4}$	0.30	0.20	0.72	0.27
Small Cell Lung Cancer Signaling	0.18	$2.19*10^{-3}$	0.17	0.30	0.11	0.10
Colorectal Cancer Metastasis Signaling	0.19	$7.41*10^{-5}$	0.10	0.22	0.56	0.20
Leptin Signaling in Obesity	0.20	$6.46*10^{-3}$	0.26	0.22	0.74	0.48
FLT3 Signaling in Hematopoietic Progenitor Cells	0.20	$1.02*10^{-4}$	$1.02*10^{-3}$	0.26	0.78	0.44
Clathrin-mediated Endocytosis Signaling	0.20	$1.02*10^{-4}$	$4.57*10^{-2}$	0.41	0.51	0.48

Ingenuity pathway	all groups	Braak α-synuclein 1-2 compared to controls	Braak α-synuclein 3-4 compared to 1-2	Braak α-synuclein 5-6 compared to 3-4	Braak α-synuclein 3-4 compared to controls	Braak α-synuclein 5-6 compared to controls
PAK Signaling	0.20	$1.00*10^{-3}$	$4.68*10^{-2}$	0.67	0.54	0.11
Sertoli Cell-Sertoli Cell Junction Signaling	0.22	$7.76*10^{-3}$	5.92E-01	0.30	0.61	$8.51*10^{-2}$
Sphingosine-1-phosphate Signaling	0.23	$2.29*10^{-3}$	0.35	0.17	0.76	0.27
Erythropoietin Signaling	0.23	$1.23*10^{-4}$	0.14	0.13	0.78	0.28
Melanoma Signaling	0.23	$5.75*10^{-4}$	$3.47*10^{-2}$	0.24	$8.13*10^{-2}$	0.19
Antiproliferative Role of Somatostatin Receptor 2	0.24	$9.33*10^{-4}$	0.32	0.25	0.78	0.43
Macropinocytosis Signaling	0.25	$1.38*10^{-3}$	0.22	0.31	0.79	0.49
Type II Diabetes Mellitus Signaling	0.26	$5.62*10^{-3}$	0.15	0.43	0.54	0.38
TR/RXR Activation	0.27	$2.24*10^{-3}$	$4.07*10^{-2}$	0.70	0.61	0.67
Glioblastoma Multiforme Signaling	0.27	$5.62*10^{-4}$	0.16	0.26	0.77	0.66
IL-2 Signaling	0.28	$2.09*10^{-3}$	$7.76*10^{-2}$	0.32	0.75	0.51
Glucocorticoid Receptor Signaling	0.28	$1.66*10^{-3}$	0.42	0.55	0.54	0.67
Role of JAK family kinases in IL-6-type Cytokine Signaling	0.28	$2.14*10^{-3}$	$1.58*10^{-2}$	0.40	0.78	0.52
IL-17A Signaling in Airway Cells	0.28	$2.51*10^{-3}$	0.10	0.16	0.75	0.18
CD28 Signaling in T Helper Cells	0.31	$1.78*10^{-3}$	0.33	0.20	0.67	0.18
JAK/Stat Signaling	0.32	$5.50*10^{-4}$	$8.71*10^{-2}$	0.32	0.78	0.62
Paxillin Signaling	0.34	$1.07*10^{-3}$	$7.76*10^{-2}$	0.43	0.32	0.12
Leukocyte Extravasation Signaling	0.35	$1.32*10^{-3}$	0.31	0.33	0.58	0.24
β-Adrenergic Signaling	0.35	$6.17*10^{-3}$	0.15	0.43	0.54	0.28
IL-17 Signaling	0.35	$2.51*10^{-3}$	$7.76*10^{-2}$	0.40	0.78	0.45
Estrogen-Dependent Breast Cancer Signaling	0.36	$6.76*10^{-4}$	0.12	0.16	0.77	0.54
T Cell Receptor Signaling	0.38	$3.47*10^{-3}$	0.26	0.16	0.80	0.25
Glioma Invasiveness Signaling	0.41	$4.27*10^{-3}$	0.51	0.24	0.77	0.37
Role of NANOG in Mammalian Embryonic Stem Cell Pluripotency	0.41	$2.09*10^{-3}$	0.34	0.54	0.68	0.75
PDGF Signaling	0.42	$1.23*10^{-4}$	$2.63*10^{-2}$	0.30	0.75	0.42
Melanocyte Development and Pigmentation Signaling	0.42	$8.91*10^{-3}$	0.17	0.26	0.08	0.24
Growth Hormone Signaling	0.42	$6.17*10^{-3}$	0.31	0.31	0.77	$2.95*10^{-2}$
Actin Nucleation by ARP-WASP Complex	0.48	$3.55*10^{-3}$	$6.17*10^{-2}$	0.49	0.67	0.25
IL-9 Signaling	0.54	$8.71*10^{-3}$	0.23	0.43	0.54	0.11
BMP signaling pathway	0.67	$2.51*10^{-3}$	0.12	0.40	0.54	0.28
PPAR/RXR Activation	0.67	$1.58*10^{-3}$	0.52	0.51	0.51	0.37

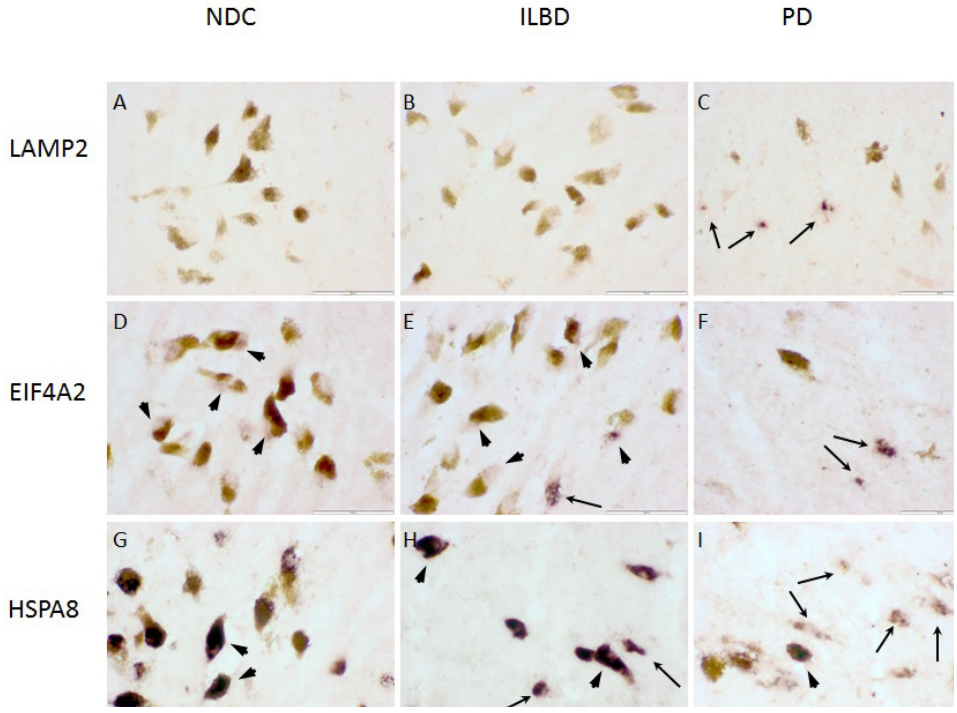

Supplementary figure 3.1. *In situ* hybridization of LAMP2, EIF4A2 and HSPA8 in the substantia nigra of non-demented control (A, D, G), iLBD (B, E, H) and PD (C, F, I) donors. LAMP2 expression (A, B, C) is present only in glial cells in PD substantia nigra. EIF4A2 (D, E, F) showed light expression in dopaminergic neurons in control and iLBD cases, and strong expression in glial cells in ILBD and PD donors. HSPA8 (G, H, I) showed strong expression in the dopaminergic neurons in all groups and increased number of positive glial cells in PD cases compared to iLBDs. Arrow heads indicate reactive dopaminergic neurons; arrows indicate glial cells.

3